

SECONDARY ELECTRON EMISSION FROM
MONOCRYSTALLINE METAL AND ALKALI-HALIDE
CRYSTALS

Kristin Lloyd Allen

Library
Naval Postgraduate School
Monterey, California 93940

NAVAL POSTGRADUATE SCHOOL

Monterey, California



THESIS

SECONDARY ELECTRON EMISSION
FROM MONOCRYSTALLINE METAL
AND ALKALI-HALIDE CRYSTALS

by

Kristin Lloyd Allen

Thesis Advisor:

D. E. Harrison, Jr.

June 1973

T153741

Approved for public release; distribution unlimited.

Secondary Electron Emission from Monocrystalline
Metal and Alkali-Halide Crystals

by

Kristin Lloyd Allen
Ensign, United States Navy
B.S.N.E., University of Virginia, 1972

Submitted in partial fulfillment of the
requirements for the degree of

MASTER OF SCIENCE IN PHYSICS

from the

NAVAL POSTGRADUATE SCHOOL
June 1973

ABSTRACT

This thesis is a computer simulation of secondary electron emission (SEE) from monocrystalline metals and alkali-halides using a modified version of the Harrison, Carlston and Magnuson single collision theory of SEE. Three cases of SEE are investigated: the angular dependence of SEE from Cu bombarded by Ar^+ , the dependence of SEE as a function of energy for rare gas ions normally incident on the (100), (110) and (111) faces of metal single crystals, and the dependence of SEE as a function of energy for Ar^+ and Ne^+ ions normally incident on the (100), (110) and (111) faces of KCl. The theory does not accurately describe the angular dependence of SEE for monocrystalline Cu targets, but does accurately predict the modified $\sec \theta$ dependence found experimentally in polycrystalline studies. For the metal targets, the difference between the theoretical kinetic secondary emission result and the experimental datum is identified as potential secondary emission. The alkali-halide SEE simulation agrees reasonably well with experiment.

TABLE OF CONTENTS

I.	INTRODUCTION - - - - -	10
II.	STUDY OBJECTIVES - - - - -	12
III.	SECONDARY ELECTRON EMISSION THEORY - - - - -	13
IV.	THEORIES CONCERNING SECONDARY ELECTRON EMISSION- -	19
	A. THEORY OF PARILIS AND KISHINEVSKII - - - - -	19
	B. THEORY OF HARRISON, CARLSTON AND MAGNUSON- - -	25
	1. Inelastic Energy Transfer- - - - -	28
	2. Collision Parameters - - - - -	30
	3. Number of Electrons Emitted - Russek Model- - - - -	36
	4. HCM Results- - - - -	38
V.	MODIFICATIONS TO THE HCM THEORETICAL MODEL - - - -	41
	A. INTERATOMIC POTENTIAL- - - - -	41
	B. THE BASIC INTERACTION- - - - -	43
	C. THE DISTRIBUTION OF IMPACT PARAMETERS- - - -	44
VI.	NUMERICAL METHODS AND COMPUTER PROGRAMS- - - - -	53
VII.	RESULTS- - - - -	60
	A. ANGULARLY DEPENDENT RESULTS- - - - -	61
	B. METAL TARGET RESULTS - - - - -	61
	1. Copper Bombarded by Ar, Ne, Kr and Xe Ions- - - - -	61
	2. Silver Bombarded by Ar, Ne and Kr Ions - -	72
	3. Molybdenum Bombarded by Ar, Ne, Kr and Xe Ions- - - - -	80
	4. Aluminum Bombarded by Ar, Kr and Xe Ions- - - - -	80

C. ALKALI-HALIDE RESULTS - - - - -	80
1. Potassium-Chloride Bombarded by Ar Ions - - - - -	102
2. Potassium-Chloride Bombarded by Ne Ions - - - - -	109
VIII. CONCLUSIONS AND RECOMMENDATIONS - - - - -	112
APPENDIX A - COMPUTER PROGRAM PARAMETERS - - - - -	116
COMPUTER PROGRAM - HERMAN-SKILLMAN RADIAL ELECTRON DENSITY PROGRAM - - - - -	121
COMPUTER PROGRAM - POTENTIAL PROGRAM - - - - -	139
COMPUTER PROGRAM - DISTRIBUTION OF IMPACT PARAMETERS PROGRAM- - - - -	149
COMPUTER PROGRAM - KSE PROGRAM - - - - -	155
LIST OF REFERENCES - - - - -	170
INITIAL DISTRIBUTION LIST- - - - -	172
FORM DD 1473 - - - - -	173

LIST OF FIGURES

Figure	Page
1. Potential energy diagram for a helium ion as it undergoes Auger neutralization at a tungsten surface. (3) - - - - -	16
2. Potential energy diagram for a metastable atom (He) as it undergoes Auger de-excitation at a tungsten surface. (3) - - - - -	17
3. Relationships between various quantities appearing in the Dynamic Integral - - - - -	31
4. Representative areas for normal incidence. After (2) - - - - -	33
5. Distribution of impact parameters for normal incidence on face-centered cubic crystals - - -	34
6. Distribution of impact parameters for normal incidence on body-centered cubic crystals - - -	35
7. Ar ⁺ - Cu results obtained from the HCM original model- - - - -	39
8. Representative area of a (100) FCC crystal face rotated about $\langle 110 \rangle$ in either a positive or negative sense - - - - -	47
9. Representative area of the (100) face of an FCC crystal rotated in a positive sense about the $\langle 110 \rangle$ direction - - - - -	48
10. Rotation geometry for a (100) face of an FCC crystal about an arbitrary crystallographic direction - - - - -	49
11. Unnormalized distribution of impact parameters for FCC (100) rotated through various angles about $\langle 110 \rangle$ - - - - -	52
12. Deck setup for running the Electron Density Program - - - - -	55
13. Deck setup for running the Potential Program- -	56

14.	Deck setup for running the Distribution of Impact Parameters Program- - - - -	57
15.	Deck setup for running the Interpolation Program - - - - -	58
16.	Deck setup for running the KSE Program- - - - -	59
17.	SEE coefficient vs. angle of rotation for (100) FCC Copper crystal. Direction of rotation was about $\langle 110 \rangle$ - - - - -	62
18.	Cu bombarded by Ar^+ ions normally incident on the (100), (110) and (111) planes- - - - -	64
19.	Cu bombarded by Ne^+ ions normally incident on the (100), (110) and (111) faces - - - - -	65
20.	Cu bombarded by Kr^+ ions normally incident on the (100), (110) and (111) faces - - - - -	66
21.	Cu bombarded by Xe^+ ions normally incident on the (100), (110) and (111) faces - - - - -	67
22.	PSE contribution to $^+$ secondary electron emission for the Ar^+ - Cu system- - - - -	68
23.	PSE contribution to $^+$ secondary electron emission for the Ne^+ - Cu system- - - - -	69
24.	PSE contribution to $^+$ secondary electron emission for the Kr^+ - Cu system- - - - -	70
25.	PSE contrubition to $^+$ secondary electron emission for the Xe^+ - Cu system- - - - -	71
26.	Ag bombarded by Ar^+ ions normally incident on the (100), (110) and (111) faces - - - - -	73
27.	Ag bombarded by Ne^+ ions normally incident on the (100), (110) and (111) faces - - - - -	74
28.	Ag bombarded by Kr^+ ions normally incident on the (100), (110) and (111) faces - - - - -	75
29.	PSE contribution to $^+$ secondary electron emission for the Ar^+ - Ag system- - - - -	76
30.	PSE contribution to $^+$ secondary electron emission for the Ne^+ - Ag system- - - - -	77

31.	PSE contribution to secondary electron emission for the Kr^+ - Ag system- - - - -	78
32.	Effect of varying target atom ionization in the HCM model on secondary electron emission from the Ar^+ - Mo system - - - - -	81
33.	Effect of varying target atom ionization in the HCM model on secondary electron emission from the Ar^+ - Mo system - - - - -	82
34.	Effect of varying target atom ionization in the HCM model on secondary electron emission in the Ar^+ - Mo system - - - - -	83
35.	Effect on varying target atom ionization in the HCM model on secondary electron emission from the Ne^+ - Mo system- - - - -	84
36.	Effect of varying target atom ionization in the HCM model on secondary electron emission from the Ne^+ - Mo system - - - - -	85
37.	Effect of varying target atom ionization in the HCM model on secondary electron emission from the Ne^+ - Mo system - - - - -	86
38.	Effect of varying target atom ionization in the HCM model on secondary electron emission from the Kr^+ - Mo system - - - - -	87
39.	Effect of varying target atom ionization in the HCM model on secondary electron emission from the Kr^+ - Mo system - - - - -	88
40.	Effect of varying target atom ionization in the HCM model on secondary electron emission from the Kr^+ - Mo system - - - - -	89
41.	Effect of varying target atom ionization in the HCM model on secondary electron emission from the Xe^+ - Mo system - - - - -	90
42.	Effect of varying target atom ionization in the HCM model on secondary electron emission from the Xe^+ - Mo system - - - - -	91
43.	Effect of varying target atom ionization in the HCM model on secondary electron emission from the Xe^+ - Mo system - - - - -	92

44.	Effect of varying target atom ionization in the HCM model on secondary electron emission from the Ar ⁺ - Al system - - - - -	93
45.	Effect of varying target atom ionization in the HCM model on secondary electron emission from the Ar ⁺ - Al system - - - - -	94
46.	Effect of varying target atom ionization in the HCM model on secondary electron emission from the Ar ⁺ - Al system - - - - -	95
47.	Effect of varying target atom ionization in the HCM model on secondary electron emission from the Kr ⁺ - Al system - - - - -	96
48.	Effect of varying target atom ionization in the HCM model on secondary electron emission from the Kr ⁺ - Al system - - - - -	97
49.	Effect of varying target atom ionization in the HCM model on secondary electron emission from the Kr ⁺ - Al system - - - - -	98
50.	Effect of varying target atom ionization in the HCM model on secondary electron emission from the Xe ⁺ - Al system - - - - -	99
51.	Effect of varying target atom ionization in the HCM model on secondary electron emission from the Xe ⁺ - Al system - - - - -	100
52.	Effect of varying target atom ionization in the HCM model on secondary electron emission from the Xe ⁺ - Al system - - - - -	101
53.	Representative area KCl (100) - - - - -	103
54.	Representative area KCl (110) - - - - -	104
55.	Representative area KCl (111) - - - - -	105
56.	Potassium distribution of impact parameters in KCl - - - - -	106
57.	Chlorine distribution of impact parameters in KCl - - - - -	107
58.	SEE coefficient as a function of energy for KCl bombarded by Ar ⁺ ions - - - - -	108
59.	SEE coefficient as a function of energy for KCl bombarded by Ne ⁺ ions - - - - -	111

ACKNOWLEDGEMENT

I would like to thank Dr. Don E. Harrison, Jr. of the Naval Postgraduate School for his assistance in the preparation of this manuscript and for the many hours of conversation that resulted in a better understanding of the theories presented here. To my wife, Sarah, I express my sincere appreciation for her patience and understanding during the long hours spent in gathering data and writing this manuscript.

I. INTRODUCTION

Secondary electron emission is the release of electrons from target materials bombarded by primary ions. The first observation of secondary electron emission in 1889 was by Villard who noticed electrons being ejected from the cathode in a discharge tube. Secondary electron mission (SEE) is characterized by the coefficient of ion-electron emission, γ , which is defined as the number of electrons liberated per incident ion.

Secondary electron emission can be produced by two mechanisms, potential emission (PSE) and kinetic emission (KSE). Potential emission arises from the fact that as an ion approaches a target material it may become energetically feasible for a free electron to be emitted from the target surface either by Auger neutralization or Auger recombination. On the other hand, kinetic emission arises from the actual collision between the electrons of the impinging ion and the electrons in the target atom. In general, γ depends primarily upon the PSE mechanism at ion energies below one Kev and the KSE begins to contribute at ion energies above one Kev. Although this is a fairly good rule of thumb, variables such as the work function of the target material, ion charge, surface state of the target, target temperature, and whether the monocrystalline or polycrystalline nature of the target affect the value of the KSE threshold.

Medved et al. [1] have shown that potential emission from Ar^+ and Ar° on Mo increases with energy, with the total SEE at higher energies consisting partly of a KSE component and partly of a PSE component. In general there exists a transition region that is not sharply defined and for this reason it is felt that PSE contributes to secondary emission in the energy range above one Kev, even though the KSE should be the dominant emission mechanism in the one to ten Kev energy range. Both types of emission are investigated in this thesis.

II. STUDY OBJECTIVES

In 1964 Harrison, Carlston and Magnuson [2] proposed a single collision theory of secondary electron emission from monocrystalline target materials in the one to ten Kev primary ion energy range. The original paper develops a theory applicable to monocrystalline targets bombarded by inert gas ion beams directed normal to the (100), (110) and (111) crystal faces. This thesis will extend this theory to explain the following phenomena in the one to ten Kev primary ion energy range:

1. Secondary electron emission from a single crystal plane rotated arbitrarily about a crystallographic axis,
2. Secondary electron emission from metal single crystals, and
3. Secondary electron emission from alkali-halide monocrystals.

III. SECONDARY ELECTRON EMISSION THEORY

Secondary electron ejection mechanisms are either of the potential or kinetic type. Potential ejection can be caused by resonance neutralization, resonance ionization, Auger neutralization, or Auger de-excitation. Kinetic ejection requires the direct transfer of the ion's kinetic energy to the electrons of the target atom. Both mechanisms are discussed below.

Resonance neutralization occurs when it is energetically feasible for an electron in the target material to "tunnel" through its potential barrier and approach the position of the incoming ion. This stage of the process increases the energy of the ion and target atom system by an amount equal to the energy needed to remove an electron from the metal. This energy can range from near zero to ϕ , the work function of the target material. In the second stage of resonance neutralization, the electron and the ion combine, effectively at infinity, to reduce the system energy to an amount V_i , the ionization potential of the ion. This mechanism is not quite as simple as it seems, since it is affected by the image potential and coulombic forces of the electronic structure of the atoms in the crystal. According to the Franck-Condon principle, the electronic transition of the electron from the target material to the ion can only occur with appreciable probability when the position and velocity

of the ion are not affected by the transition. By this principle we expect a crossover of the initial and final potential energy curves of the system. Taking the image potential into account, resonance neutralization can occur for reasonable separations of ion and target atom when

$$(V_i - V_e) - \phi + I_s < W_a - \phi ,$$

and

$$(V_i - V_e) + I_s > \phi .$$

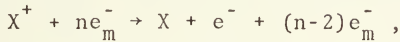
Therefore $\phi < (V_i - V_e) + I_s < W_a$,

where ϕ is the work function of the target material, V_i , the ionization potential of the ion, V_e , the excitation potential of the primary ion, I_s , the surface image potential and W_a , the initial kinetic energy of the primary ion.

The second possible potential ejection mechanism is resonance ionization which is essentially the reverse process of resonance neutralization. In resonance ionization an excited atom at infinity is ionized into an electron and an ion. The electron then proceeds to the metal surface and occupies any of the unfilled available states above the Fermi level of the metal. As in resonance neutralization, there is a range of ion-target atom separation for which the process is most likely to occur. There is also the possibility that a highly excited atom will be ionized very close to the target surface with a subsequent high probability that a secondary electron will be produced.

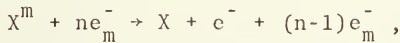
Although the above processes are possible, they are not the ones that make the largest contributions to secondary electron emission at low energies. Auger processes, which occur at distances of approach of 3 \AA or less, are the primary mechanisms contributing to PSE in the low Kev energy range. These can be summarized as follows [3]:

Auger neutralization:



and

Auger de-excitation:



where X^+ and X^m refer to the bombarding ion or metastable atom, respectively, and ne_m^- is the number of free electrons initially in the target material. In both cases, the final state of the system is such that a free electron and a neutral atom are produced. Auger neutralization occurs when the energy of the initial system, target and ion, is greater than the resulting system, $X + e^- + (n-2)e_m^-$, at infinite separation. Schematically the process is shown in Figure 1 [3]. Auger de-excitation, on the other hand, involves a metastable atom which approaches the target material. As a result, the initial energy curve, shown in Figure 2 [3], is not modified by an image potential and hence the initial and final energy states never cross.

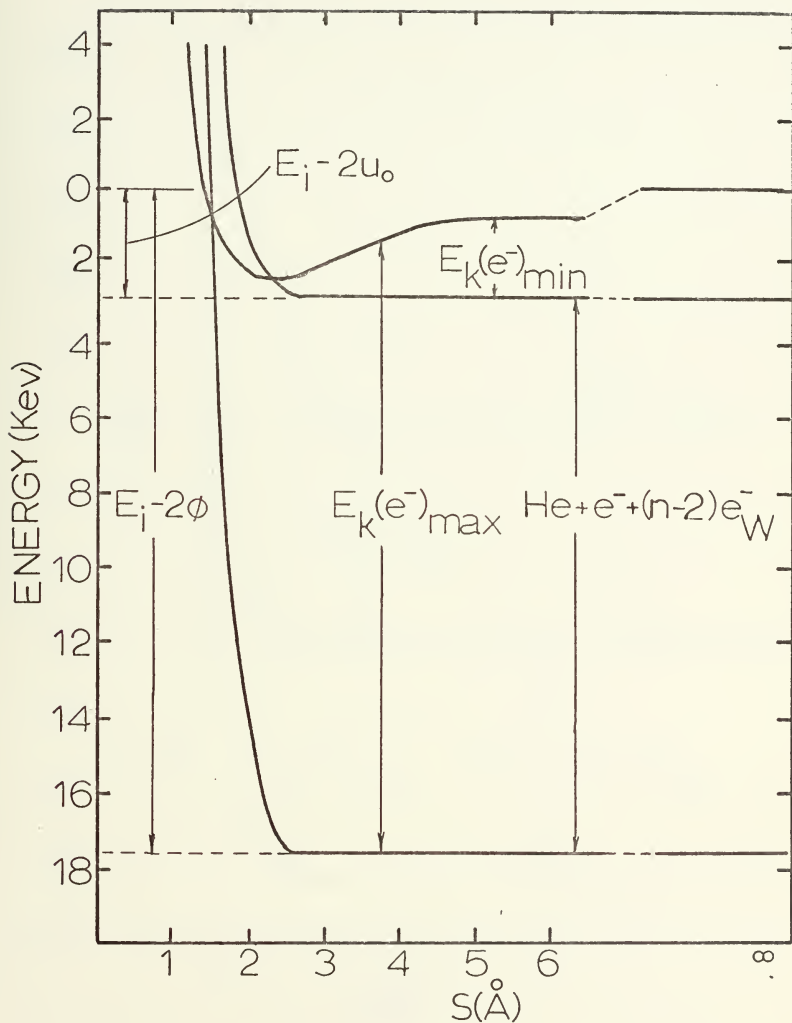


Figure 1. Potential energy diagram for a helium ion as it undergoes Auger neutralization at a tungsten surface (3).

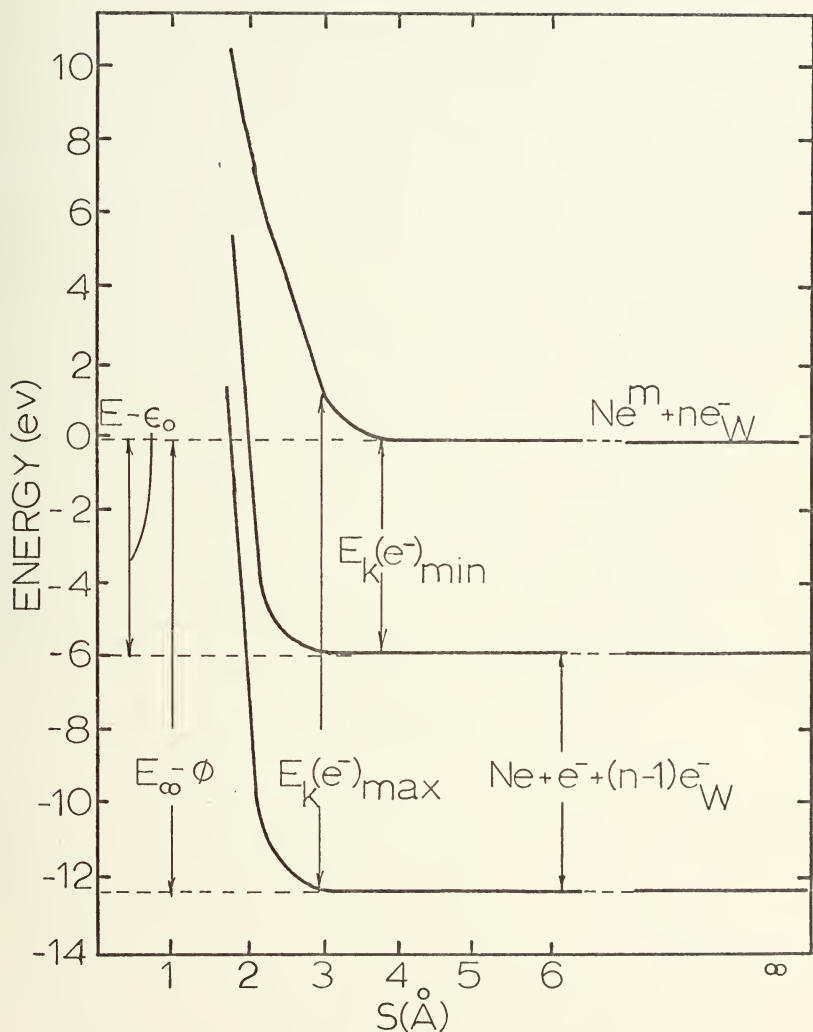


Figure 2. Potential energy diagram for a metastable atom (He) as it undergoes Auger de-excitation at a tungsten surface (3).

These two processes, to a great extent, account for low energy (ev range) secondary electron emission.

Kinetic emission is the result of the direct transfer of the incoming ion's kinetic energy to the atom's electrons. Part of this energy is absorbed in the recoil of the atom, while some of the remaining energy is transferred to the electrons of both the ion and target atom, causing an excitation of both of their electronic structures. As the two nuclei separate, some of the perturbed electrons are liberated as secondary electrons. The ion and recoiling target atom are slowed down within the crystal structure of the target material and are likely to undergo Auger neutralization or de-excitation. If this process occurs sufficiently close to the surface of the target material, there is a probability that these electrons also will escape from the target materials surface and contribute to kinetic secondary electron emission.

IV. THEORIES CONCERNING SECONDARY ELECTRON EMISSION

A. THEORY OF PARILIS AND KISHINEVSKII

Of all the theories proposed to explain kinetic secondary electron emission, the theory of Parilis and Kishinevskii (PK) seemed to be one of the most promising [4]. PK divided the secondary electron emission problem into two separate subproblems which were analyzed separately and subsequently collated to develop the theory of KSE. These two subproblems included:

1. The search for a sufficiently effective mechanism of transfer of the kinetic energy of a moving particle to the (target) electron; and
2. The description of the yield of excited electrons from the target. [4]

PK assumed that the solution to the first problem was of the form proposed by O. B. Firsov for inelastic scattering of ion-atom collisions in the Kev range [5]. Secondly, PK visualized the secondary electron emission process as one in which the primary ion ionizes many atoms as it progresses along its trajectory in the crystal. Electrons produced in this manner, or by further ionization of the primary ion, then proceed to the surface suffering collisions and energy losses as well as possible capture in route. The combination of the electron production phase and the electron escape phase then yields the KSE from the crystal.

The actual collision between the ion and the atom was seen by PK as being accompanied by an overlap of the

electron shell structure of the two collision partners, during which time there occurred an electronic interaction. Energy was transferred between colliding particles, exciting their electrons to a higher energy state. To calculate this excitation energy, a statistical picture of the electron distribution of the particles was used. The theoretical relationship, based on the Thomas-Fermi (TF) model of the atom, leads to the following formula for the energy transferred between the colliding particles:

$$E = \frac{m^2 e^2}{4\pi^2 \hbar^3} \int (\int_S \phi^2 dS) \dot{\underline{R}} \cdot d\underline{R} ,$$

where \underline{R} is the radius vector connecting the centers of the colliding particles, S is the surface separating the domain of action for the potential of the two particles, and ϕ is the potential on this surface given by:

$$\phi = \left[\frac{(Z_1 + Z_2)e}{r} \right] \chi \left[\frac{1.13(Z_1 + Z_2)^{1/3} r}{a_{TF}} \right] ,$$

where Z_i is the charge on each particle, $a_{TF} = \hbar^2/mc^2$ and χ is the TF screening function [8]. Physically, the interaction can be thought of as analogous to the collision of two tennis balls. As they impact, both deform, with the vector joining their centers being perpendicular to the area S of the plane of interaction which separates them. Obviously the total energy transferred is a function of the relative velocity with which the ion and atom impact and

the electron distribution associated with each. In terms of the tennis ball analogy, the greater the relative impact velocity, the larger the deformed area S , the shorter the radius vector distance \underline{R} , and the greater the number of electrons involved.

The analysis was rewritten by PK in terms of the impact parameter associated with the collision. Hence by changing variables

$$E(p) = \frac{\hbar u_0}{\pi a^2} (Z_1 + Z_2)^2 \int_{R_0}^{\infty} \frac{(1 - V(r))}{\left[1 - \frac{V(r)}{E} - \frac{p^2}{R^2}\right]^2} dR$$

$$\int_{R/2}^{\infty} \frac{\chi^2(\rho)}{\rho} d\rho,$$

where u_0 is the initial velocity of the ion, E is the excitation energy of the colliding particles, p is the impact parameter and $V(r)$ is the potential of repulsion between the particles.

To obtain the correct behavior of the emission curve, the cross section of electron ejection into the conduction band had to be calculated. Because more than one electron may be lifted from the valence band to the conduction band, the cross section was determined to be

$$\sigma = \sum_p (\text{constant}) \cdot (\text{Probability of ionization}) \cdot (\text{Impact parameter})$$

which in the integral limit approaches

$$\sigma = 2\pi \int_0^{P_1} \frac{E(p)}{J} p \, dp .$$

Here P_1 is the impact parameter at which $E(P_1) = \delta - \phi$, where δ is the energy depth of the filled conduction band, ϕ is the work function of the target material and J is the average ionization potential for the outer shells of the atom. For $1/4 < Z_1/Z_2 < 4$ PK found the cross section to be given by

$$\sigma(u_0) = \frac{1.39 \, a_{TF} \, h}{J} \frac{(Z_1 + Z_2)^2}{(Z_1^{1/2} + Z_2^{1/2})^2} S(u_0)$$

and $S(u_0)$ is approximated by

$$S(u_0) = 5.25 \, u_0 \, \arctan (.6 \times 10^{-7} (u_0 - u_{\min})) ,$$

where u_{\min} is the threshold velocity. After determining the probability that an electron will be promoted from a filled band to the conduction band, PK assumed that most of these electrons remained in the conduction band because of the surface potential of the metal target. However, because a hole is left in the valence band, an Auger recombination is possible with subsequent emission of an electron from the metal. The probability that this process occurs is given by PK as

$$w(\delta) = 0.016 (\delta - 2\phi) .$$

PK assumed that both PSE and KSE were due to Auger processes [4].

After the secondary electrons have been produced, they suffer collisions as they proceed to the surface of the metal. These collisions degrade their energy and increase the probability that they will be lost through recombination. PK assumed that the number of electrons which reach the surface is given by an exponential law of the form $\exp(-x/\lambda)$ where x is the depth at which the electrons are formed in the crystal and λ is the mean free path of the electrons in the material. Specifically, the number of electrons emitted per ion incident on the surface is given by

$$\gamma = \sum_x \left(\begin{array}{l} \text{Number of atoms} \\ \text{per cubic centi-} \\ \text{meter} \end{array} \right) \cdot \left(\begin{array}{l} \text{Prob. that an electron} \\ \text{will be ejected into} \\ \text{the conduction band} \\ \text{and a hole left in} \\ \text{valence band} \end{array} \right)$$

$$\cdot \left(\begin{array}{l} \text{Prob. that an electron} \\ \text{will escape to the} \\ \text{surface of the crystal} \end{array} \right)$$

which in the limit goes to

$$\gamma = \int_0^{X_n} N \sigma(u) w(\delta) \exp(-x/\lambda) dx ,$$

where X_n is the maximum depth at which the ion retains sufficient energy to ionize a target atom. Upon taking into account the degradation of energy of the primary ion as it suffers multiple collisions and the diffusion cross

section of the electrons, PK arrived at the final expression for γ :

$$\gamma = N w(\delta) \lambda [\sigma(u_o) - \Delta\sigma(u_o)] ,$$

where

$$\Delta\sigma(u_o) = \exp(-u_o/(K\lambda)) \int_{u_{\min}}^{u_o} \exp(u^2/(K\lambda)) \frac{d\sigma(u)}{du} du$$

and

$$K = \frac{2.48\pi N \cdot a_{TF} e^2 Z_1 Z_2}{(M_1 + M_2) (Z_1^{1/2} + Z_2^{1/2})^{2/3}}$$

The PK theory predicts the following trends [3]:

- "1. Low velocity region: $u_o = u_{\min}$, $\Delta\sigma(u_o)$ term is important..., γ increases slowly with u_o , $(\sigma(u_o) - \Delta\sigma(u_o)) = u_o^2 - (3/2 u_{\min})^2$. Hence initially $\gamma \propto u_o^2$, i.e., γ is a linear function of energy...
2. High velocity region: $(\sigma(u_o) - \Delta\sigma(u_o)) = u_o \tan^{-1}(.6 \times 10^{-7} (u_o - u_{\min}))$. This expression asymptotically approaches the straight line $\sigma(u_o) = c(u_o - u_{\min})$ and therefore increases linearly with velocity. Extrapolating the linear portion back to $\sigma(u_o) = 0$ a value of the intercept $u_1 = 1.05 \times 10^7$ cm/sec is obtained; this is independent of ion target combination.
3. Very high velocities: Here ion penetration depths are greater so that electrons are formed further

from the surface. The number escaping to the surface and therefore the yield is expected to pass through a maximum. This is confirmed experimentally.

4. No yield dependence on ion charge is predicted.
5. A dependence of yield on the ion target combination of the form $((Z_1 + Z_2)/(Z_1^{1/2} + Z_2^{1/2}))^2$ for heavy ions and $((Z_1^{1/2} + Z_2^{1/2})(Z_1^{1/6} + Z_2^{1/6})^3)$ for light ions. If the term $\Delta\sigma(u_0)$ is important...the yield is independent of ion-target combination to a first approximation.
6. Dependence of yield on the angle of incidence θ is expected to be of the form $\gamma_i = \sec \theta$ since the probability of electron escape is a function of the shortest distance to the surface and the probability of formation of electrons is a function of the actual distance traversed.
7. The effect of the isotopic mass on yield is anticipated to be connected with the different retardation rates for the isotopic pairs." [3]

All of these conclusions are approximately confirmed by the experimental results.

B. THE THEORY OF HARRISON, CARLSTON AND MAGNUSON

The PK theory uses many simplifying assumptions which introduce approximations into the results obtained. In

particular, the PK theory predicts secondary electrons of only average energy, two to five ev, and data obtained by Wolff [6] of SEE from copper bombarded by ten Kev argon ions indicates some secondary electrons emitted have energies greater than 140'ev.

In the PK theory secondary electron emission was viewed as a two-step process in which ions were first produced along a path in the target material and subsequently diffused to the surface with possible scattering or Auger emission occurring along the path. This model does not yield the high-energy secondary electrons which are reported experimentally. In an effort to explain this discrepancy between experimental and theoretical result, Harrison, Carlston and Magnuson [2] (HCM) proposed a "single collision" theory of secondary emission. This theory, though in many respects similar to the PK theory, has as its basic philosophy an electron production mechanism which differs from the model proposed above.

HCM proposed a model in which an ion approaching a target surface first undergoes resonance neutralization and subsequently collides with the first layer of atoms in the target material in the un-ionized state. Even though the primary particle is neutralized before the collision, the terminology of "ion" is retained here to distinguish between the primary particle and the target atom after collision. For simplicity HCM assumed that the electrons liberated due to the inelastic energy transferred between the electronic structures of the

ion and the atom all come from the ion, which allowed them to ignore the energy partition between collision partners. Theoretical work by Harrower [7] indicates that the Auger process requires a time on the order of 10^{-14} seconds while in the one to ten Kev energy range the collision process takes on the order of 5×10^{-14} seconds. This indicates that, statistically, the ion usually does not have time to neutralize before its next collision and for all practical purposes cannot contribute further to the secondary electron emission process. These results lend credence to the single collision model. Mathematically HCM proposed:

$$\gamma_{\text{KSE}}^{(\text{hkl})} = K \int_0^{s_{\text{MAX}}^{(\text{hkl})}} n_e(s, E_{\text{TFF}}) P^{(\text{hkl})}(s) ds ,$$

where $\gamma_{\text{KSE}}^{(\text{hkl})}$ is the number of electrons emitted per incident ion when the ions are normally incident upon the (hkl) surface; s is the impact parameter of the ion on the atom; E_{TFF} is the inelastic energy transfer between the ion and the atom; $n_e^{(\text{hkl})}(s, E_{\text{TFF}})$ is the number of electrons this energy will produce; and $P^{(\text{hkl})}(s)$ is the probability that the impact parameter s will occur in the (hkl) surface. This equation contains three adjustable parameters, the constant K and two constants which enter into the calculation of ϕ , the electron density, and the interaction potential $V(r)$. By symmetry, these last two constants must be the same for all orientations of the particular crystal plane, (hkl), in question.

According to HCM, the constant K is a factor which accounts for three physical processes:

1. The probability that an electron will be emitted from the surface (a value close to 1/2);
2. The probability of additional emission by an Auger process; and
3. The probability that a high energy electron escapes before it is scattered back into a conduction band. [2]

All of these processes are orientation independent. The factors which appear in the formulation of the HCM secondary electron emission equation are discussed in detail below.

1. The Inelastic Energy Transfer

In the HCM theory E_{TFF} is the inelastic energy transferred in the collision process and is basically the same as $E(p)$ in the PK theory. However, as HCM point out, because the interaction involves atoms spaced regularly in a lattice array, the inelastic energy integral does not have an infinite upper limit as was assumed by PK. Specifically,

$$E_{\text{TFF}}(s, E_0) = K_{\text{TFF}} \int_{r_{\min}}^{r_{\max}} \frac{(1-V(r)/E_0) dr}{(1-V(r)/E_0 - s^2/r^2)^{1/2}}$$

$$\cdot \int_{r/2}^{r_{\text{EM}}} \phi^2 \frac{(\rho) d\rho}{\rho}$$

where

$$K_{\text{TF}} = \frac{h}{\pi a_H} (E_0 / (2m_1))^{1/2} (Z_1 + Z_2)^2 ,$$

$$a_H = h^2 / (me^2) = .529 \text{ \AA}$$

and E_0 is the energy of the ion in the center of mass system; Z_1 and Z_2 are the ion and atom nuclear charges, respectively; r_{\min} is the distance of closest approach; and ϕ is the Thomas-Fermi (TF) screening function:

$$\phi(\rho) = [1 + (a_F \rho)^{0.8034}]^{-3.734}$$

where

$$a_F = \frac{a_{\text{TF}}((Z_1 + Z_2)/144)^{1/3}}{0.8853}$$

and a_{TF} is one of the adjustable constants introduced above. By experimenting with different sets of potentials, in conjunction with the screened electron distribution, HCM found that the best agreement with experiment was obtained when the potential $V(r)$ was of the Born-Mayer form [2]:

$$V(r) = \exp(A + Br) = A' \exp(Br)$$

with B always negative, and where A is the second of the above mentioned arbitrary constants. HCM referred to the integral containing dp as the electron integral. The convention is retained here.

Several important results were noted by HCM in the formulation of their original model. First, the dynamical integral was extremely sensitive to its upper limit $r_{\max}^{(s)}$, whereas the electron integral was not sensitive to variations in r_{EM} . For this reason r_{EM} was set at a value somewhat larger than the nearest neighbor distance R_o , in the crystal lattice, and retained this value for all orientations of the crystal lattice. On the other hand, the upper limit of the dynamical integral was extremely sensitive to the nearest neighbor distance. Such a behavior is expected because as each ion collision with a particular atom terminates, another must begin with one of its neighbors. From a particle dynamics point of view, HCM found that by treating the actual collision with the lattice as a binary collision between the incoming ion and any single atom within the first repeat distance of the crystal plane, the theory yielded results which approximated those obtained by experiment. Figure 3 indicates the geometrical relationship between various quantities associated with the dynamical integral [2].

2. Collision Parameters

Because of the repetitive nature of the lattice, or lattice plane, it is not unreasonable to think of a "representative area" which characterizes the lattice plane as a whole and hence its distribution of impact parameters. If no lattice were present, and only one target atom, there would be no characteristic area and the occurrence of a

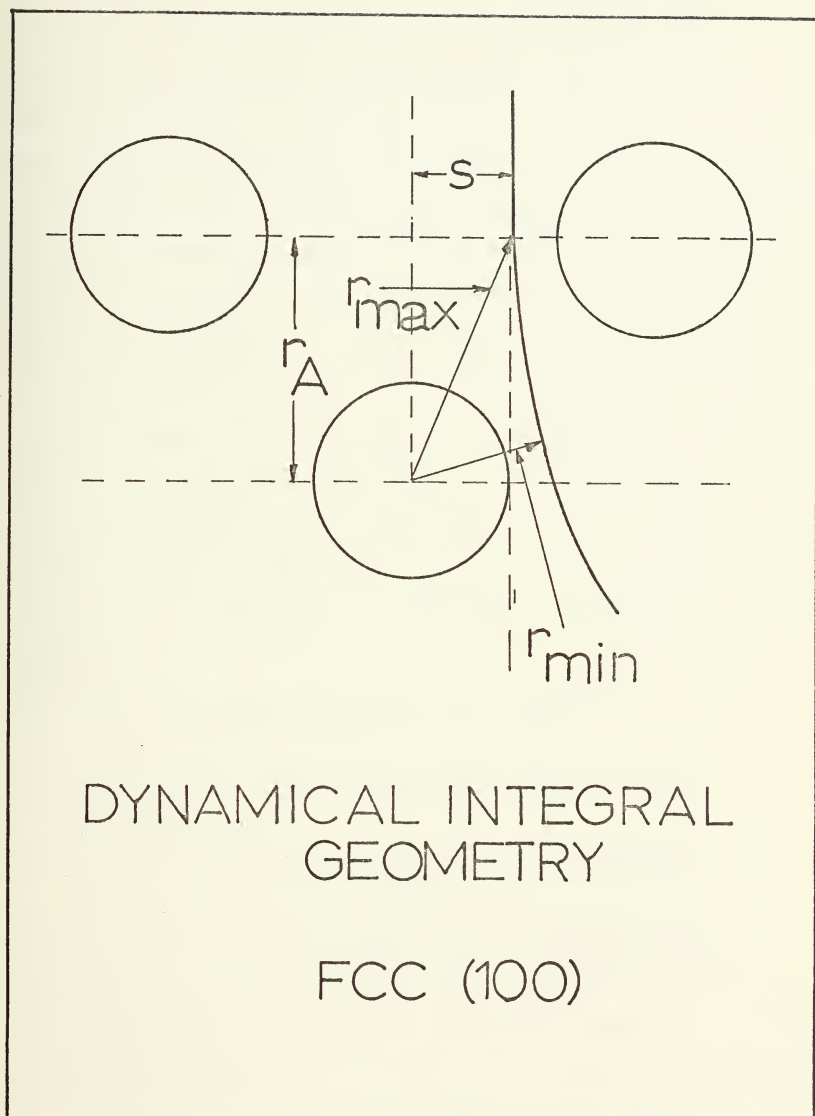


Figure 3. Relationships between various quantities appearing in the Dynamical Integral.

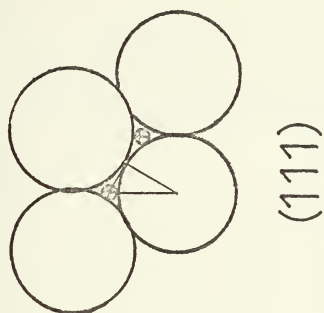
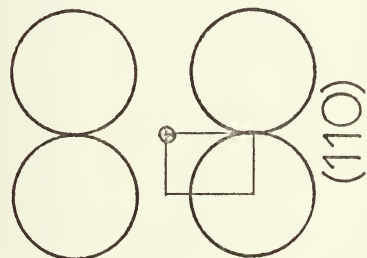
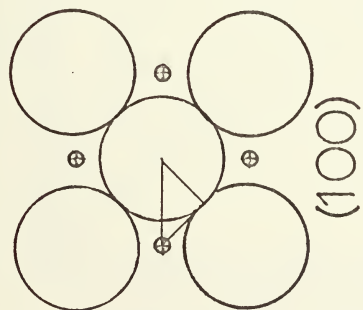
collision with any impact parameter would be possible, yielding an infinite collision cross section. As an ion approaches a plane of atoms in a crystal, however, there exists an allowable set of impact parameters for the ion-atom collision. Specifically, in a lattice there exists an impact probability distribution, $p^{(hkl)}(s)$, for each crystal orientation. For normal incidence HCM proposed the areas shown in Figure 4. These areas are representative of the normal impact of an ion with any atom on the specified crystal surface, viz., by symmetry operations they fill plane space and are representative under any of these symmetry operations of what an ion "sees" as it approaches the planar surface normally. There are many distributions which could be considered probability distributions. HCM considered the following:

1. The distribution of values of s measured to the nearest surface atom;
2. The distribution of all values measured to all atoms which project their area into the representative area;
3. The distribution of smallest impact parameters when all atoms are considered [2].

The third case was the only one which yielded results in agreement with the experimental data. The distributions for normal incidence on FCC and BCC metal targets are shown in Figures 5 and 6.

Operationally, the distributions are determined as follows: First, the representative area is chosen. "Points" are shot at the representative area, and the distances

FACE CENTERED CUBIC



BODY CENTERED CUBIC

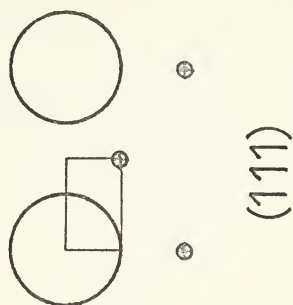
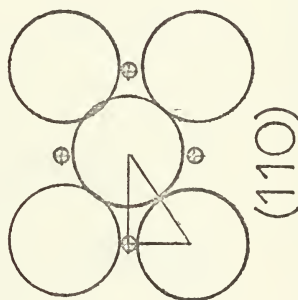
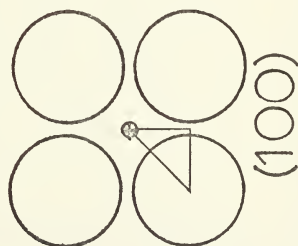


Figure 4. Representative areas for normal incidence.
After (2).

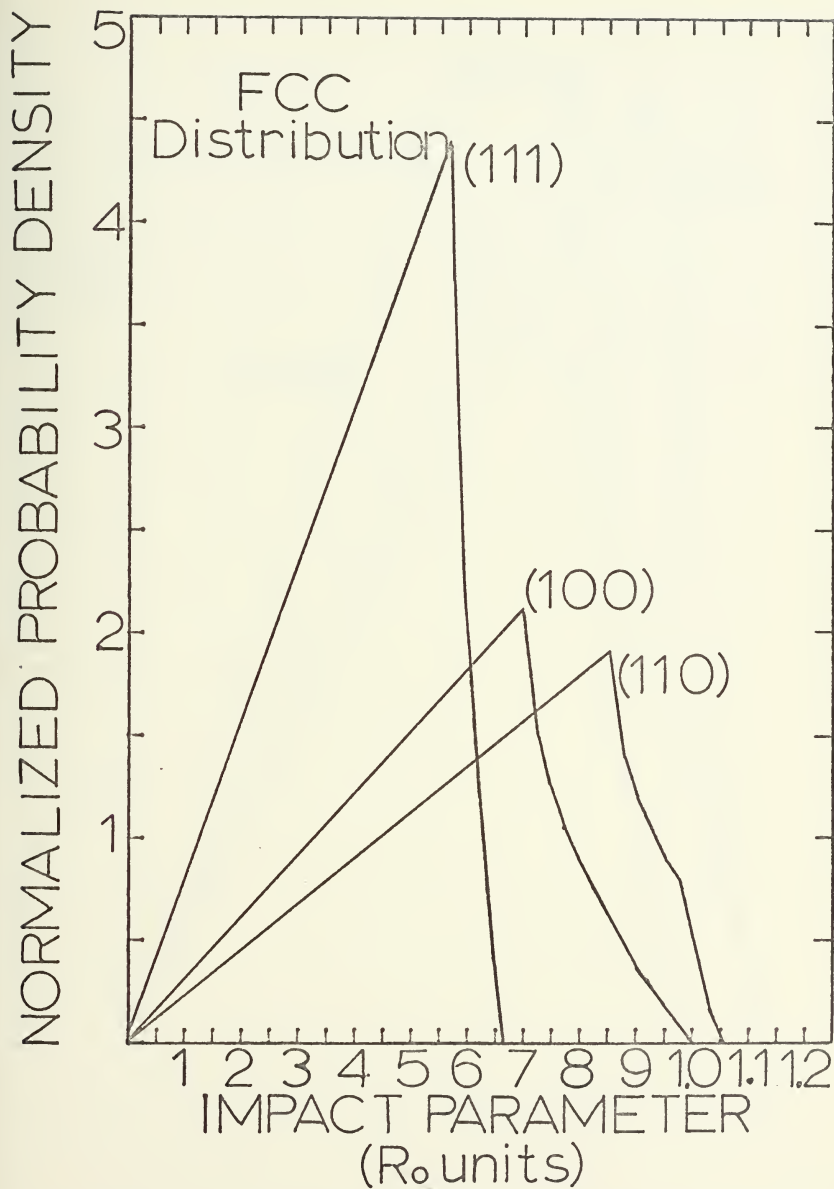


Figure 5. Distribution of impact parameters for normal incidence on face-centered cubic crystals.

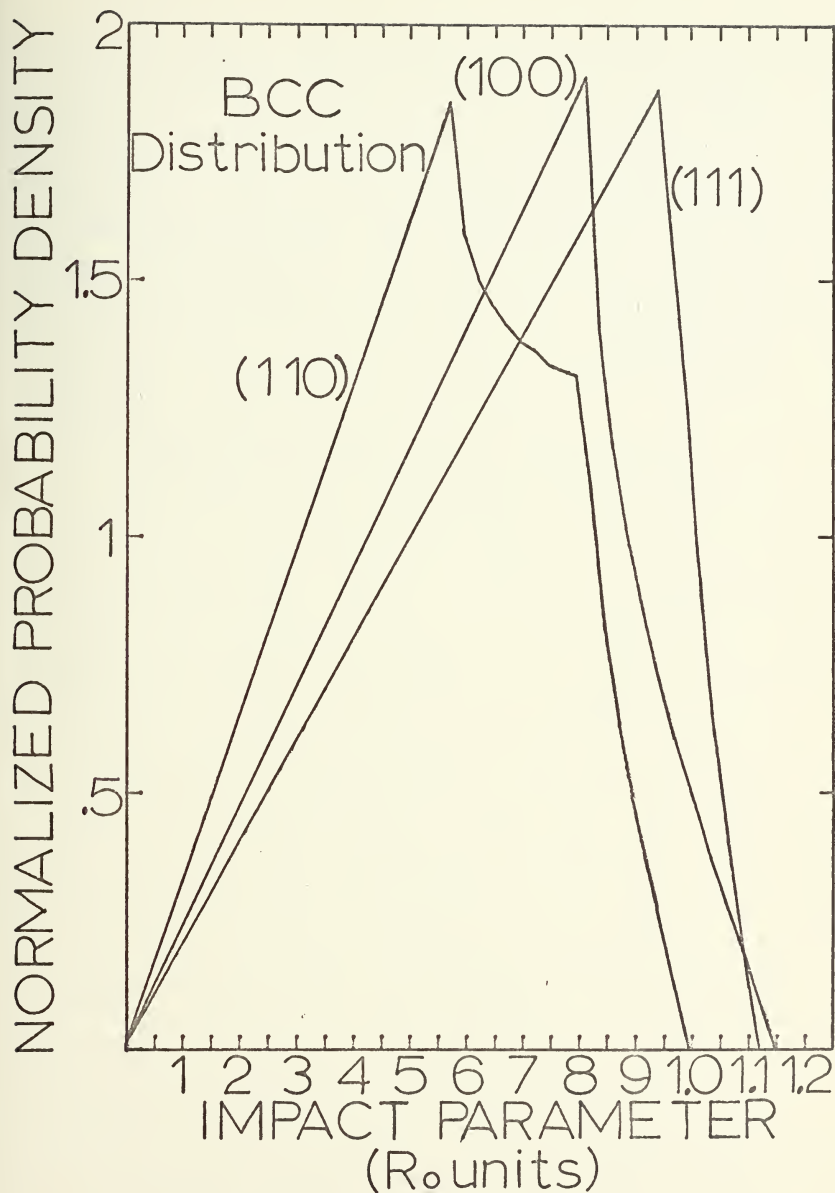


Figure 6. Distribution of impact parameters for normal incidence on body-centered cubic crystals.

between the impact point and the centers of the atoms lying in the representative area are measured. For each atom the distances for points that are measured to be closest to it are tallied. After a sufficient number of points are tallied to yield good statistics, the distribution for each atom is weighted by a factor to account for the fractional portion of atom lying in the representative area. The atoms' distributions are then added and scaled so that the total area under the resulting curve is unity.

3. Number of Electrons Emitted--Russek Model

One of the major shortcomings of the PK theory was that it used average ionization energies to obtain an ionization cross section. This is to say the PK theory did not consider the electronic structure of the target atom. HCM adopted a model proposed by Russek [9] to obtain the number of electrons liberated per collision, $n_e^{(hk\ell)}(s, E_{TFF})$. In his original paper, Russek proposed two ionization models of interest, the uniform ionization model (UI), and the staggered ionization model (SI). The UI model assumed that as electrons were liberated by the collision process, the amount of energy required to liberate any one electron was the same as that required to liberate any other electron. On the other hand, the SI model assumed that each electron liberated required more energy than was required to liberate the preceding electron. For the SI case Russek shows that the probability that n electrons will be liberated from a shell, which contains M electrons is given by:

$$P_n^{(M)} \sim \binom{M}{n} \sum_{i=0}^k (-1)^i \binom{M-n}{i} \left(\frac{1 - n E_n^{\text{ION}} + i E_{n+1}^{\text{ION}}}{E_{\text{TFF}}} \right)^{M-1}$$

where $k \leq (E_{\text{TFF}}/E_{n+1}^{\text{ION}} - n E_{n+1}^{\text{ION}}/E_{n+1}^{\text{ION}}) \leq k+1$ and M is the number

of electrons available in the outermost shell of the atom;

E_n^{ION} is the energy required to remove the n^{th} of these electrons and E_{TFF} is the energy available to cause this

removal. Two things should be noted. First, the impact parameter enters this calculation through the inelastic energy transfer. Second, when $E_{n+1}^{\text{ION}} = E_n^{\text{ION}}$ one obtains

the UI model. After normalizing the function, $P_n^{(M)}$, viz.,

$$\sum_{n=0}^N P_n^{(M)} = 1$$

then, from probability arguments, the number of electrons liberated is:

$$\overline{n_e(E_{\text{TFF}})} = \sum_{n=0}^M P_n^{(M)} n_e.$$

HCM were unable to obtain good results with the Russek UI model. In all cases, γ increased much too rapidly as a function of energy. On the other hand, the SI model yielded reasonably good results, where spectroscopic values for E_n^{ION} were used.

4. HCM Results

HCM investigated the Ar - Cu system in detail.

They first examined the E_{TF} dynamical integral for various types of potential functions and found that the PK potential which was of the Thomas-Fermi-Firsov type was too hard for small values of E_0 , viz., the hard core radius of the target atom was too large, in this energy range, to yield acceptable results. Attempts at softening the potential by decreasing a_{TF} failed. For this reason HCM assumed a potential function of the Born-Mayer type. The potential function used in each case was found by matching the exponential to the TF screening function at some separation.

HCM assumed that the experimental data contained both potential, γ_{PSE} , and kinetic, γ_{KSE} , contributions to the total secondary electron emission coefficient. Therefore, HCM identified the γ at which KSE begins to contribute as γ_{PSE} and assumed this value remains constant for all energies. This value for γ_{PSE} was then subtracted from the experimentally determined γ for the (111) surface at 10 Kev. The (111) value of γ_{KSE} at 10 Kev, obtained from theory, was scaled to this point, and all other points were multiplied by the scale factor used in performing this operation. Finally the constant value of γ_{PSE} was added to all the scaled theoretical values. The result is the HCM value for the total secondary electron emission. The results of the HCM theory for the Ar^+ - Cu system are presented in Figure 7.

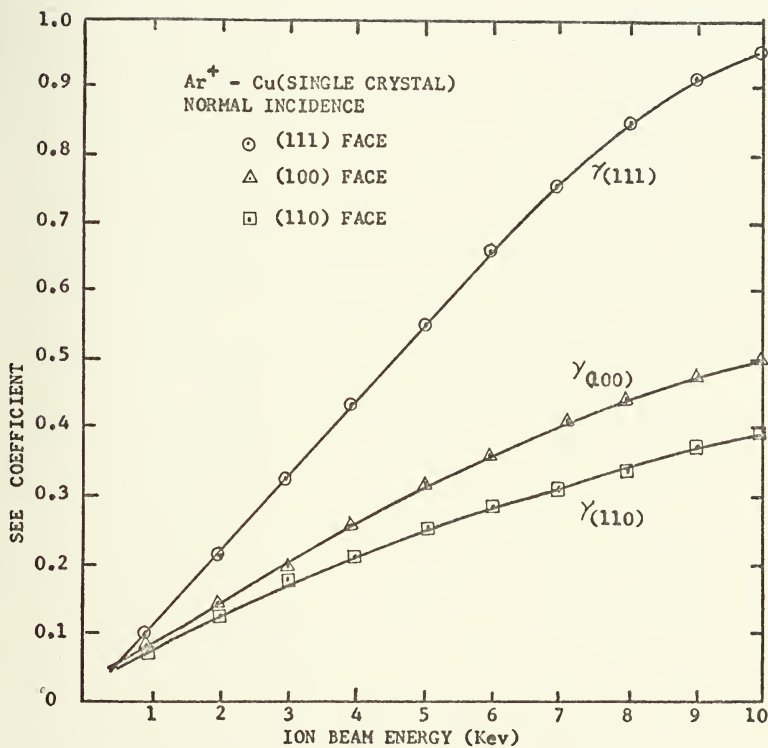


Figure 7. Ar⁺ - Cu results obtained from the HCM original model. Taken from (2).

In general, HCM's theory agrees reasonably well with experimental results for all systems studied except Ar - Mo.

V. MODIFICATIONS TO THE HCM THEORETICAL MODEL

A. INTERATOMIC POTENTIAL

Independent of the philosophy behind the basic interaction, the HCM theory, like the PK theory, is highly dependent on two specific assumptions. First, both assume that the inelastic energy transferred is of the form proposed by Firsov. Second, both theories must assume an interatomic potential function which is consistent with the electron distributions of the ion and atom. Since the Firsov model is presently the only comprehensive model available for the inelastic energy transfer, it has been retained here as an approximate model of the inelastic collision process and is assumed to be sufficiently accurate for our purposes. However, the interaction potential used in the Firsov model need not be of the Thomas-Fermi form, but may be derived from a more accurate representation of the electron distributions of the ion and atom.

The interaction potential is derived from the electron distributions of the collision partners. These potentials exist on three general levels of sophistication: (1) The Bohr and Born-Mayer potentials which are derived from electron distributions which provide screening of the nucleus in a self-consistent, but not necessarily accurate, manner; (2) Thomas-Fermi and Thomas-Fermi-Dirac potentials which are derived from statistical pictures of the electron

distributions of the collision partners; and

(3) Potentials generated from electron densities derived numerically from Schroedinger's equation.

Parilis and Kishinevskii used a Thomas-Fermi potential function in the theory they proposed. Statistical models of the atomic electron distribution, such as in the TF model, are based on studies of inhomogeneous gases and approximate solutions of Schroedinger's equation consistent with this picture [10, 11]. They require that the total electron energy be a minimum and that the electron density integrate to the total number of electrons in the system. Approximations may be made to evaluate the exchange and correlation energies. When the exchange and correlation energies are omitted and the kinetic energy is approximated by a plane wave, the TF atomic model results [11]. If the exchange energy is retained and the kinetic energy is approximated by a plane wave, the TFD atomic model results [11]. The TF model of the atom has been used extensively by Firsov, whereas the TFD model appears in papers by Abrahmson [13].

Potential functions based on Hartree-Fock solutions of the atomic Schroedinger equation have been discussed by Wedepohl [12], Harrison [13], and Wilson [14]. These potentials assume the adiabatic approximation, use spherically symmetric electron distributions which have shell structure, and take into account the correlation,

kinetic and exchange energies through various approximations. They appear to lead to improved calculations of the interaction potential [8, 14, 15]. The present investigation utilizes an interaction energy calculation similar to that proposed by Wedepohl [12]. However, the electron densities from which the potential is derived are calculated from the Hartree-Fock-Slater self-consistent wave functions calculated from the Herman-Skillman [16] computer program. The reader is referred to the original book [16] for detailed information on the calculation of the atomic electron distribution functions and to the work by Torrens [8] for a general discussion of the interaction potential.

B. THE BASIC INTERACTION

Harrison, Carlston and Magnuson assumed that all of the secondary electrons produced in the single collision model came from the ion. This assumption was tested by choosing various values of E_n^{ION} in the Russek model and noting the dependence of $n_e(E_{\text{TFF}})$ on E_1^{ION} . This experiment was carried out for the $\text{Ar}^+ - \text{Cu}$ system. The results were most favorable for E_1^{ION} equal to 15.8 eV, the first ionization potential of argon, and least favorable for neutral copper's first ionization potential. This approximation was an attempt to simplify the model so that detailed models of energy sharing mechanisms could be avoided. In this present investigation, this assumption has been relaxed to include contributions to the secondary emission by the target atom.

Theoretically, the interaction is viewed as the collision of two atoms having spherically-symmetric, shell structured electron distributions. As the atoms collide, they are assumed to form a "molecular" structure whose electron ionization potential distribution is comprised of the separate ionization potentials of the electrons of the atoms involved in the collision. Since electrons are ejected on a "least energy" principle, the values of E_n^{ION} used in the Russek model have been modified by include both primary ion and target atom ionization energies which are arranged in increasing order of magnitude, irrespective of the atom to which they belong. The mean number of electrons is a complicated function of the inelastic energy transfer and the energy necessary to effect each electron's removal.

C. THE DISTRIBUTION OF IMPACT PARAMETERS

To accomplish the objectives of this present investigation, one additional modification to HCM's original paper had to be made. Since the angular dependence of γ was to be studied, a new distribution of impact parameters had to be calculated. Fortunately, according to the HCM paper, this modification to the mathematical model is the only change required to take into account rotations of the crystal plane around an arbitrary crystallographic direction. No other factor entering into the secondary electron emission equation is orientation dependent [2].

Two possible solutions to this problem are proposed below. First, a crystal plane normal to the direction of incidence of the ion beam can be found, from which a representative area can be constructed. Such a formulation would be analogous to cutting the crystal in such a manner that it presented a planar area normal to the incident ion beam and finding an area on this plane which would be representative of that orientation. Alternatively, a representative area constructed from the crystal face which was experimentally rotated can be used and mathematically rotated about the specified crystallographic axis. In practice, the first method is computationally restrictive because it requires that a representative area on a plane normal to the incident ion beam be found for each orientation. For this reason it is not pursued further here.

The second method mentioned above yields a result that is more in line with the reasoning behind HCM's original definition of the distribution of impact parameters. Practically speaking, a representative area is found for each crystal face which fills plane space and is representative of what an ion sees as it approaches the crystal plane from an arbitrary direction. Unlike the representative areas for normal incidence, angularly dependent representative areas must be truly representative for all possible rotations of the plane and not simply for one particular orientation. The representative area for the FCC (100) surface which can be rotated in either a positive or negative

sense about the $\langle \bar{1}10 \rangle$ crystallographic axis is shown in Figure 8. Note that atoms which lie within the first repeat distance of the crystal plane are eligible target atoms in the representative area by HCM's definition of representative area. Also note that these atoms from the lower atomic plane appear to move as the crystal plane is rotated in a positive sense about the $\langle \bar{1}10 \rangle$ axis (see Figure 9). This behavior can be verified by physically rotating a stick and ball model of the lattice structure about the indicated axis.

Once the representative area is chosen, its rotational properties and corresponding distribution of impact parameters are calculated as follows. The representative area is placed in the first quadrant of a rectangular coordinate system (x,y) (see Figure 10). In this system, the crystallographic axis of rotation is specified by two parameters:

1. The angle of the crystallographic axis makes with the x-axis of the rectangular coordinate system (x,y) ; and
2. The y-axis intercept of the crystallographic axis in the rectangular coordinate system (x,y) .

This system of coordinates is then transformed into a primed rectangular reference frame (x',y') for which the crystallographic axis of rotation is the x' -axis, and whose origin is the point at which the crystallographic axis intercepts the y-axis, (x_R, y_R) (see Figure 10). The equations relating the transformation of points from the (x,y) coordinate

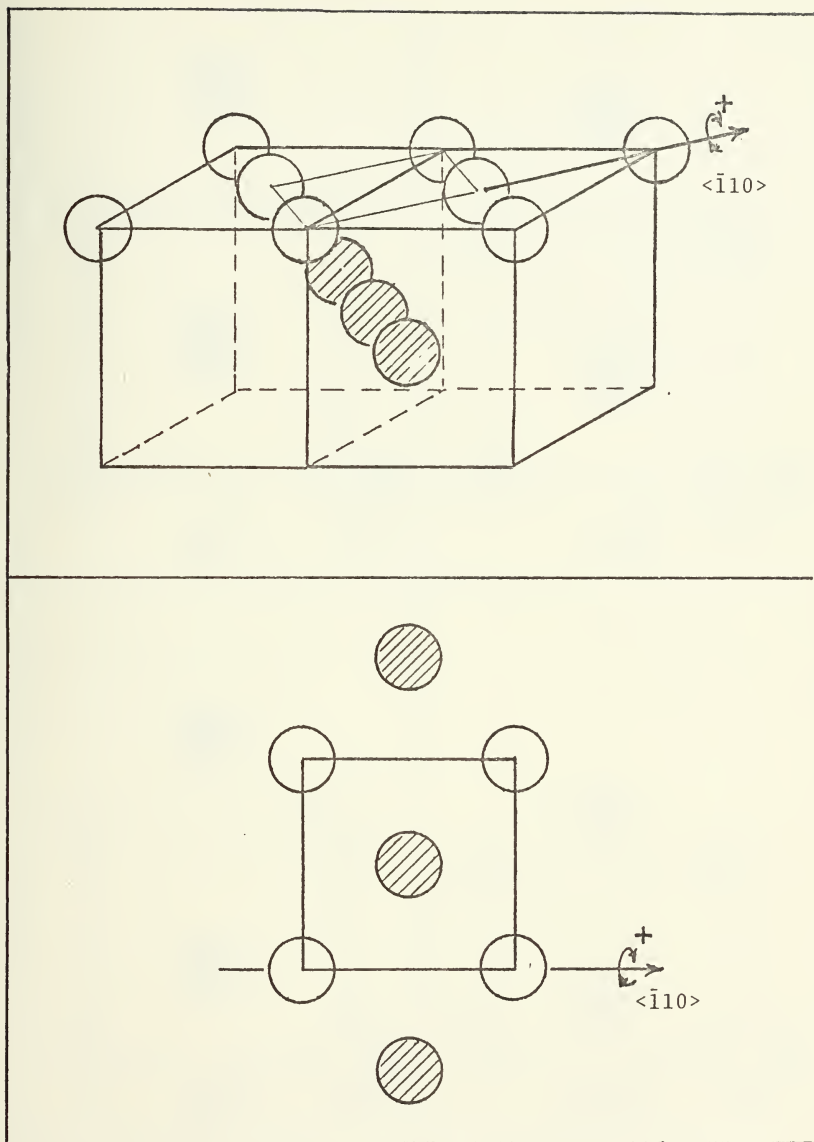


Figure 8. Representative area of a (100) FCC crystal face rotated about $\langle \bar{1}10 \rangle$ in either a positive or negative sense.

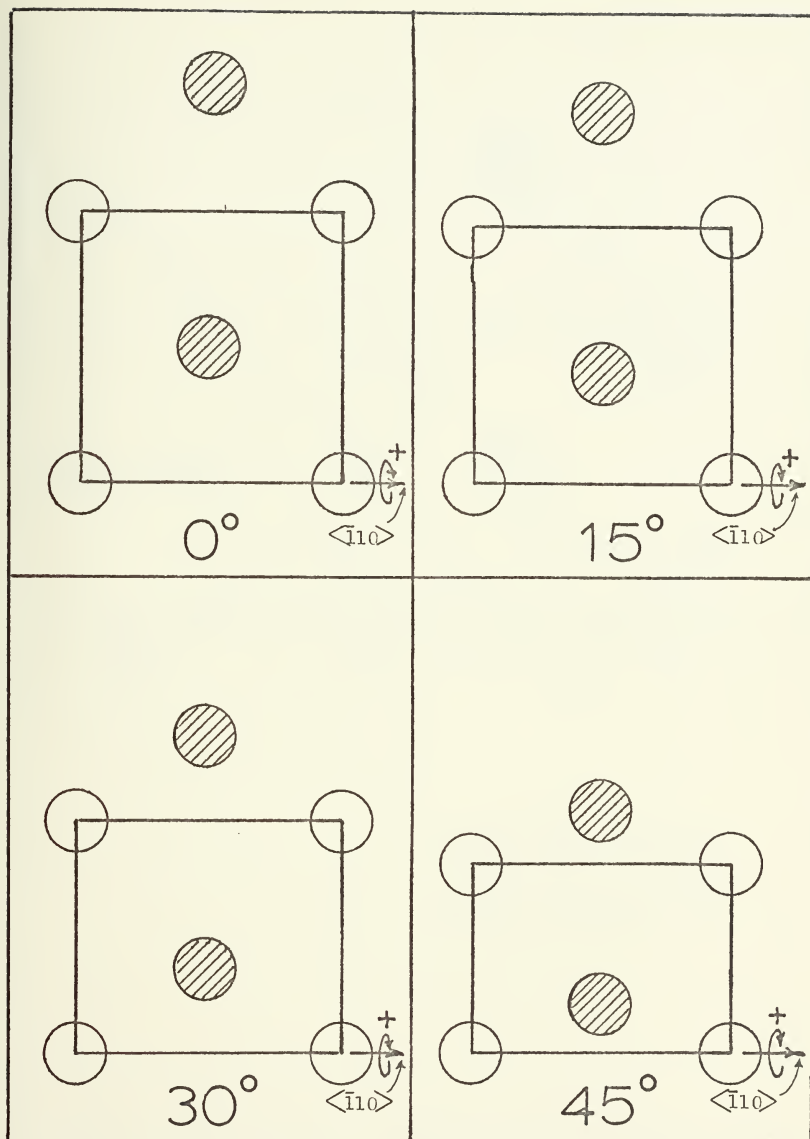


Figure 9. Representative area of the (100) face of an FCC crystal rotated in a positive sense about the $\langle 110 \rangle$ direction.

system to the (x', y') coordinate system are:

$$x' = R \cos (\theta - \phi) - (y_R \sin \phi + x_R \cos \phi),$$

$$y' = R \sin (\theta - \phi) + (x_R \sin \phi - y_R \cos \phi).$$

where

$$R = (x^2 + y^2)^{1/2}$$

$$\theta = \arctan (y/x)$$

and ϕ is the angle that the crystallographic axis makes with the x -axis. If the system is rotated through an angle α about the x' -axis, distances to any point (x', y') appear to be shortened by an amount $\cos \alpha$ in the y' dimension, leaving the x' dimension unchanged. Also, if the atom whose projected position lies at (x', y') before rotation is an atom whose actual position is R_a units below the plane being rotated, then its new apparent position on a plane perpendicular to the direction of incidence after rotation is given by the coordinates $(x', y' \cos \alpha - R_a \sin \alpha)$. In general then the final transformation equations become:

$$x' = R \cos (\theta - \phi) - (y_R \sin \phi + x_R \cos \phi) ,$$

$$y' = (R \sin (\theta - \phi) + (x_R \sin \phi - y_R \cos \phi)) \cos \alpha - R_a \sin \alpha .$$

The geometry implicit in these calculations is shown in Figure 10.

The actual calculation of the distribution of impact parameters is performed as follows. A mathematically constructed, rectangular grid is placed over the area and points which lie within the representative area are

systematically chosen. Using the transformation equations and the known position of the atoms in the representative area, the distance from the points chosen in the area to each respective atom are calculated in (x',y') coordinates and the shortest distance is chosen. The shortest impact parameter is tallied against the atom with which it is associated, in an array. In the case of equal distances between two atoms, the atom with which the ion impacts is chosen by a uniformly distributed pseudorandom process [17]. The final array contains the distribution of all impact parameters tallied with each atom in the representative area. To obtain the final distribution of impact parameters for the crystal face, the individual distributions are weighted, added, and the area under the curve is normalized to unity. The number of points used in calculating these distributions are on the order of 100,000 per representative area. The final unnormalized distribution of impact parameters for (100) FCC crystals for various angles of rotation is shown in Figure 11. Note that all dimensions used in calculating these distributions are in terms of R_0 , the nearest neighbor distance in the crystal lattice.

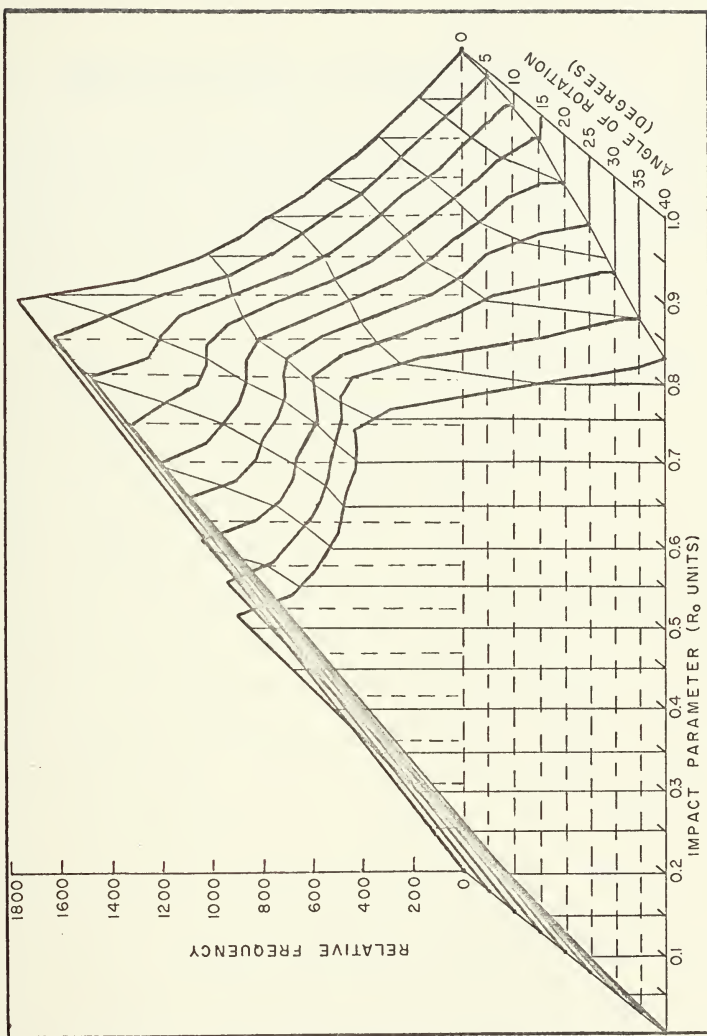


Figure 11. Unnormalized distribution of impact parameters for FCC (100) rotated through various angles about $\langle 110 \rangle$.

VI. NUMERICAL METHODS AND COMPUTER PROGRAMS

The theory presented in the preceding chapters has been incorporated into five FORTRAN IV computer programs which are presented in the appendix to this thesis. They appear in the order of their use. Specifically, these programs are:

1. The Herman-Skillman radial-electron density program,
2. The Harrison potential program,
3. Distribution of impact parameters program,
4. Numerical interpolation program, and
5. The Harrison KSE program.

To calculate the coefficient of ion-electron emission (SEE coefficient), these programs are utilized in the following manner. The ion-atom-radial-electron densities are calculated using the Herman-Skillman computer program [16]. These densities are put into the Harrison potential program which calculates the interatomic potential, $V(r)$, used in the calculation of the inelastic energy transfer, E_{TFF} . The distribution of impact parameters program calculates the distribution of impact parameters for each crystal face under investigation. Since this is a statistical process, the distributions recovered from this program are "smoothed" using a first and tenth degree Legendre orthogonal least squares interpolating polynomial, which is generated by the numerical interpolation program [18]. Finally the

smoothed distribution of impact parameters and potential function are inserted into the Harrison KSE program which has been modified to include all the changes to the original theory presented in the "Modifications" chapter of this thesis. This program performs the actual calculation of the SEE coefficient using the HCM model. The input data format to each of these programs is shown in Figures 12 through 16. The definitions of the input variables used in the programs are presented in Appendix A to this thesis. The results presented in the following chapter were run on the Naval Postgraduate School IBM/360 Computer System.

Data Input for the Electron Density Program

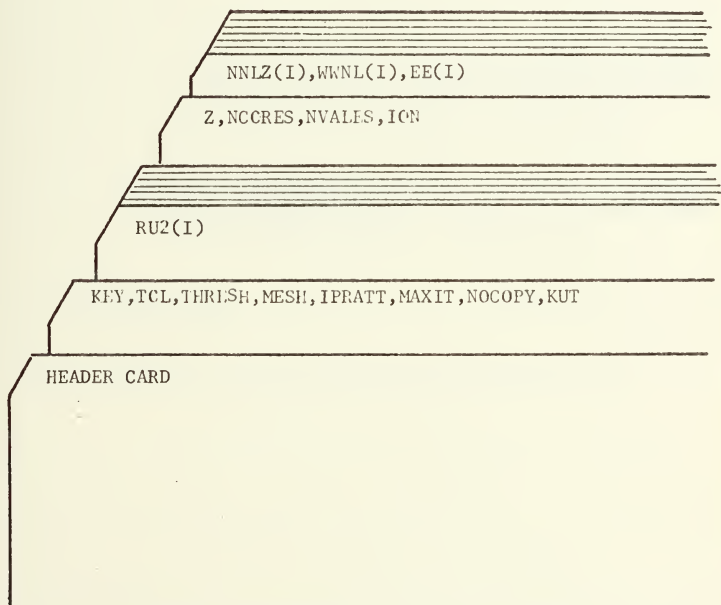


Figure 12. Deck setup for running the Electron Density Program.

Data Input for the Potential Program

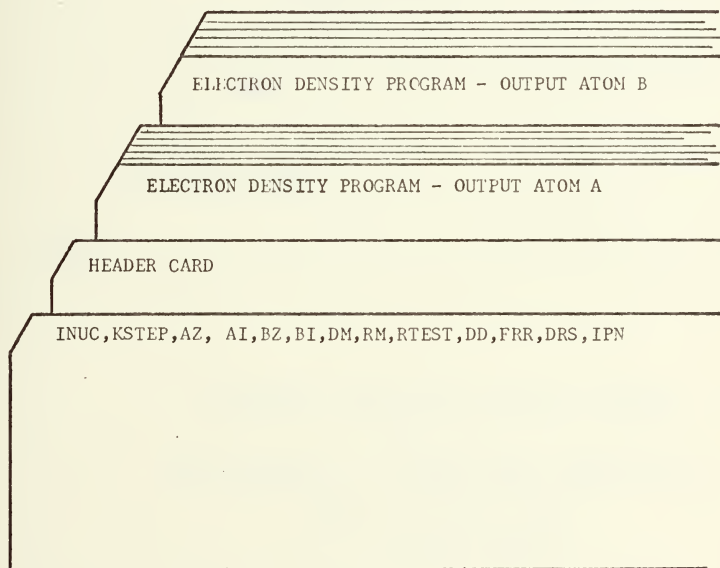


Figure 13. Deck setup for running the Potential Program.

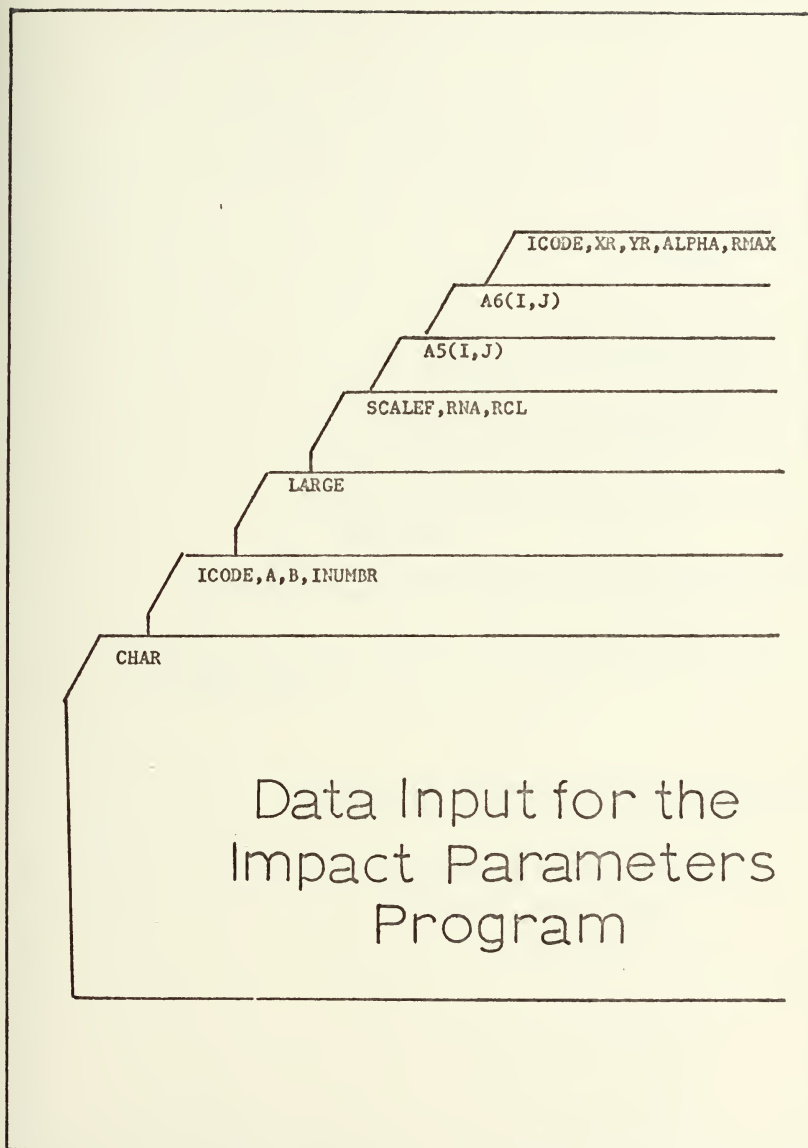


Figure 14. Deck setup for running the Distribution of Impact Parameters Program.

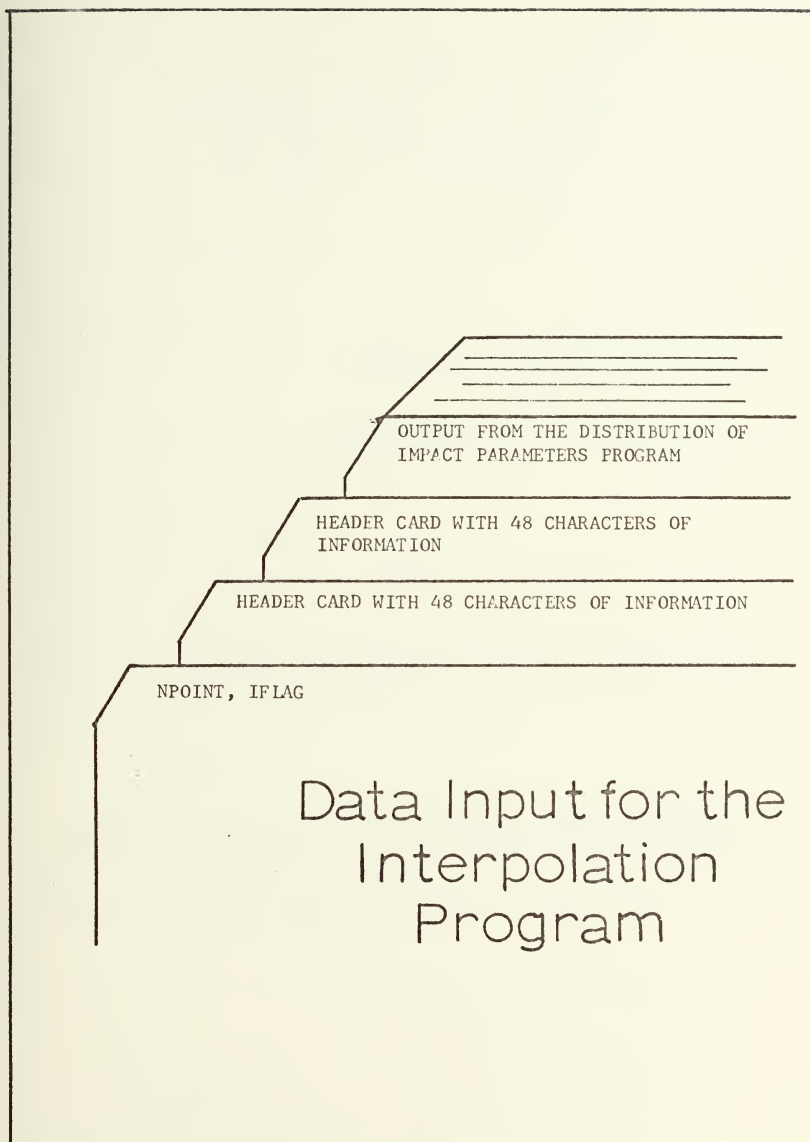


Figure 15. Deck setup for running the Interpolation Program.

Data Input for the KSE Program

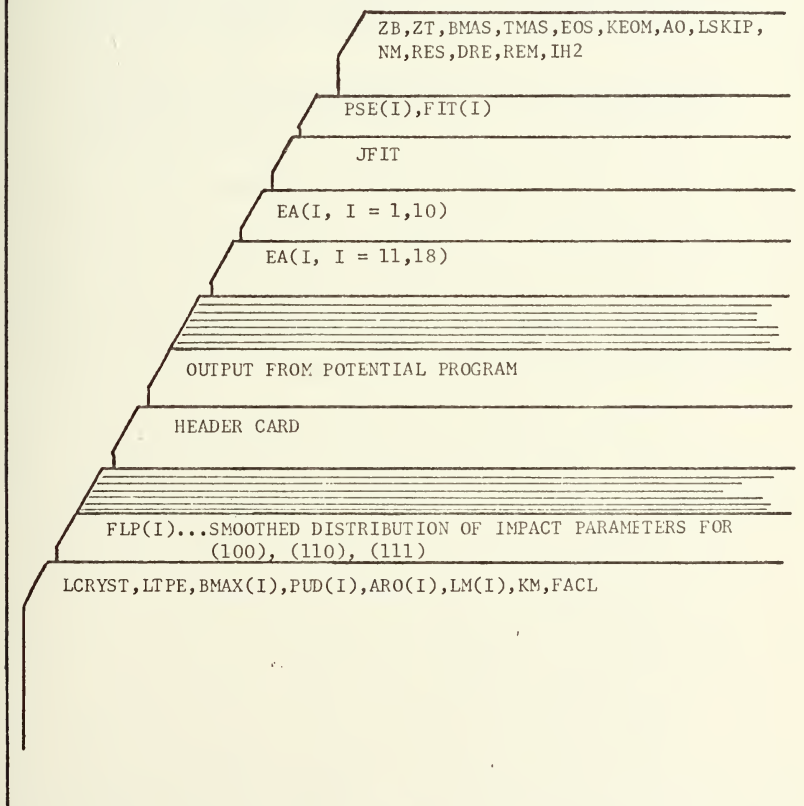


Figure 16. Deck setup for running the KSE Program.

VII. RESULTS

Three separate cases of secondary electron emission were investigated using the modified HCM model. These were:

1. Angularly dependent secondary electron emission from the (100) face of a copper single crystal rotated about a $\langle 110 \rangle$ axis;
2. Secondary electron emission from Ar, Ne, Kr and Xe ions normally incident on the (100), (110) and (111) faces of Cu, Ag, Mo, and Al single crystals; and
3. Secondary electron emission from Ar and Ne ions normally incident on the (100), (110) and (111) faces of KCl.

In the HCM theoretical model, the primary ion is assumed to be neutralized before it strikes the target surface. The target atoms in the metal are assumed to be ion cores in a sea of valence electrons. For these reasons, the actual results presented here are obtained by modeling the binary collision process as a collision between a neutral, inert gas atom and an ion core of the target atom. In the cases of copper and silver, the ion cores are fairly well defined, since both appear in column I.B. of the periodic table. However, in the cases of molybdenum and aluminum which appear in the VI.B. and III.A. columns of the periodic table, respectively, there are several possible ion core configurations that could be used in the HCM model. For this reason, various degrees of ionization of the molybdenum and aluminum target atoms were used in computing the SEE coefficient for these target atoms by way of the HCM model.

In the cases of copper and silver, results indicate that the best ion core configuration for both target materials is the singly ionized state. Note that all graph titles refer to the HCM model used, whereas the figure captions indicate the physical system actually investigated.

A. ANGULARLY DEPENDENT RESULTS

The results obtained from the bombardment of Cu single crystals by Ar ions for various angles of rotation about the $\langle 110 \rangle$ crystallographic axis are shown in Figure 17. It is interesting that the HCM model did not predict the correct behavior of the SEE coefficient for monocrystalline, angularly rotated targets, but did accurately reproduce the results obtained for polycrystalline targets [19]. This seems to indicate that the single collision model is not an accurate one for arbitrary rotations about the crystallographic axis, but needs to be modified to account for a more complicated interaction with the crystal lattice.

B. METAL TARGET RESULTS

An attempt was made in this thesis to verify those calculations performed by HCM in their original paper. Not too surprisingly, the results obtained here differ appreciably from those obtained by HCM using their original model. Each system is discussed in detail below.

1. Copper Bombarded by Ar, Ne, Kr and Xe Ions

In HCM's original paper, the $\text{Ar}^+ - \text{Cu}$ system was treated in detail. Using their original model, they

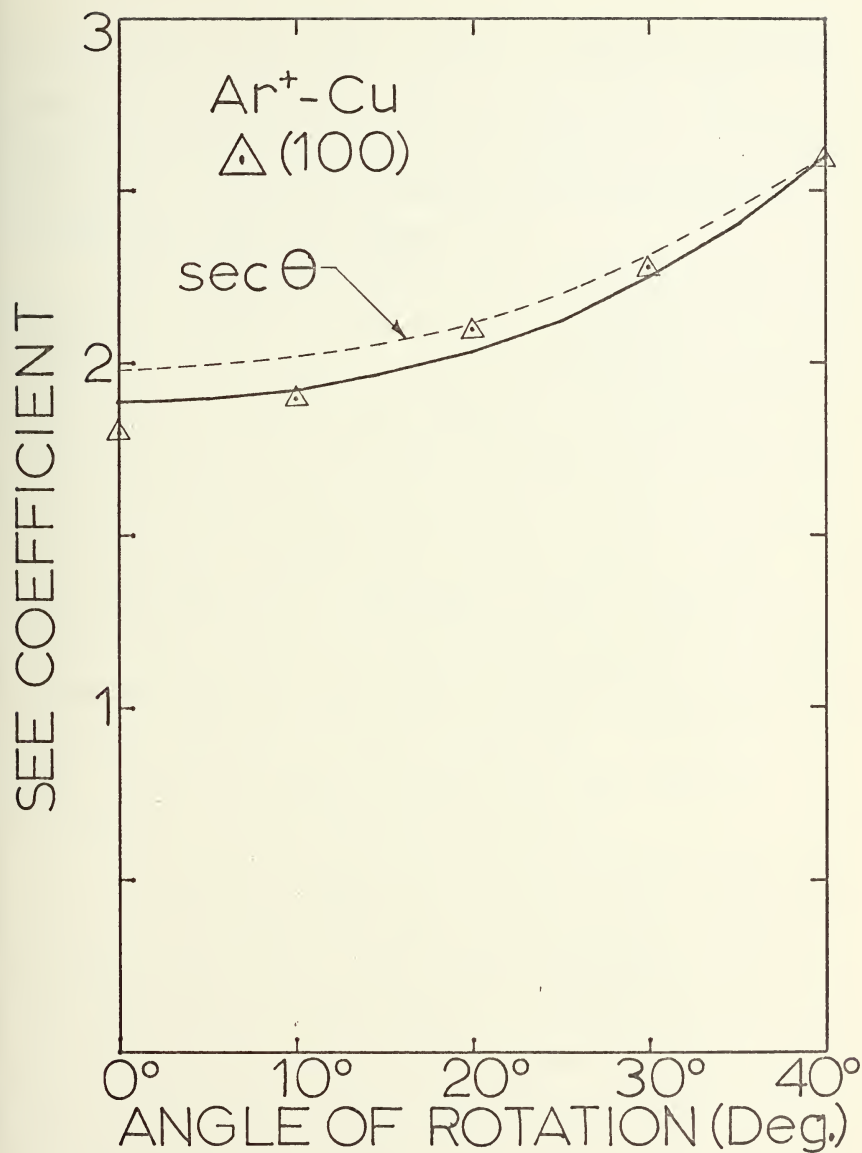


Figure 17. SEE coefficient vs. angle of rotation for (100) FCC Copper crystal. Direction of rotation was about $\langle 110 \rangle$.

obtained the results shown in Figure 7, which show excellent agreement with experiment. After altering their model, using the modifications presented in Chapter IV, the results do not agree so well with experiment as did those obtained by HCM. (See Figures 18 through 21.)

In an attempt to explain this discrepancy, the difference between the experimentally observed SEE coefficient and that obtained here was plotted as a function of energy. Theoretically, if the results obtained in this present investigation are to be physically meaningful, this difference must be due to the potential ejection mechanism operating at higher energies. Experimentally, Medvel et al. [1] have ascertained that for Ar bombardment of polycrystalline Mo targets, the potential ejection mechanism is still operating at energies up to 2.5 Kev, and the PSE contribution is still tending to increase with increasing energy. If this is in fact the case, the results obtained here have physical significance. (See Figures 22 through 25.)

It is interesting to note that the PSE contribution from all three faces investigated exhibit similar behavior in that they all peak at approximately the same energy, and tend to decrease at higher energies. The exact location of the peak, however, varies with the primary ion type. Furthermore, in all four primary ion cases, the PSE contribution curves for the (100) and (110) faces cross at approximately seven to nine Kev, indicating that the PSE mechanism may be somewhat independent of ion type, while showing some

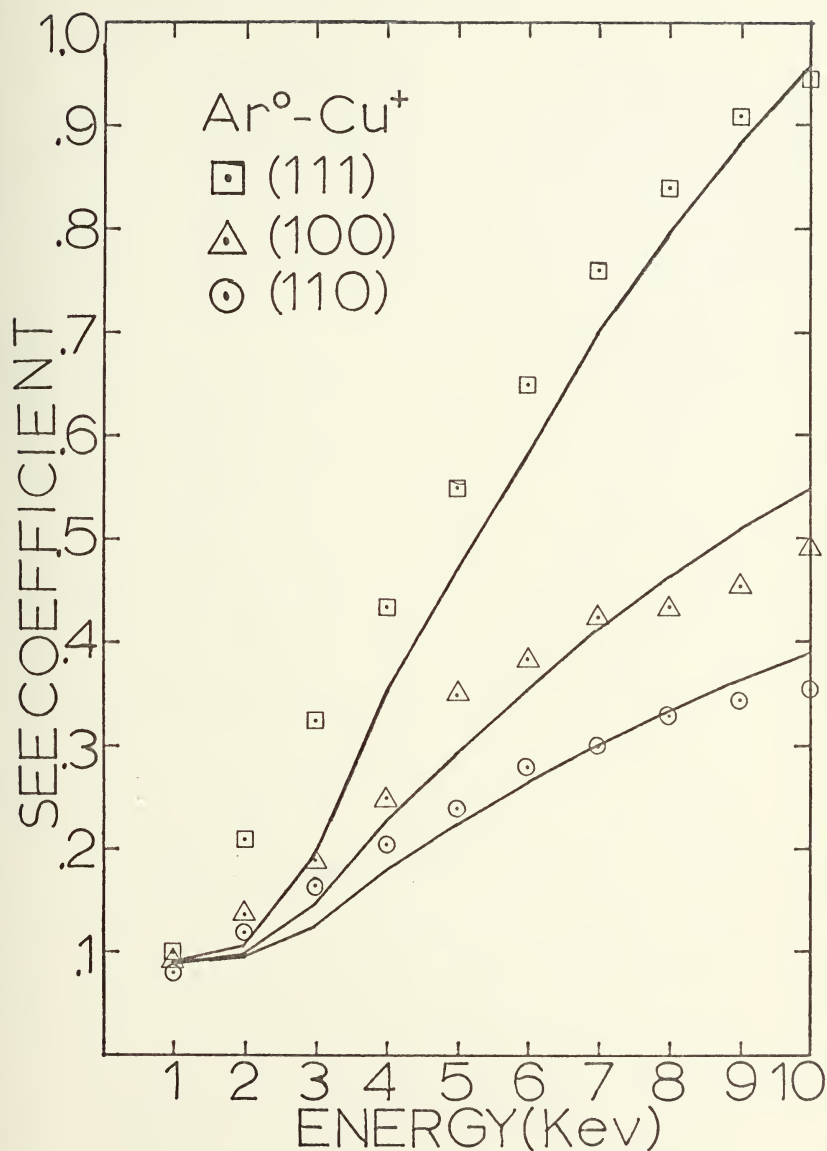


Figure 18. Cu bombarded by Ar^+ ions normally incident on the (100), (110) and (111) planes.

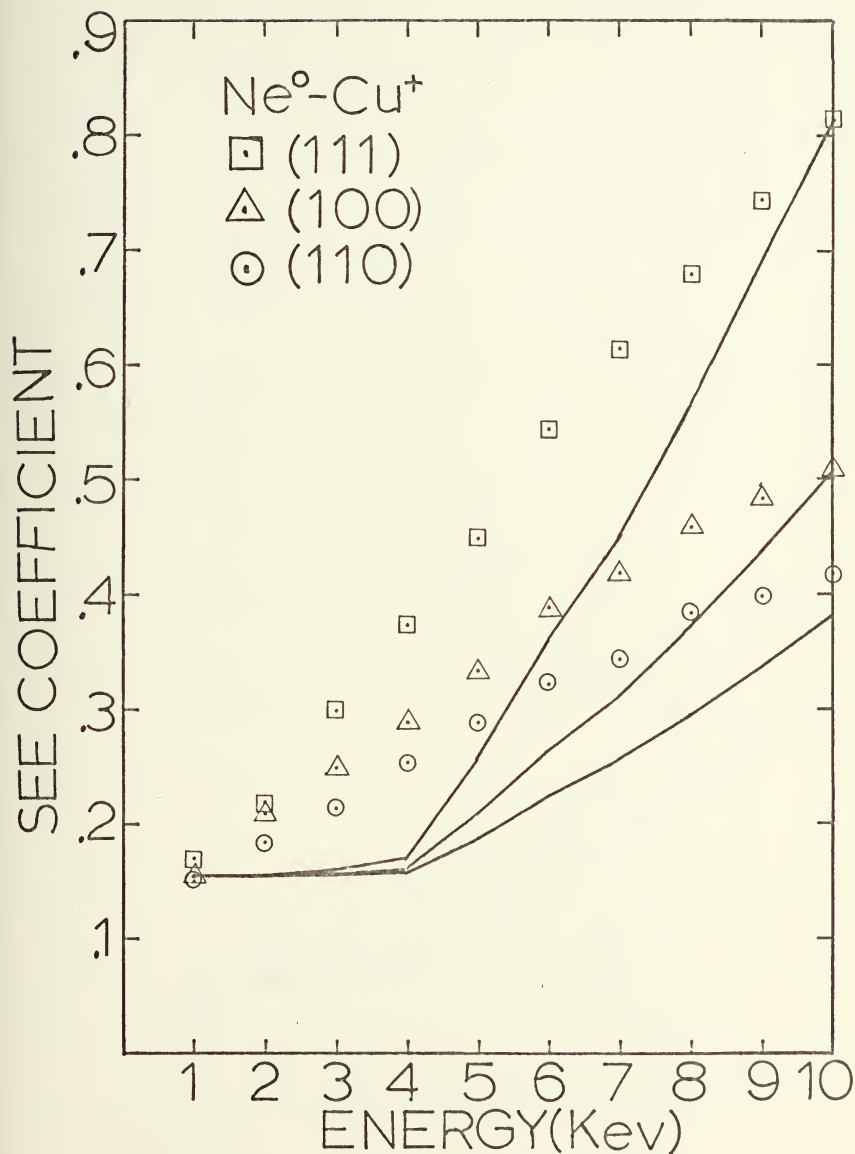


Figure 19. Cu bombarded by Ne^+ ions normally incident on the (100), (110) and (111) faces.

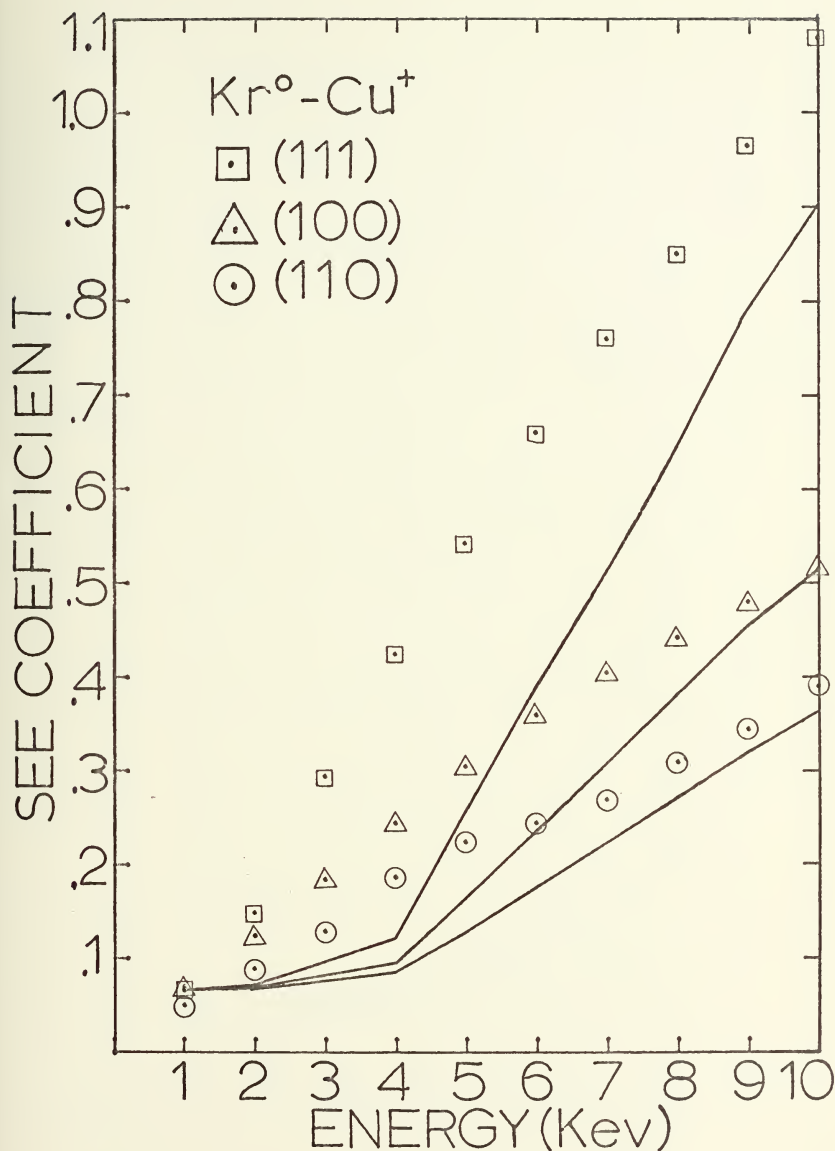


Figure 20. Cu bombarded by Kr^+ ions normally incident on the (100), (110) and (111) faces.

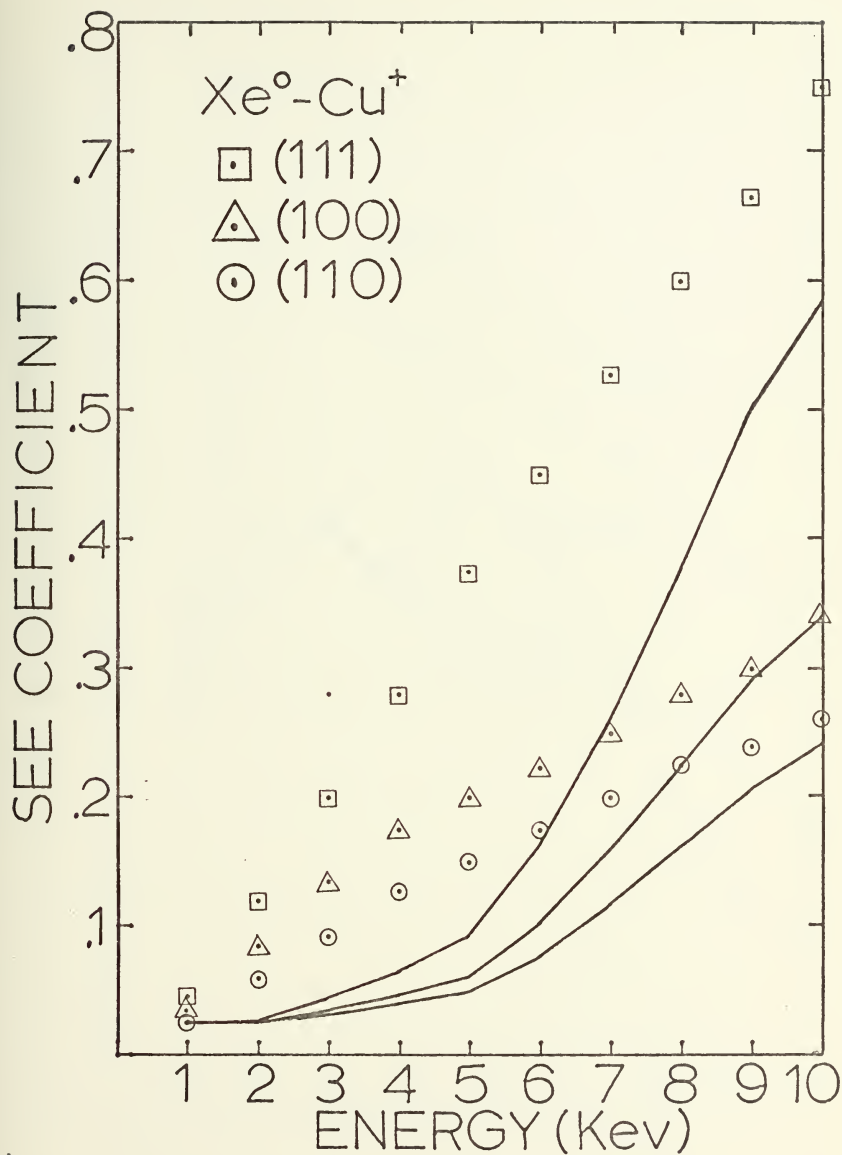


Figure 21. Cu bombarded by Xe^+ ions normally incident on the (100), (110) and (111) faces.

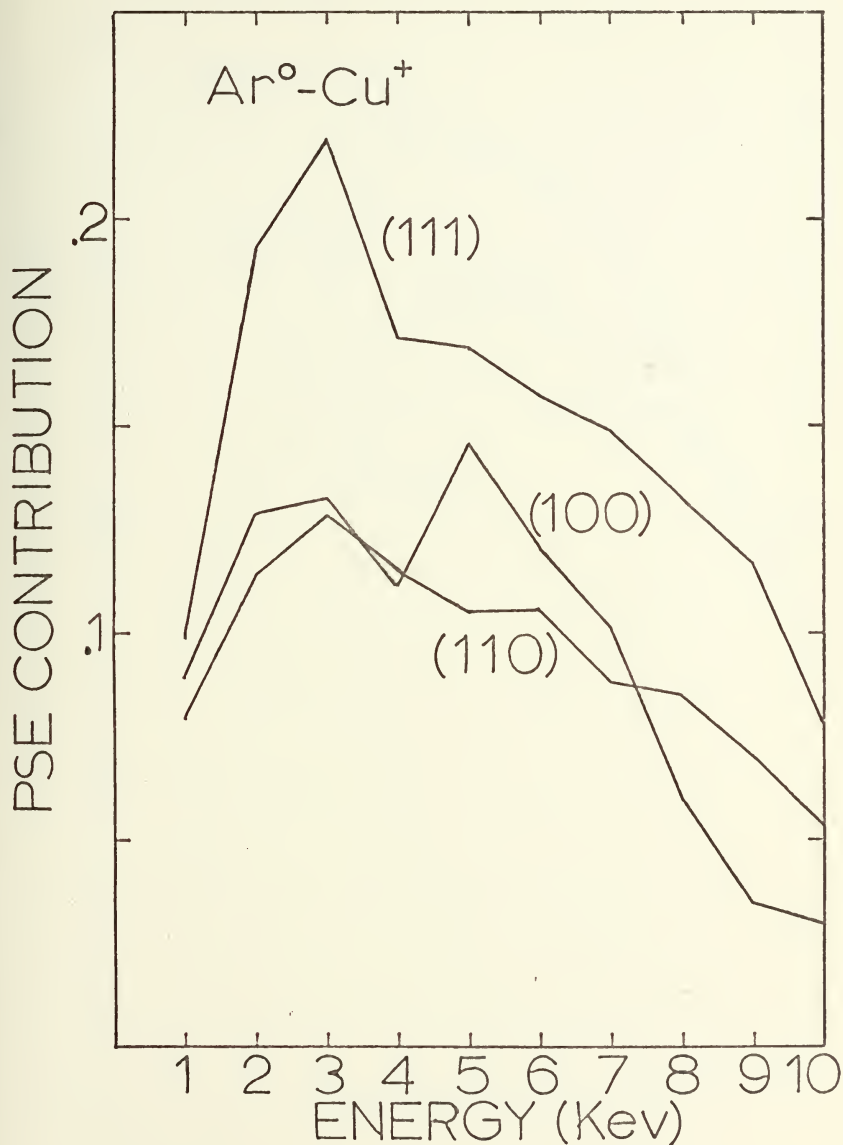


Figure 22. PSE contribution to secondary electron emission for the $\text{Ar}^0\text{-Cu}^+$ system.

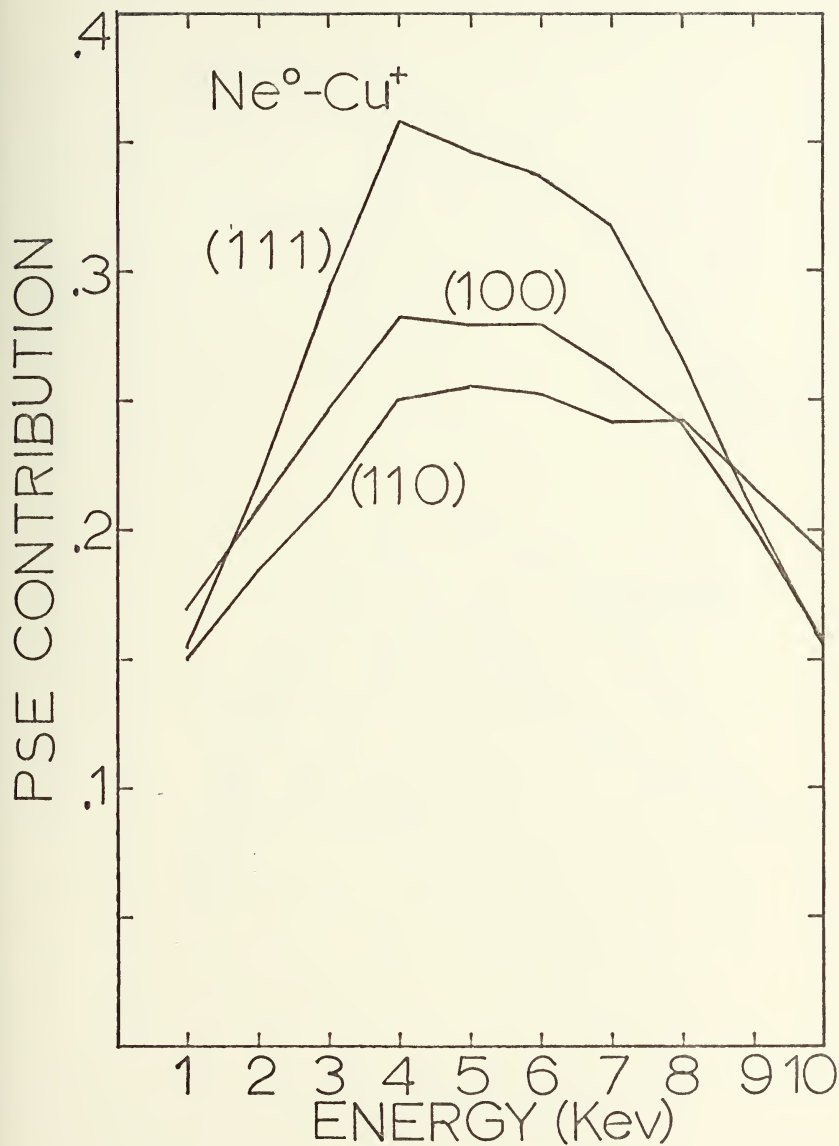


Figure 23. PSE contribution to secondary electron emission for the Ne⁰ - Cu system.

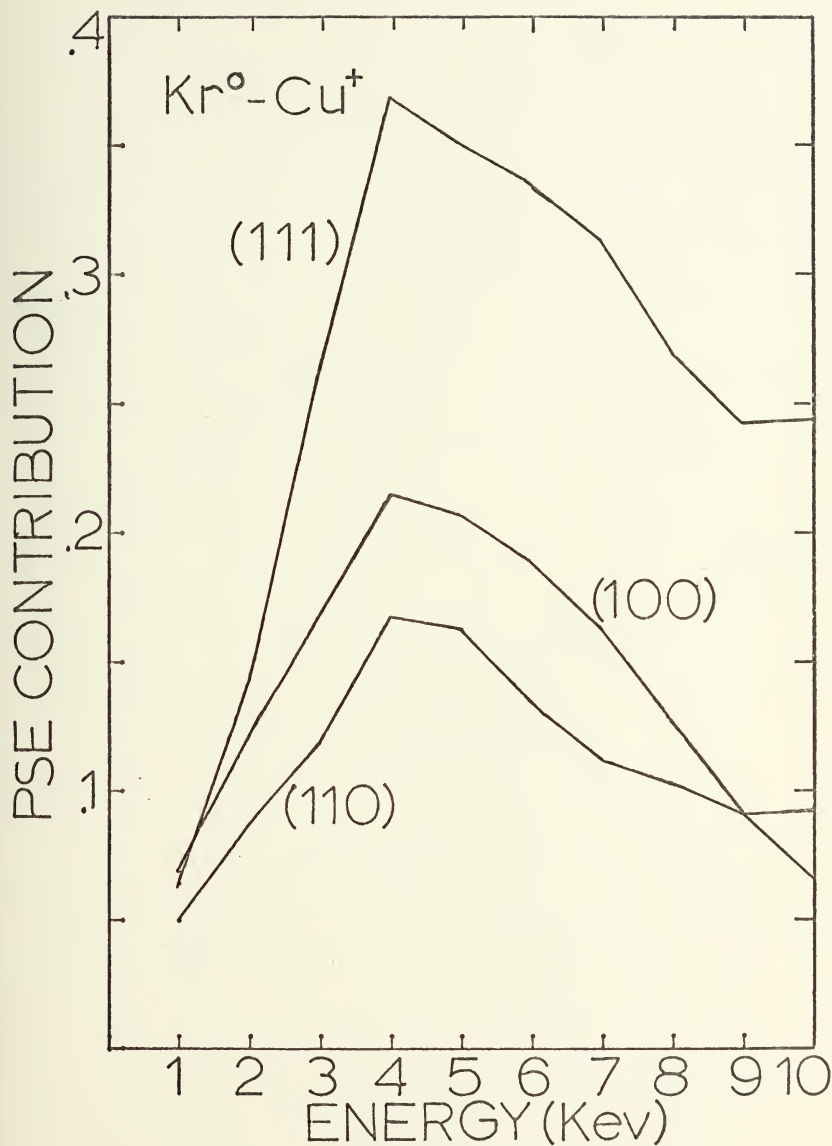


Figure 24. PSE contribution to secondary electron emission for the $\text{Kr}^+ - \text{Cu}$ system.

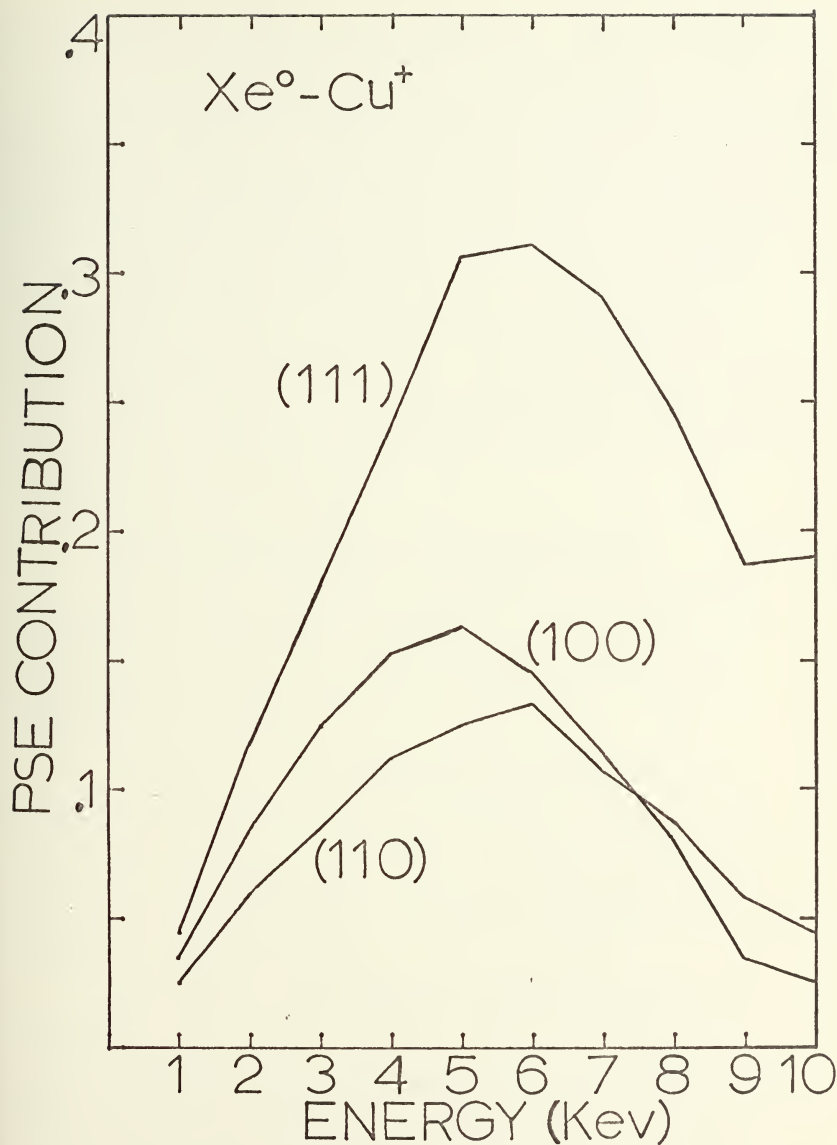


Figure 25. PSE contribution to secondary electron emission for the $\text{Xe}^\circ - \text{Cu}^+$ system.

dependence on the plane being bombarded. Such a crossing behavior in the PSE contribution as a function of energy would not be expected simply by analyzing the SEE coefficient curves, since these curves do not cross at any energy. If this is the case, then it would follow that the theoretical results obtained for each crystal face should be independently fitted to the experimental data, without regard to the other planes being bombarded. In most cases this would yield results that are in closer agreement with experiment and yet do not eliminate the PSE contribution to secondary electron emission entirely.

2. Silver Bombarded by Ar, Ne, and Kr Ions

The silver systems also indicate the possibility of the PSE mechanism being dependent on the crystal face being bombarded as well as the primary ion type. (See Figures 26 through 31.)

In the Ar^+ - Ag system the PSE contribution to secondary electron emission is initially largest for the (100) face, followed by the (111) and (110) faces, respectively. In all three cases the PSE contribution decreases slightly at higher energies.

In the Kr^+ - Ag system a different ordering of facial PSE contributions appear. Initially, the (111) face contributes the most to potential emission, followed by the (100) and (110) faces, in that order. At higher energies, the ordering changes, with (100) contributing the largest amount to PSE, followed by (111) and (110),

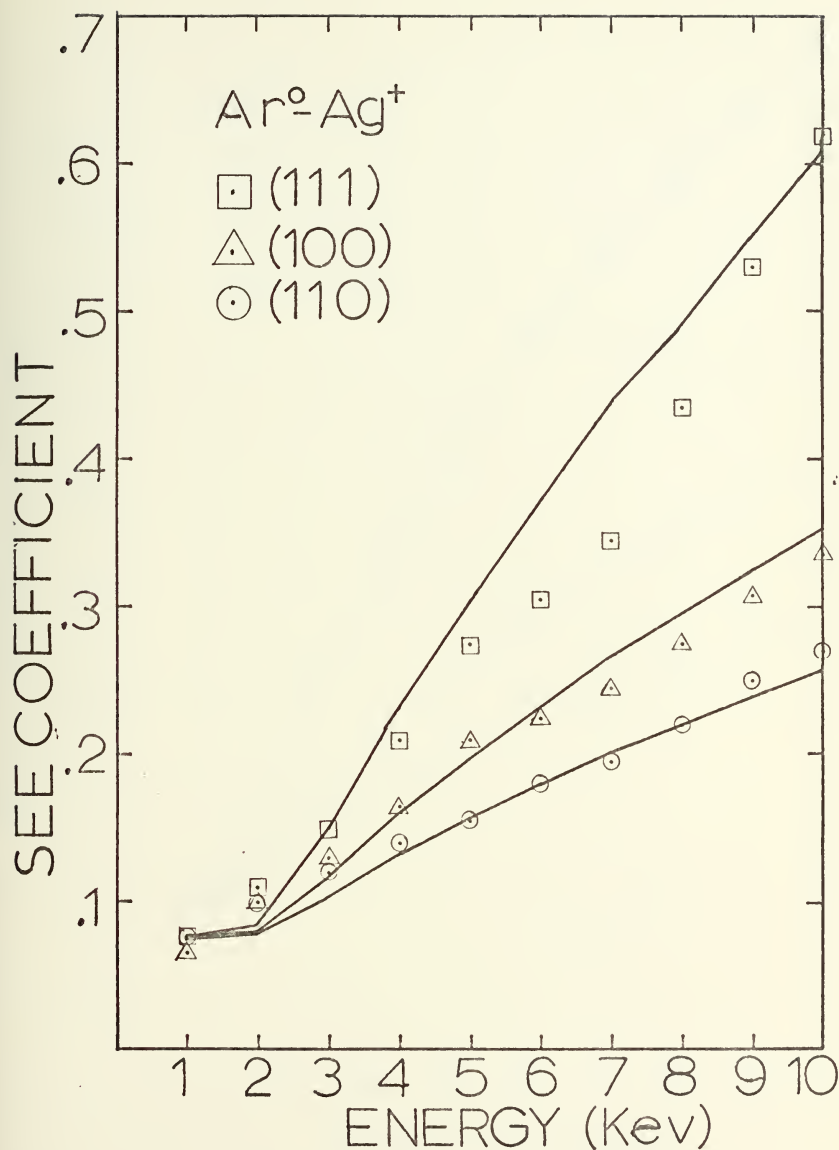


Figure 26. Ag bombarded by Ar^+ ions normally incident on the (100), (110) and (111) faces.

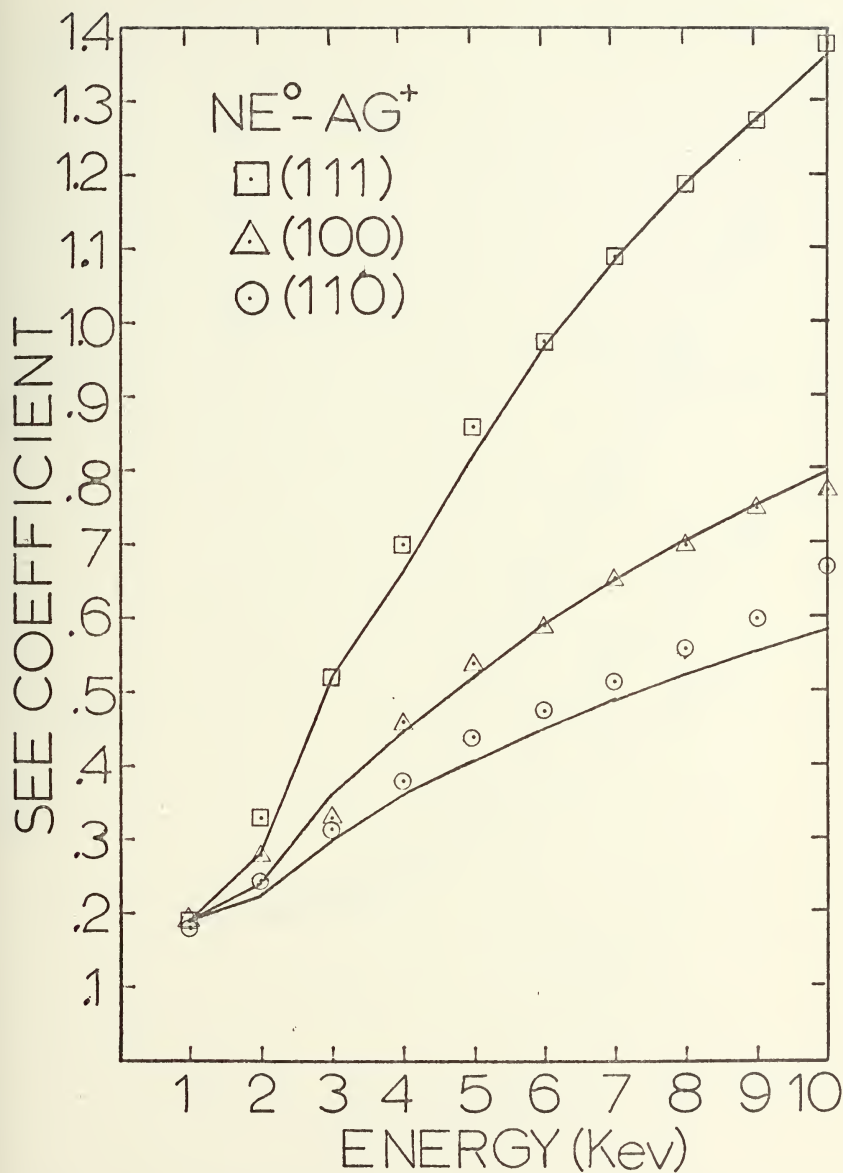


Figure 27. Ag bombarded by Ne^+ ions normally incident on the (100), (110) and (111) faces.

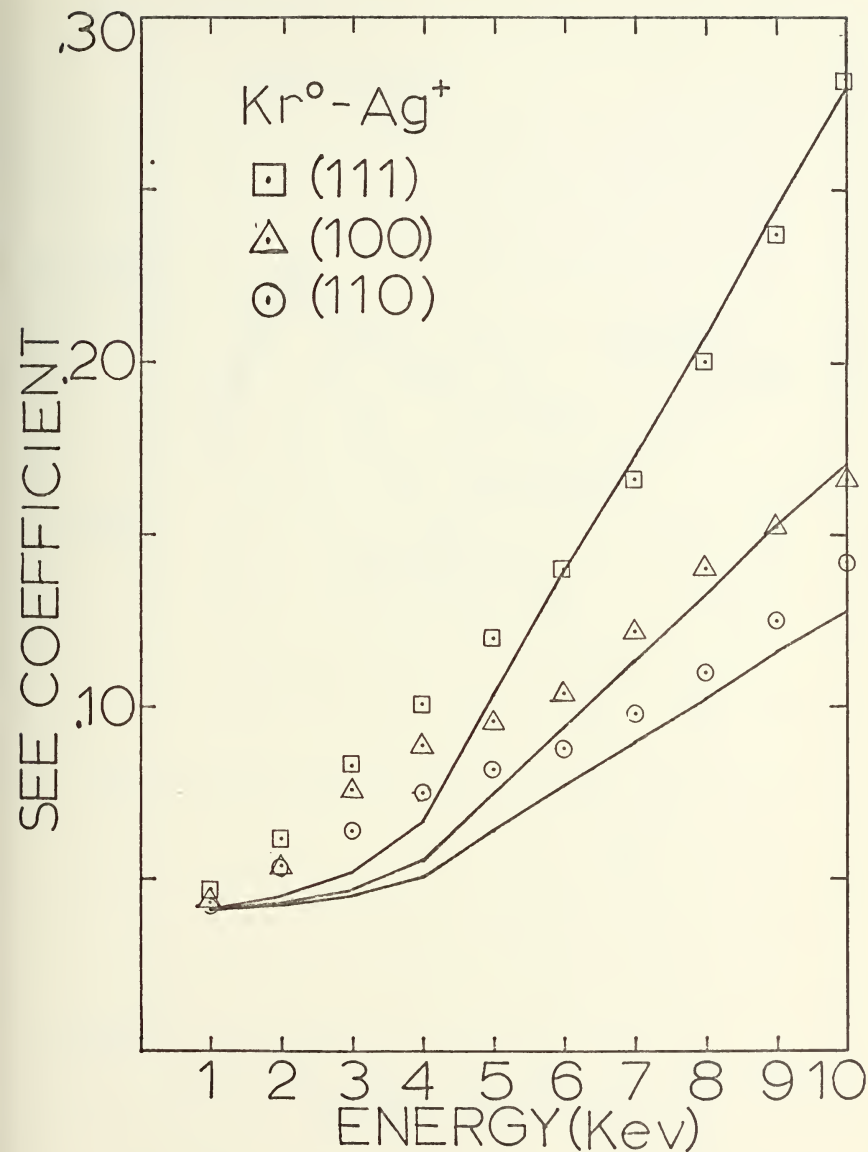


Figure 28. Ag bombarded by Kr^+ ions normally incident on the (100), (110) and (111) faces.

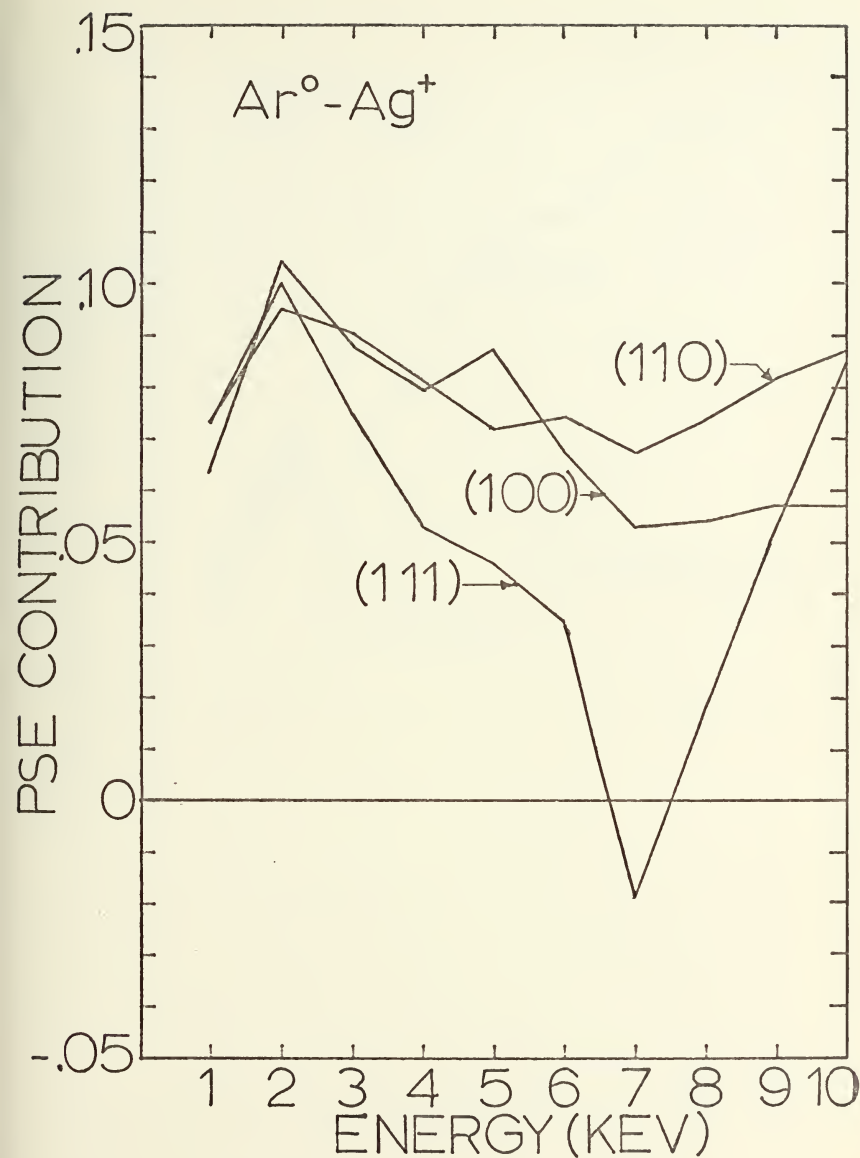


Figure 29. PSE contribution to secondary electron emission for the Ar⁺ - Ag system.

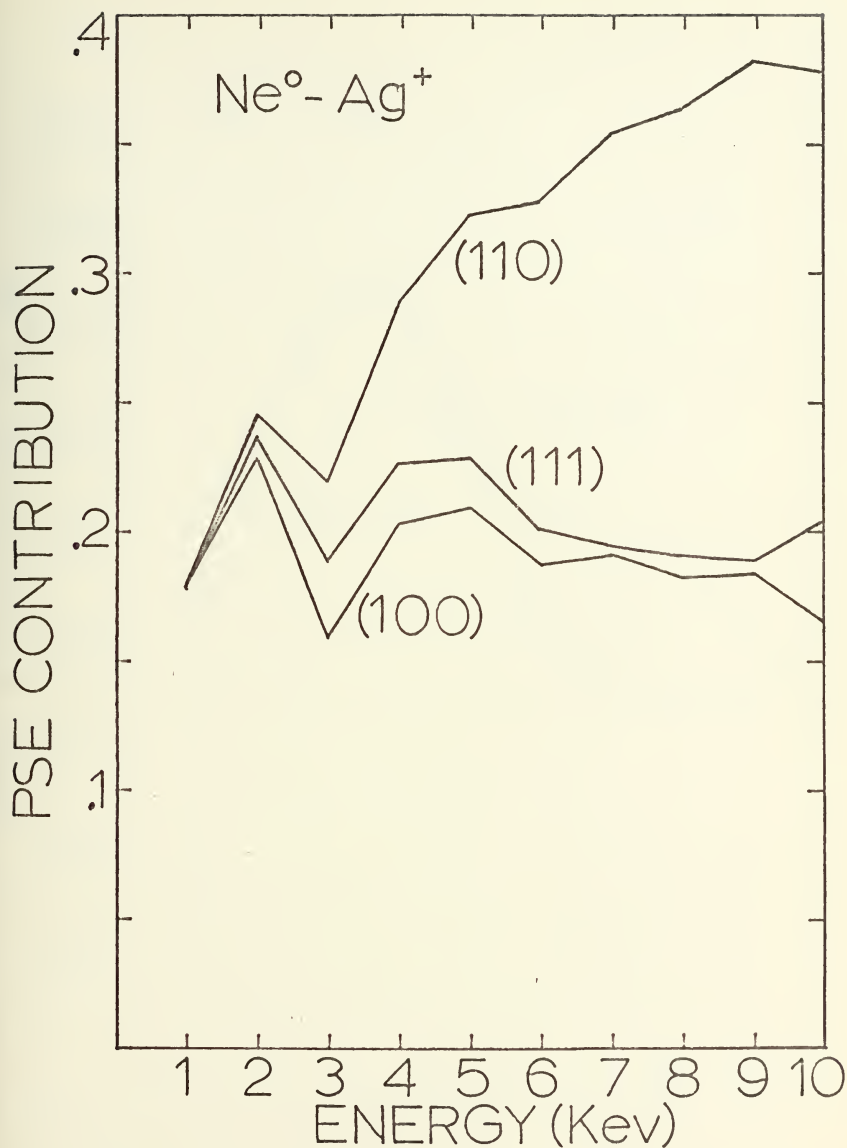


Figure 30. PSE contribution to secondary electron emission for the $\text{Ne}^\circ - \text{Ag}$ system.

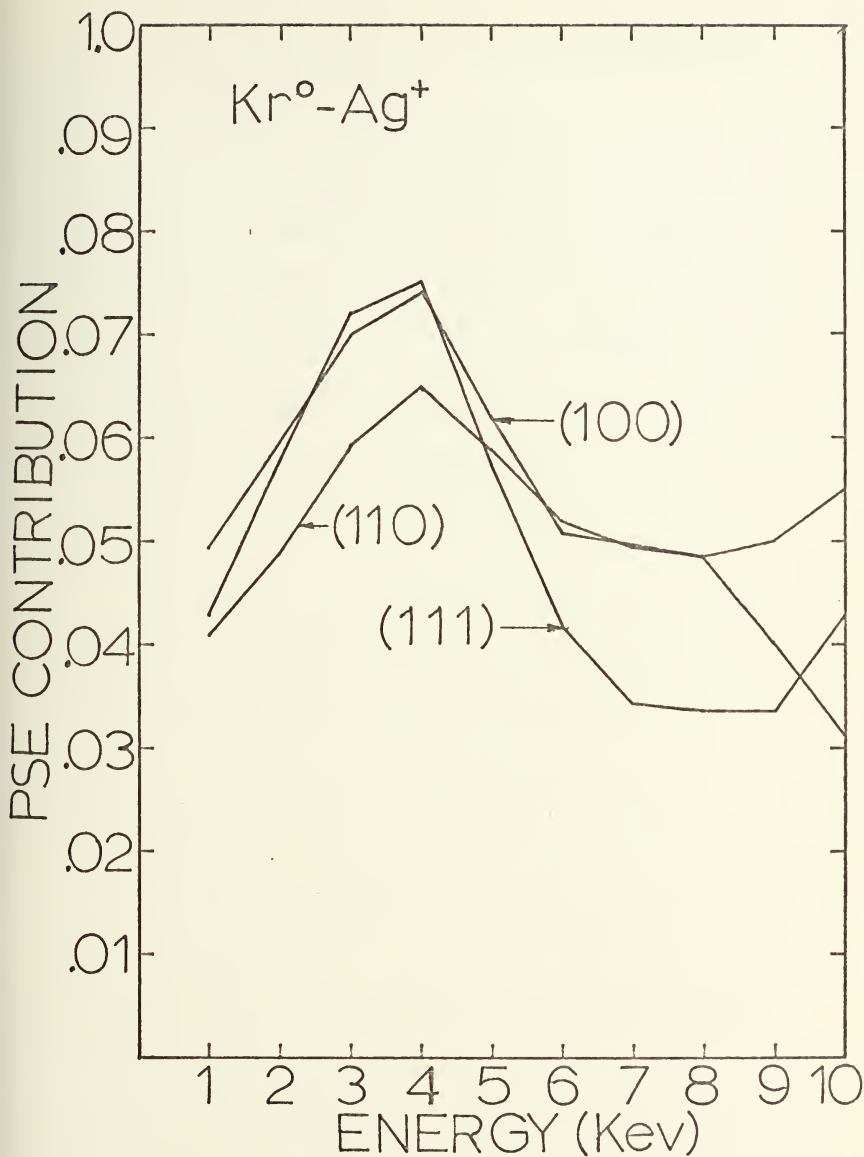


Figure 31. PSE contribution to secondary electron emission for the $\text{Kr}^0\text{-Ag}^+$ system.

respectively. Once again, the PSE contribution tends to decrease at higher energies.

In the Ne^+ - Ag system an entirely different picture arises. For all energies, the (110) face contributes the most to PSE, followed by the (111) and (100) faces, respectively. However, even at ten Kev, the potential emission for the (110) face is still rising whereas, over the entire energy range, the PSE contribution from the (111) and (100) face remains fairly constant. These results would seem to indicate, once again, that not only is potential emission dependent on primary ion type, but also on crystal face.

In the Ar^+ - Ag system, the PSE contribution from the (111) face goes to a negative value at seven Kev. The reason for this behavior can be found by analyzing the Ar^+ - Ag SEE coefficient versus energy curves shown in Figure 26. The SEE coefficient experimental data for the (111) face dips downward at seven Kev. This behavior is not demonstrated on the other faces and would tend to indicate that some experimental variation may be present in these experimental data. On the other hand, the interaction being modeled may be sufficiently complicated that the potential contribution cannot be separated simply by scaling the results. No other system investigated displays similar results.

3. Molybdenum Bombarded by Ar, Ne, Kr and Xe Ions

In Figures 32 through 43, Mo^+ initially seems to be the ion core model that best represents secondary electron emission from various target faces. This conclusion holds true for the $\text{Ne}^+ - \text{Mo}$ and $\text{Kr}^+ - \text{Mo}$ systems. However, for the $\text{Xe}^+ - \text{Mo}$ system, the best ion core model is not Mo^+ but Mo^{++} . This would seem to indicate that the primary ion type plays an important role in secondary electron emission.

4. Aluminum Bombarded by Ar, Kr, and Xe Ions

In the case of aluminum bombarded by Ar^+ (Figures 44 through 52) the Al^+ and Al^{++} ion core models for the target atoms yielded results that were almost identical. This system is contrasted with the $\text{Kr}^+ - \text{Al}$ system which shows a distinct preference for Al^{++} as the ion core model, with the Al^+ and Al^{+++} yielding similar and uniformly poor results. Similarly, the $\text{Xe}^+ - \text{Al}$ system shows the same preference for the Al^{++} ion core model and demonstrates a poorer fit when the Al^+ and Al^{+++} models are used. When all cases are considered, it would seem that secondary electron emission is sensitive to the primary ion type, as has been demonstrated by previous results.

C. ALKALI-HALIDE RESULTS

Experimental results for the bombardment of alkali-halide single crystals by inert gas ions have been obtained from experiments by Baboux and Pedrix [21, 22]. Two cases are considered in this present investigation. These include

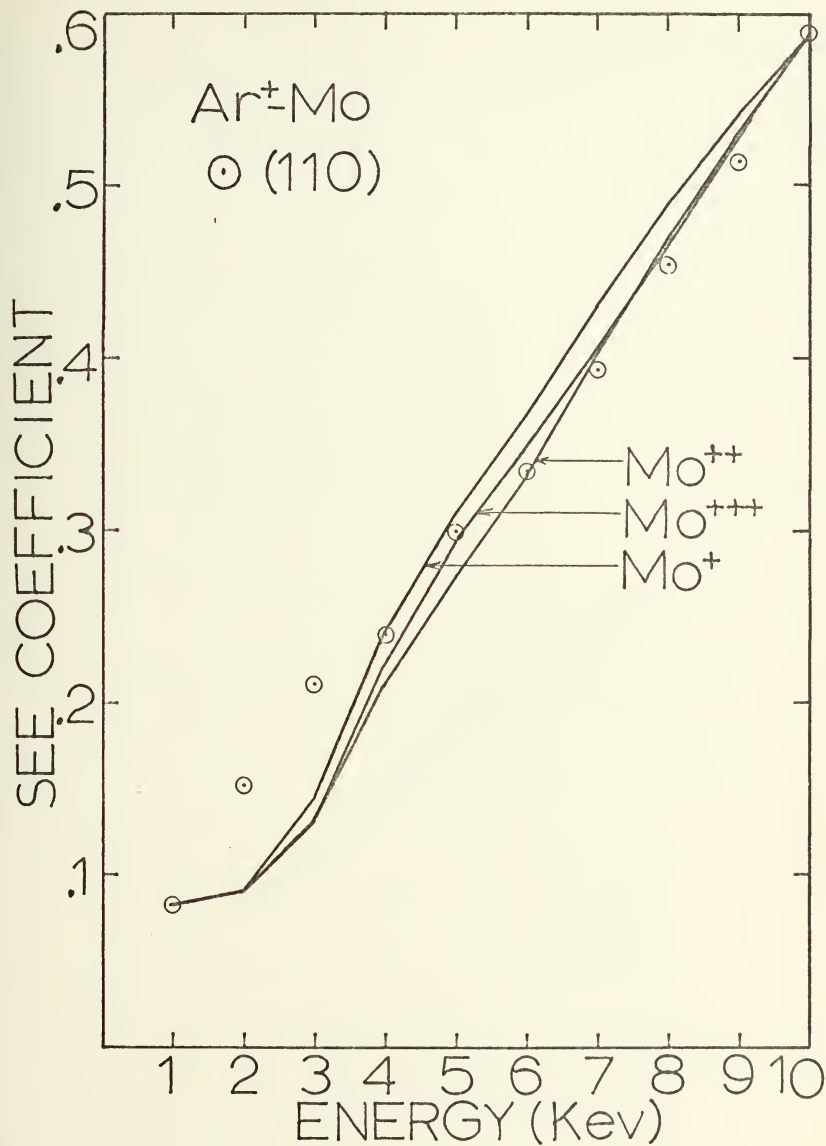


Figure 32. Effect of varying target atom ionization in the HCM model on secondary electron emission from the Ar⁺ - Mo system.

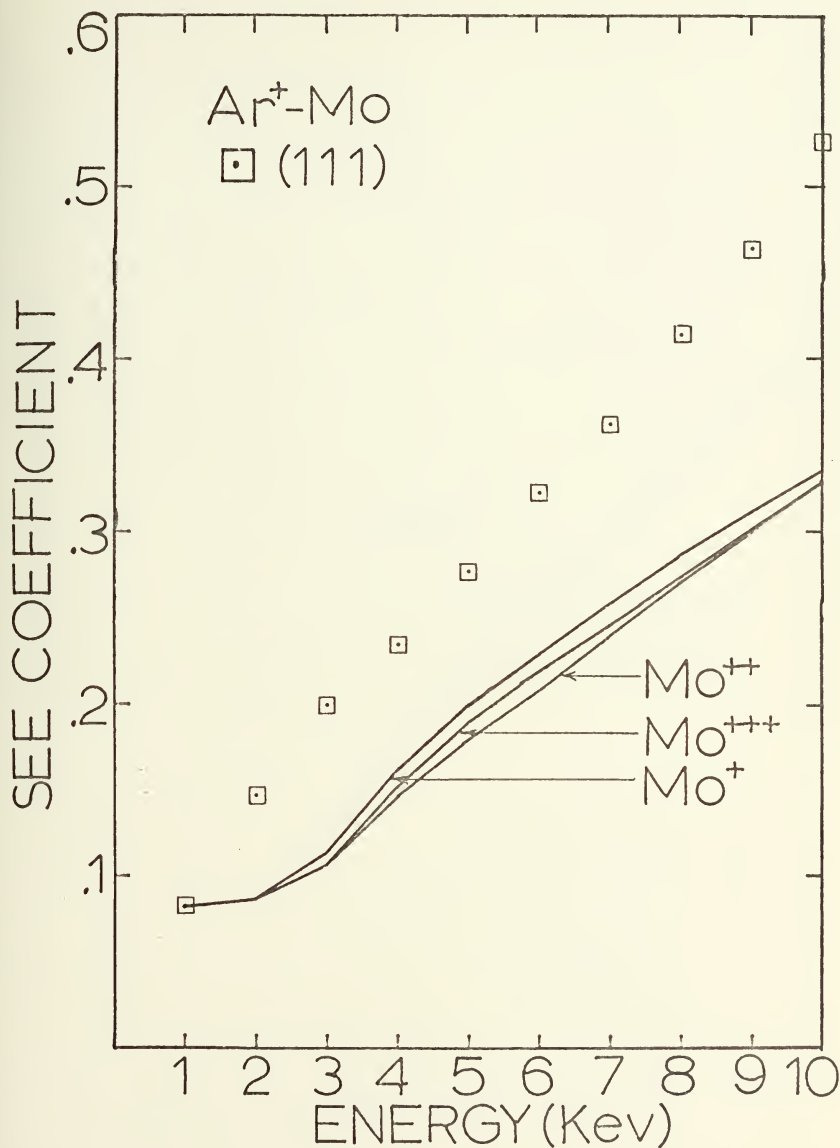


Figure 33. Effect of varying target atom ionization in the HCM model on secondary electron emission from the Ar⁺ - Mo system.

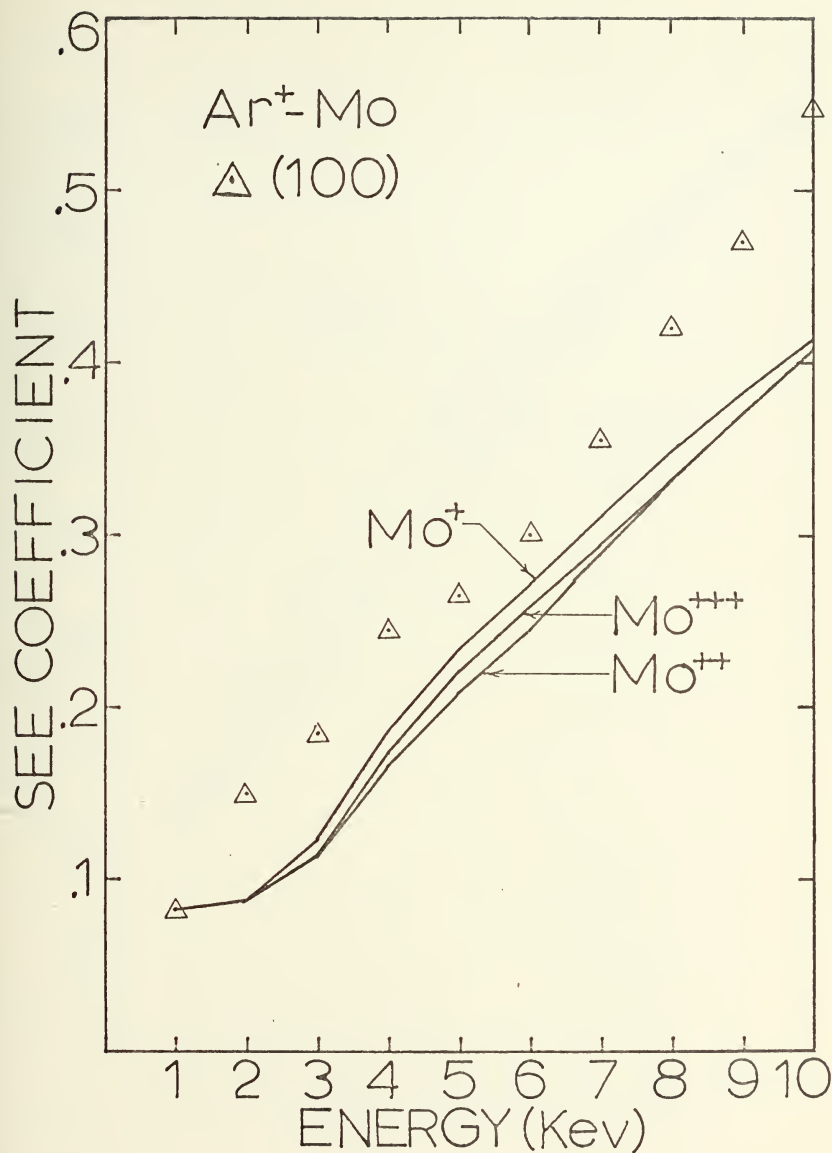


Figure 34. Effect of varying target atom ionization in the HCM model on secondary electron emission in the Ar⁺ - Mo system.

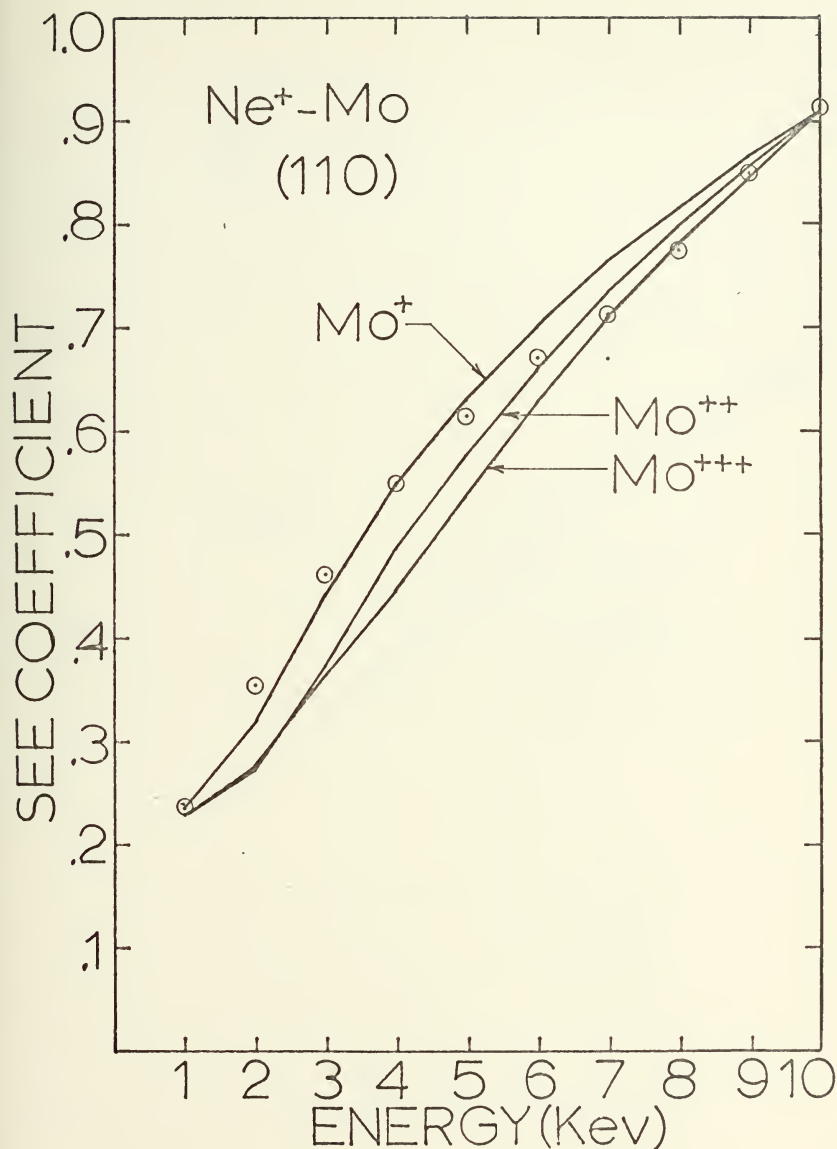


Figure 35. Effect on varying target atom ionization in the HCM model on secondary electron emission from the $\text{Ne}^+ - \text{Mo}$ system.

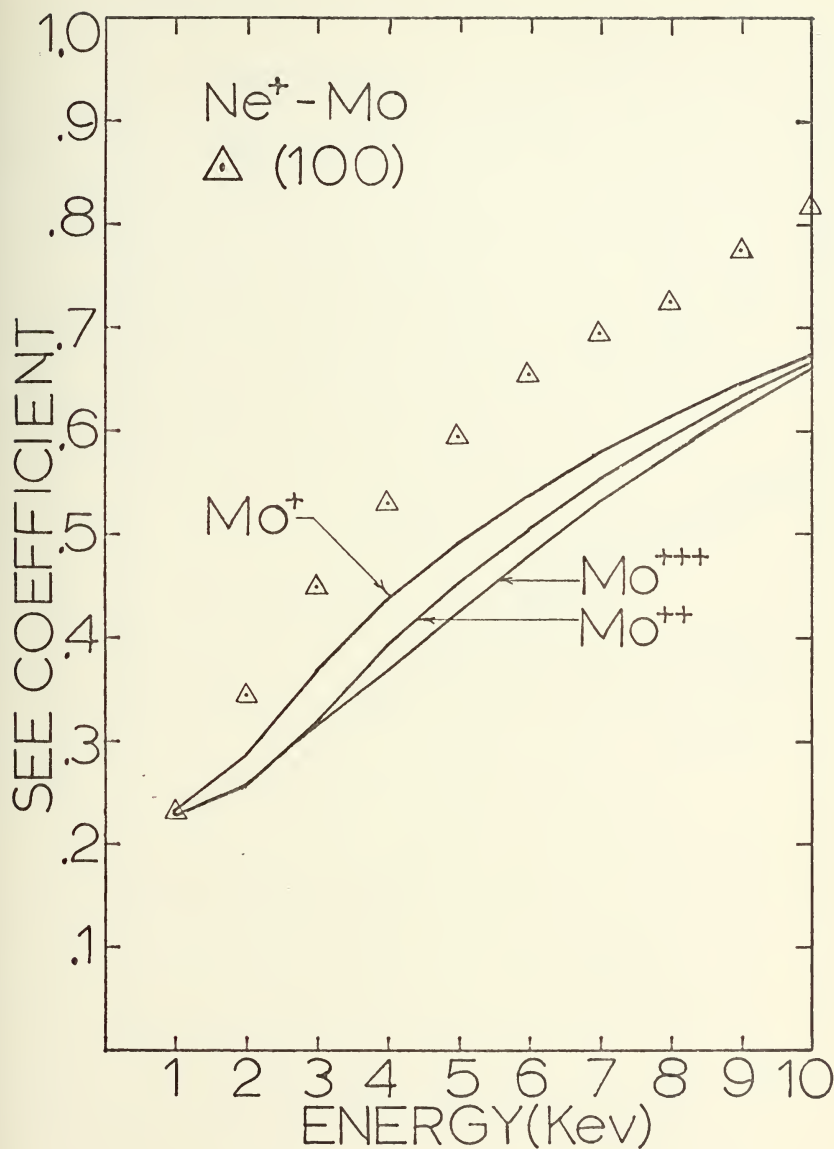


Figure 36. Effect of varying target atom ionization in the HCM model on secondary electron emission from the Ne⁺ - Mo system.

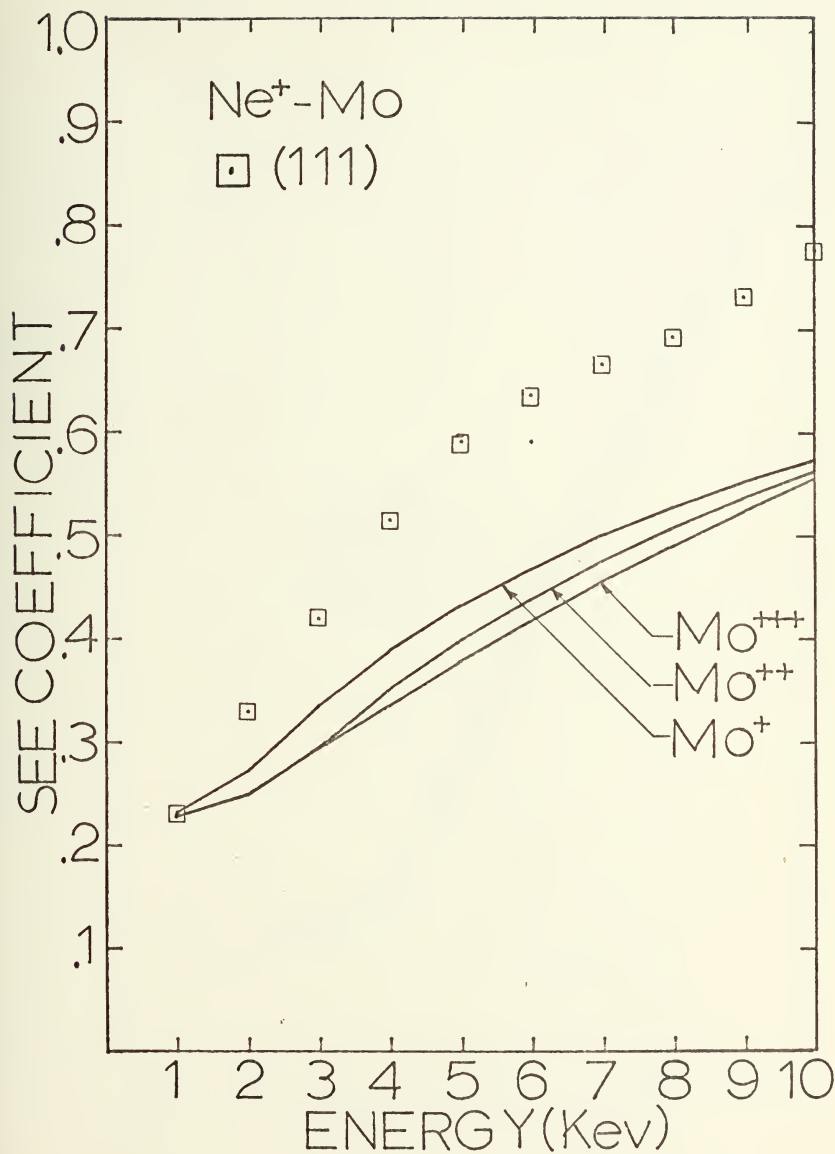


Figure 37. Effect of varying target atom ionization in the HCM model on secondary electron emission from the Ne⁺ - Mo system.

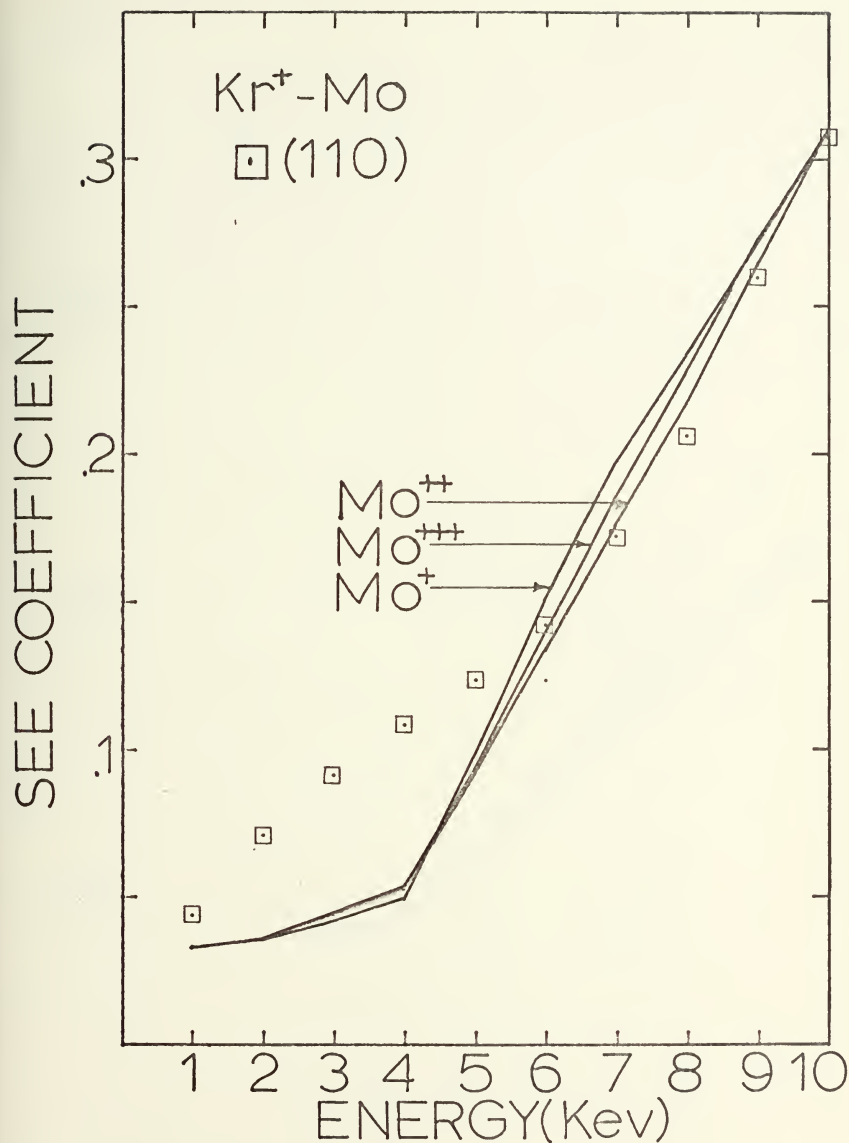


Figure 38. Effect of varying target atom ionization in the HCM model on secondary electron emission from the $\text{Kr}^+ - \text{Mo}$ system.

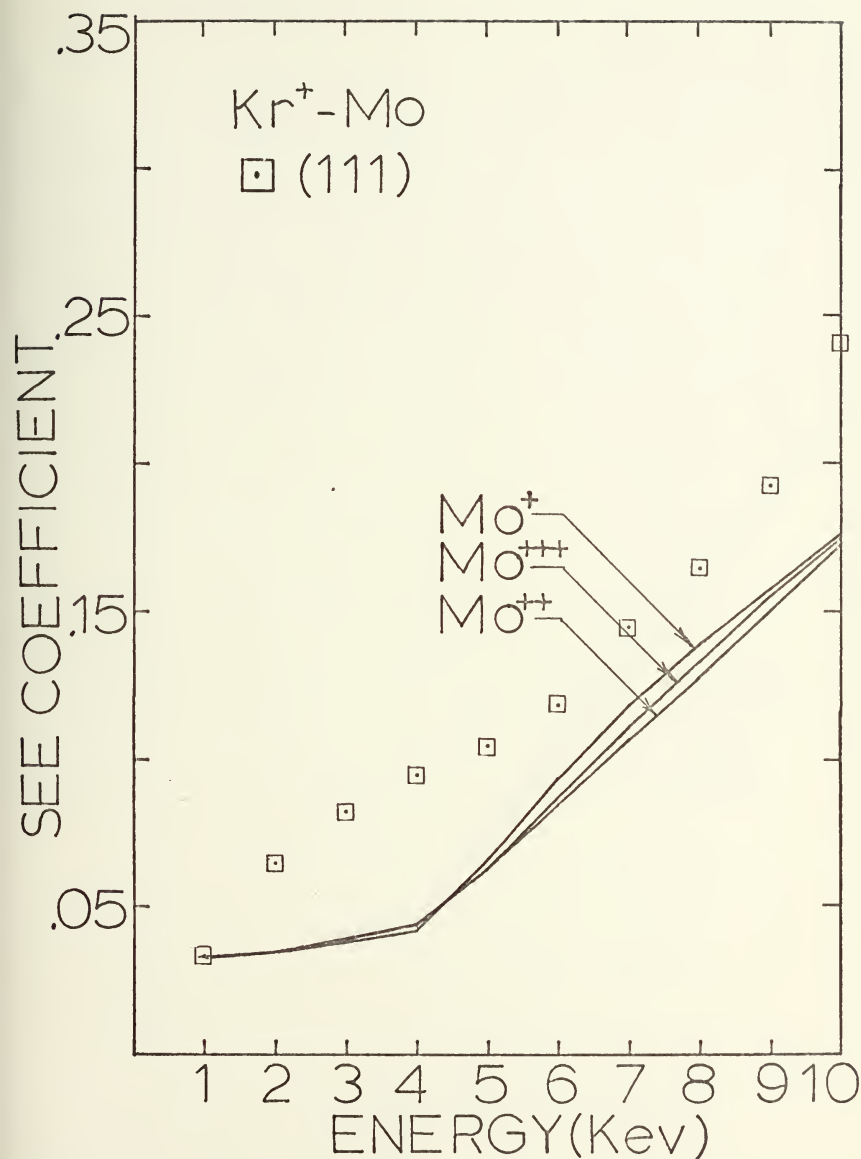


Figure 39. Effect of varying target atom ionization in the HCM model on secondary electron emission from the $\text{Kr}^+ - \text{Mo}$ system.

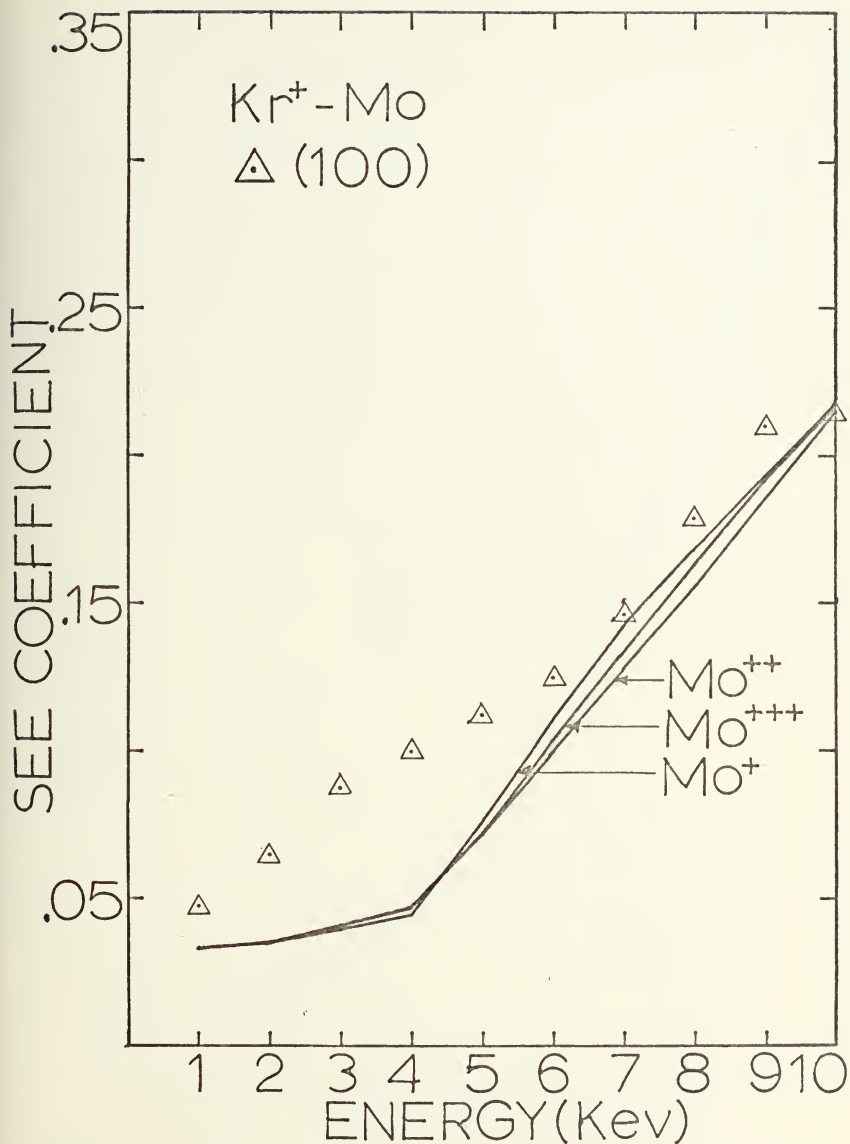


Figure 40. Effect of varying target atom ionization in the HCM model on secondary electron emission from the $Kr^+ - Mo$ system.

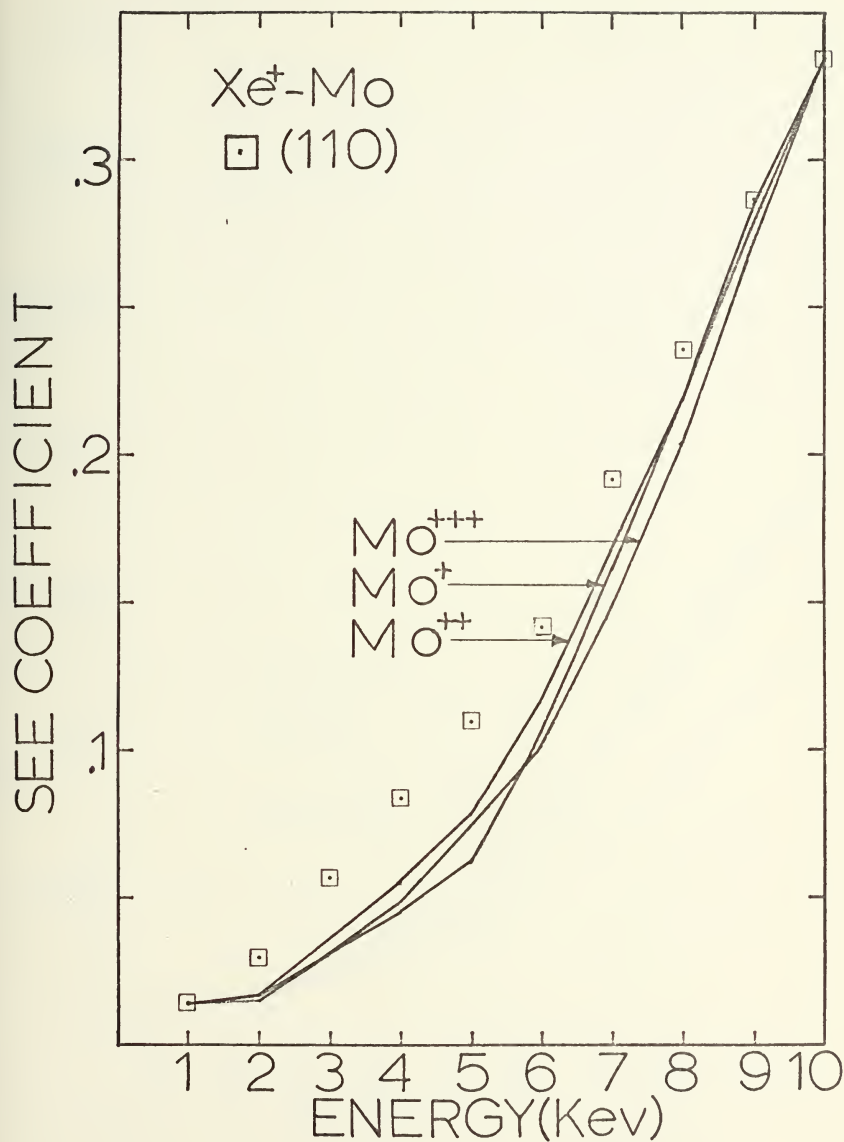


Figure 41. Effect of varying target atom ionization in the HCM model on secondary electron emission from the $\text{Xe}^+ - \text{Mo}$ system.

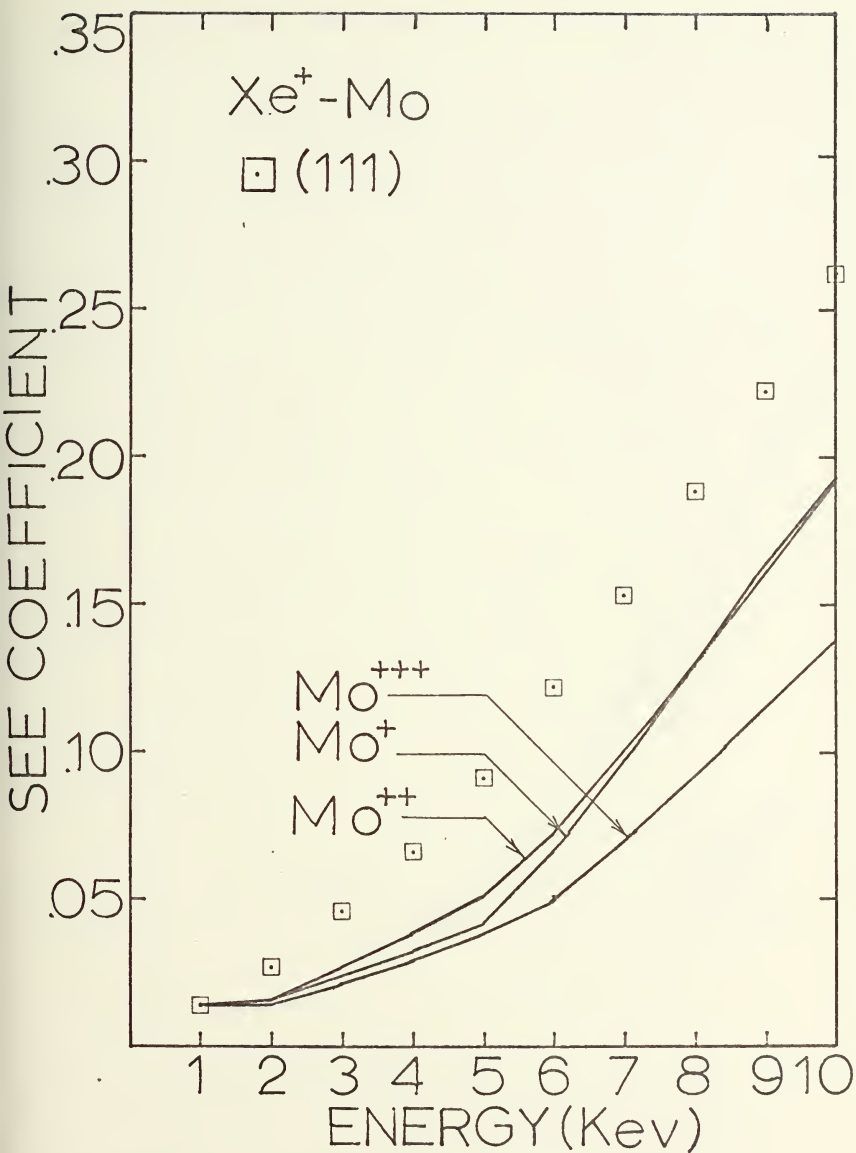


Figure 42. Effect of varying target atom ionization in the HCM model on secondary electron emission from the $\text{Xe}^+ - \text{Mo}$ system.

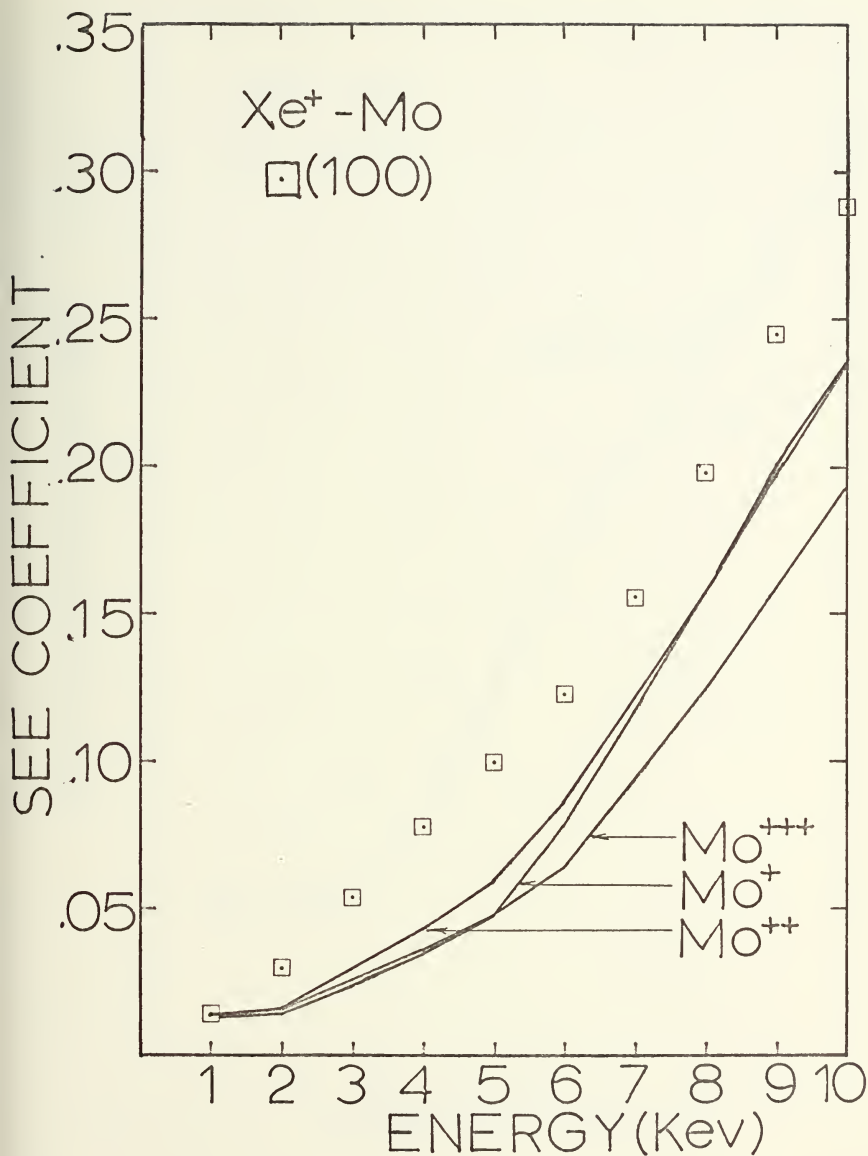


Figure 43. Effect of varying target atom ionization in the HCM model on secondary electron emission from the $\text{Xe}^+ - \text{Mo}$ system.

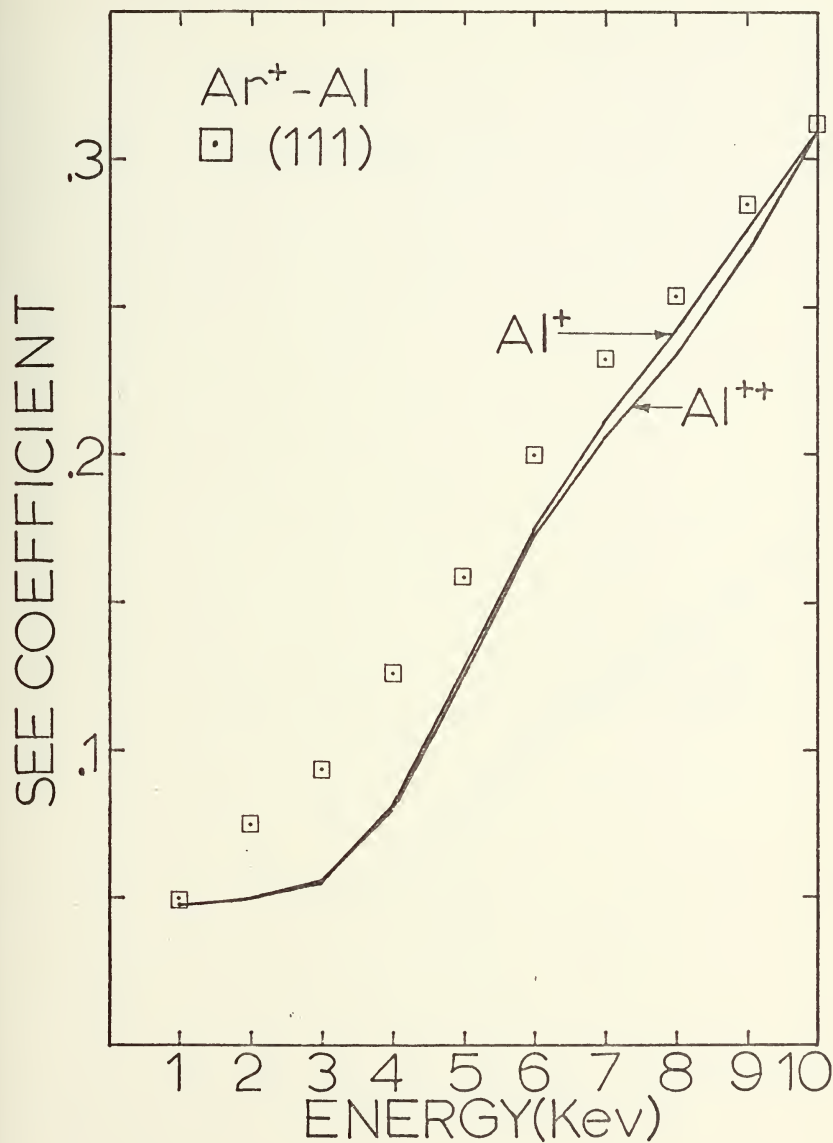


Figure 44. Effect of varying target atom ionization in the HCM model on secondary electron emission from the Ar⁺ - Al system.

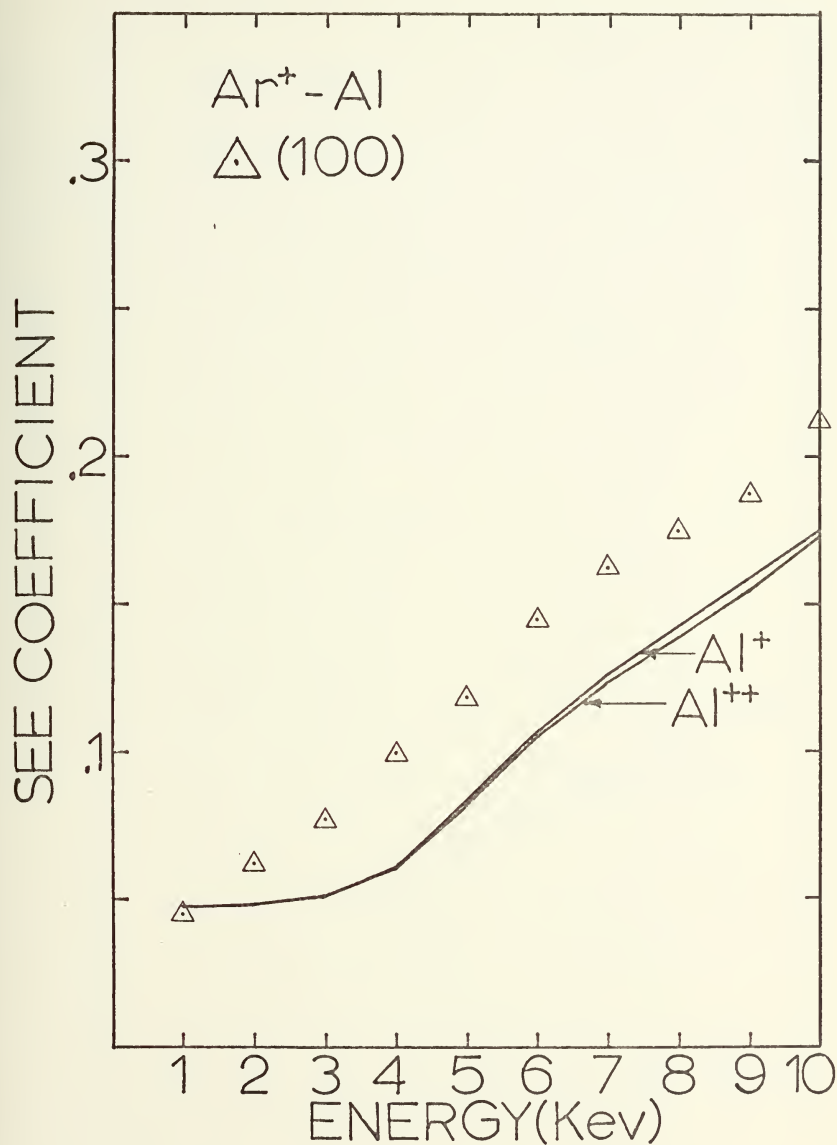


Figure 45. Effect of varying target atom ionization in the HCM model on secondary electron emission from the Ar⁺ - Al system.

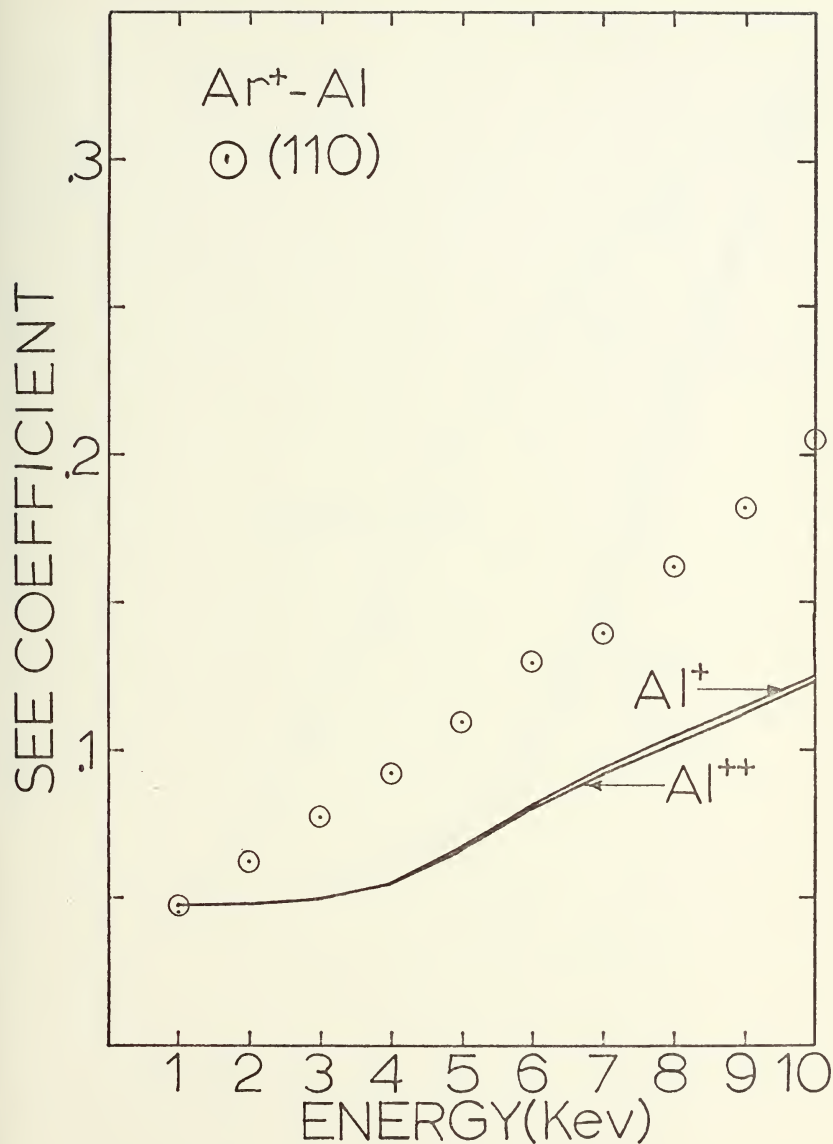


Figure 46. Effect of varying target atom ionization in the HCM model on secondary electron emission from the Ar⁺ - Al system.

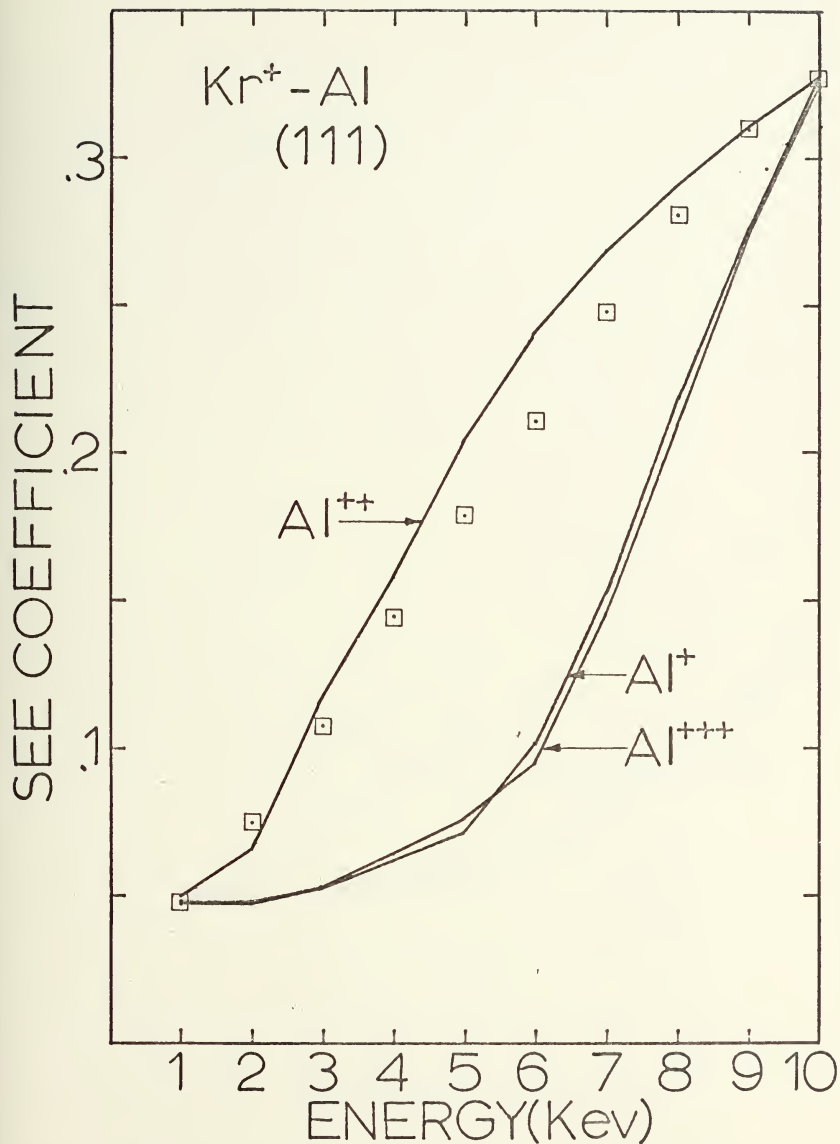


Figure 47. Effect of varying target atom ionization in the HCM model on secondary electron emission from the Kr - Al system.

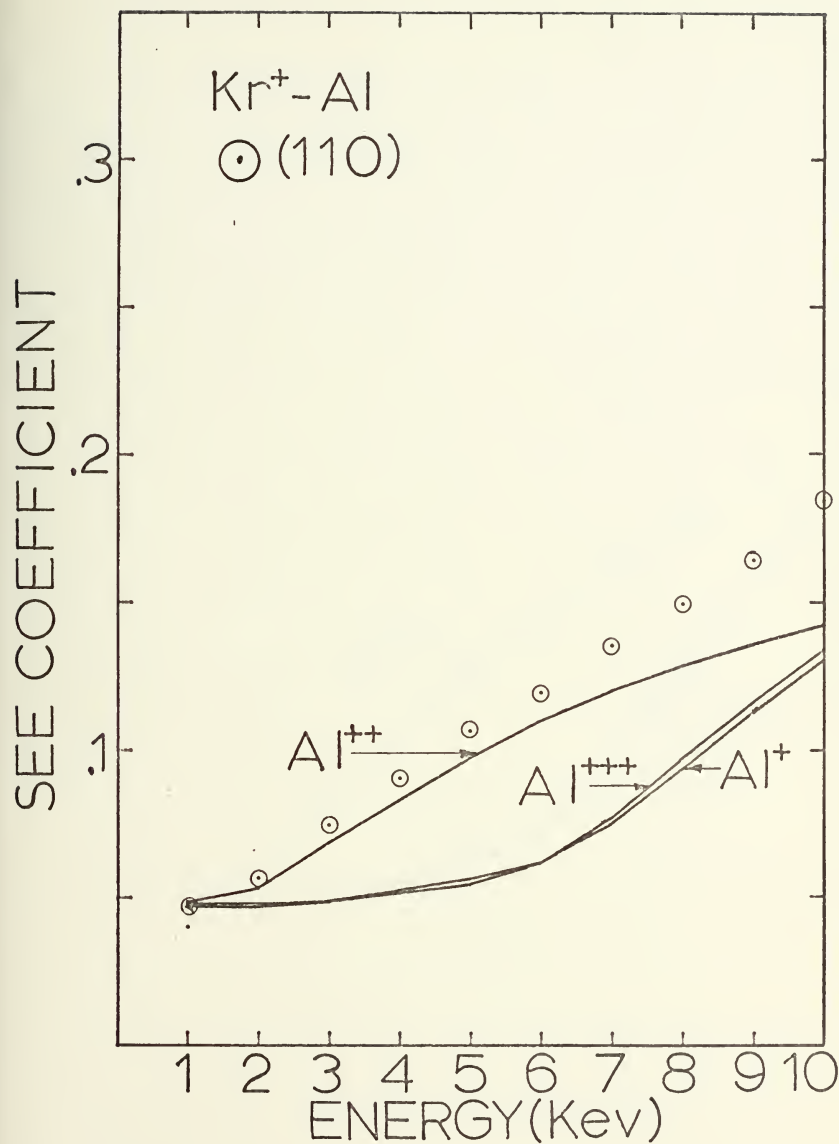


Figure 48. Effect of varying target atom ionization in the HCM model on secondary electron emission from the $\text{Kr}^+ - \text{Al}$ system.

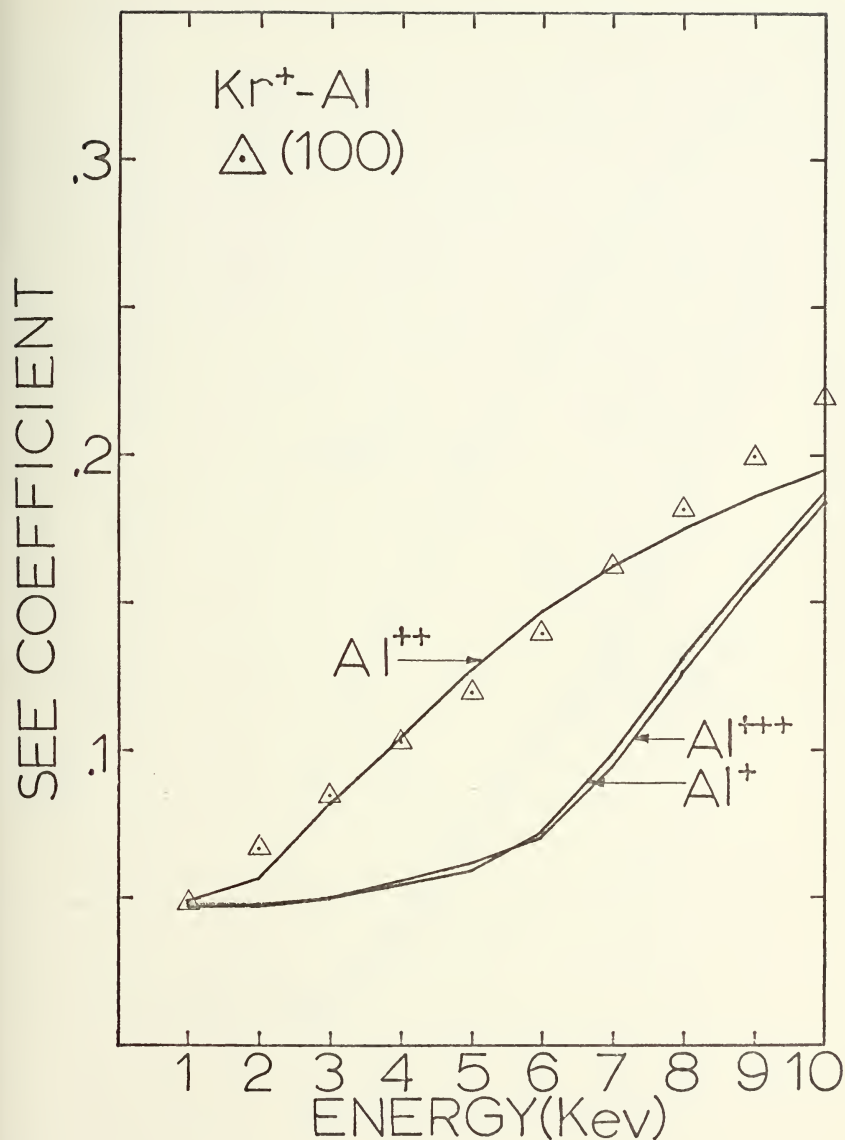


Figure 49. Effect of varying target atom ionization in the HCM model on secondary electron emission from the $\text{Kr}^+ - \text{Al}$ system.

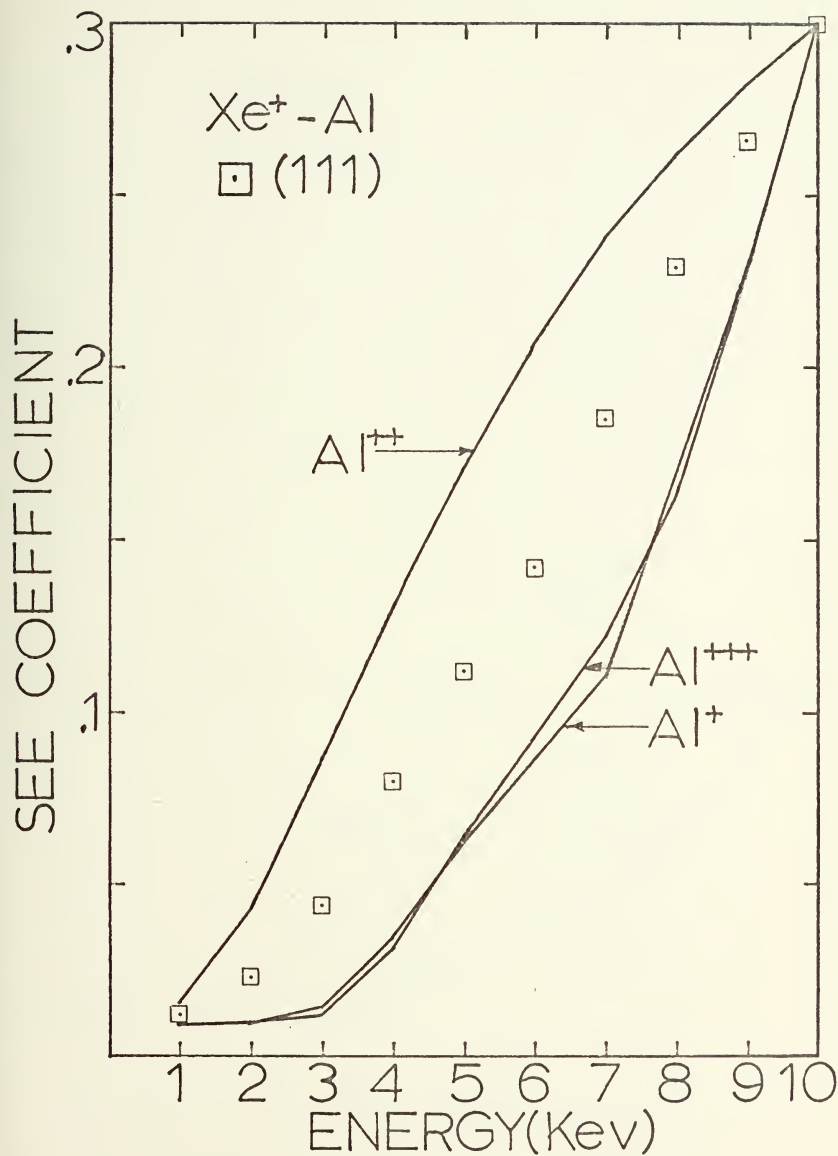


Figure 50. Effect of varying target atom ionization in the HCM model on secondary electron emission from the $\text{Xe}^+ - \text{Al}$ system.

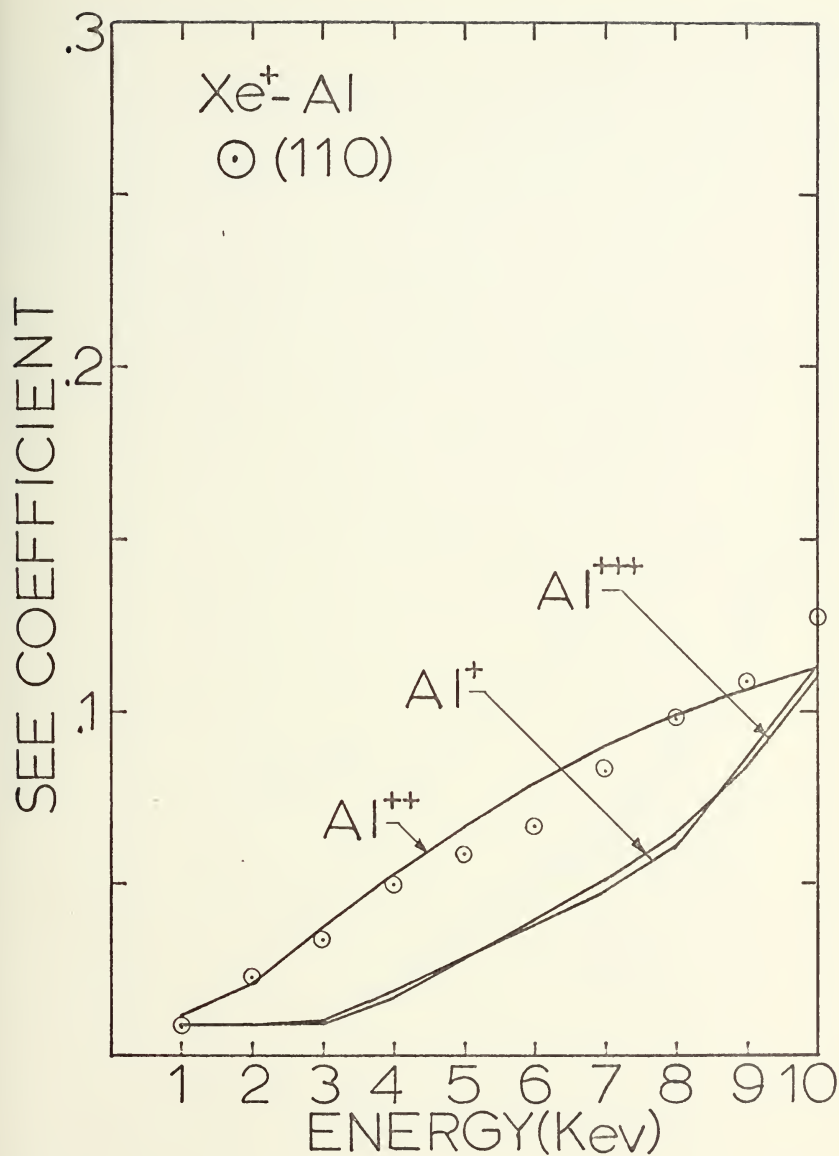


Figure 51. Effect of varying target atom ionization in the HCM model on secondary electron emission from the $\text{Xe}^+ - \text{Al}$ system.

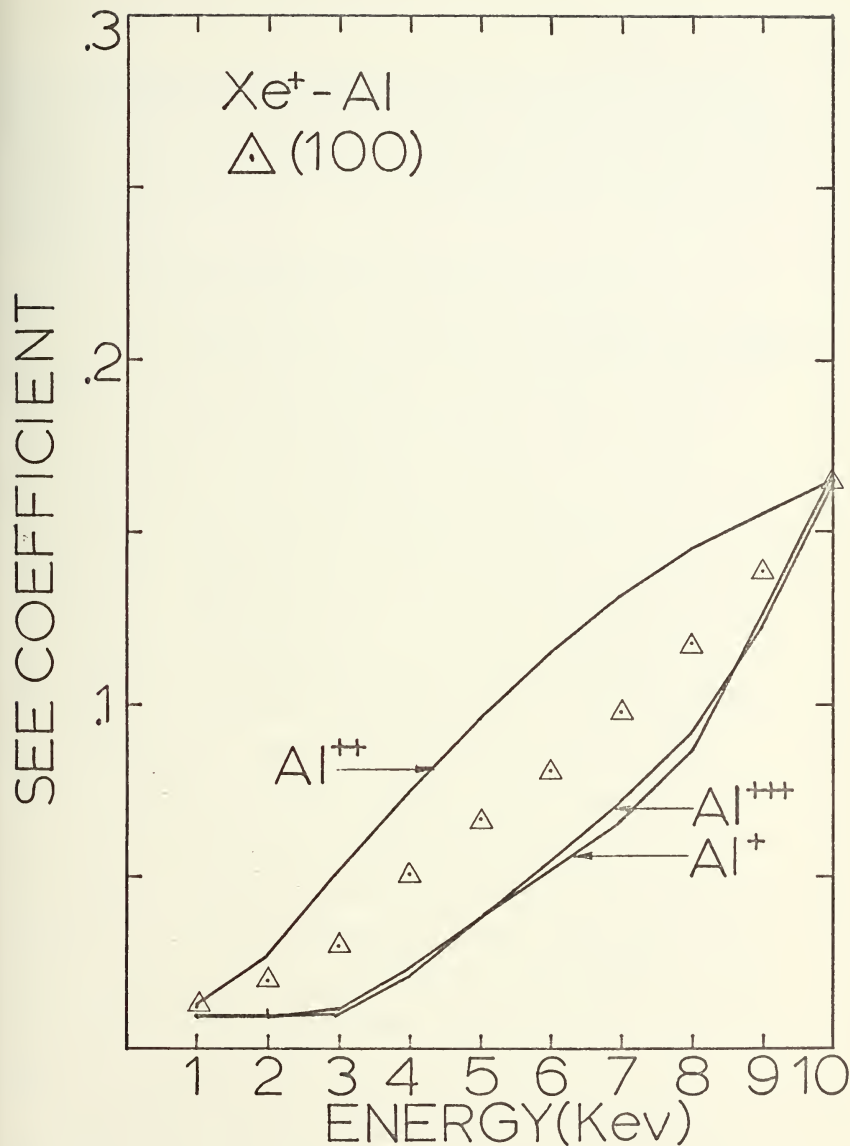


Figure 52. Effect of varying target atom ionization in the HCM model on secondary electron emission from the $\text{Xe}^+ - \text{Al}$ system.

the bombardment of potassium chloride by argon and neon ions normally incident on the (100), (110) and (111) faces of the single crystal. These two cases are discussed in detail below.

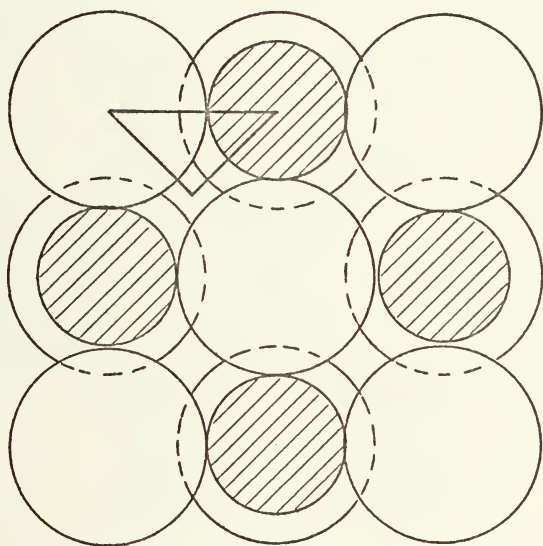
1. Potassium-Chloride Bombarded by Ar Ions

The calculations of the SEE coefficient for alkali-halide single crystals present a theoretical problem that was not addressed when the metal target results were presented. Specifically, the alkali-halide crystals in question have lattice structures comprised of two different atoms arranged in a similar fashion, but displaced in space by a distance $(1/2, 1/2, 1/2)$. Because of this, the standard FCC distribution of impact parameters does not work in the alkali-halide case and must be replaced by a distribution representative of the normal impact of an ion with the target surface. The representative areas and distribution of impact parameters are chosen in a manner similar to that for the metal case, but are weighted to include preferential impact with the larger of the two ion cores in the lattice. The representative areas and distribution of impact parameters are shown in Figures 53 through 57.

The results for KCl bombarded by Ar^+ are shown in Figure 58. Experimentally, it was found that the SEE

REPRESENTATIVE AREA

KCl (100)

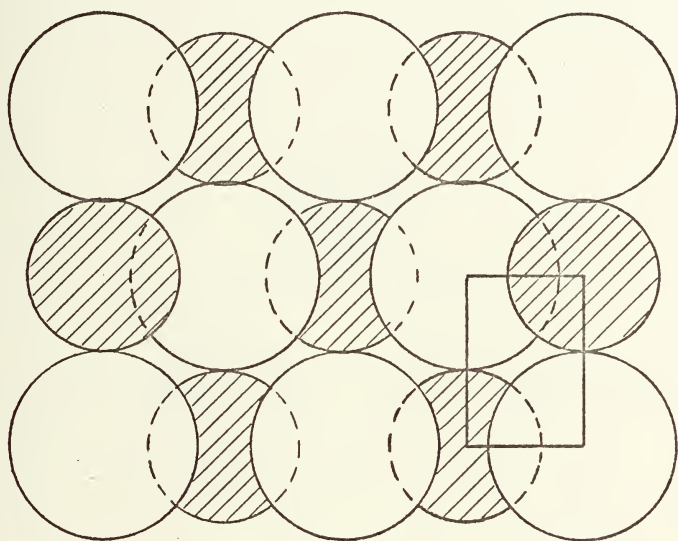


□ Cl atoms

▨ K atoms

Figure 53. Representative area KCl (100).

REPRESENTATIVE AREA
KCl (110)



□ Cl atoms

▨ K atoms

Figure 54. Representative area KCl (110).

REPRESENTATIVE AREA
KCl (111)

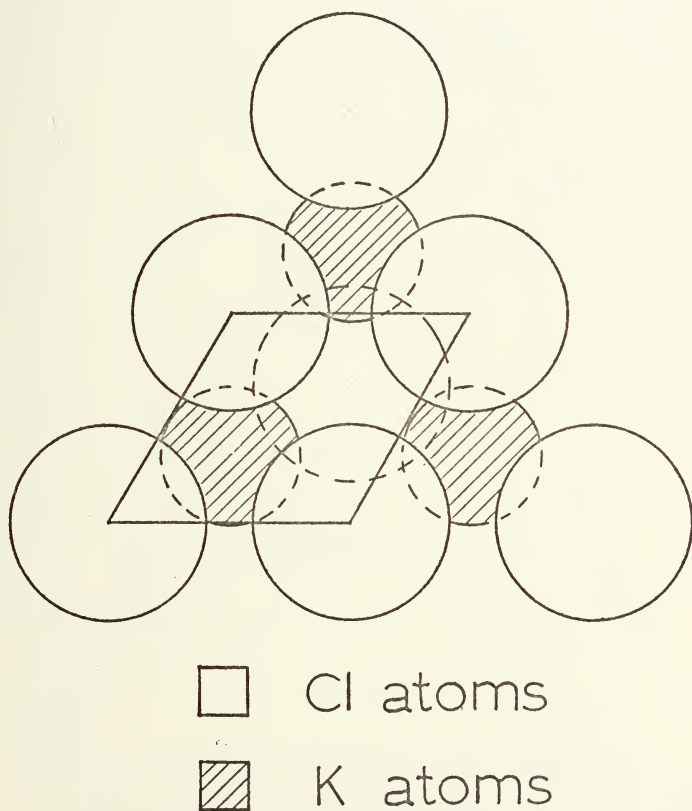


Figure 55. Representative area KCl (111).

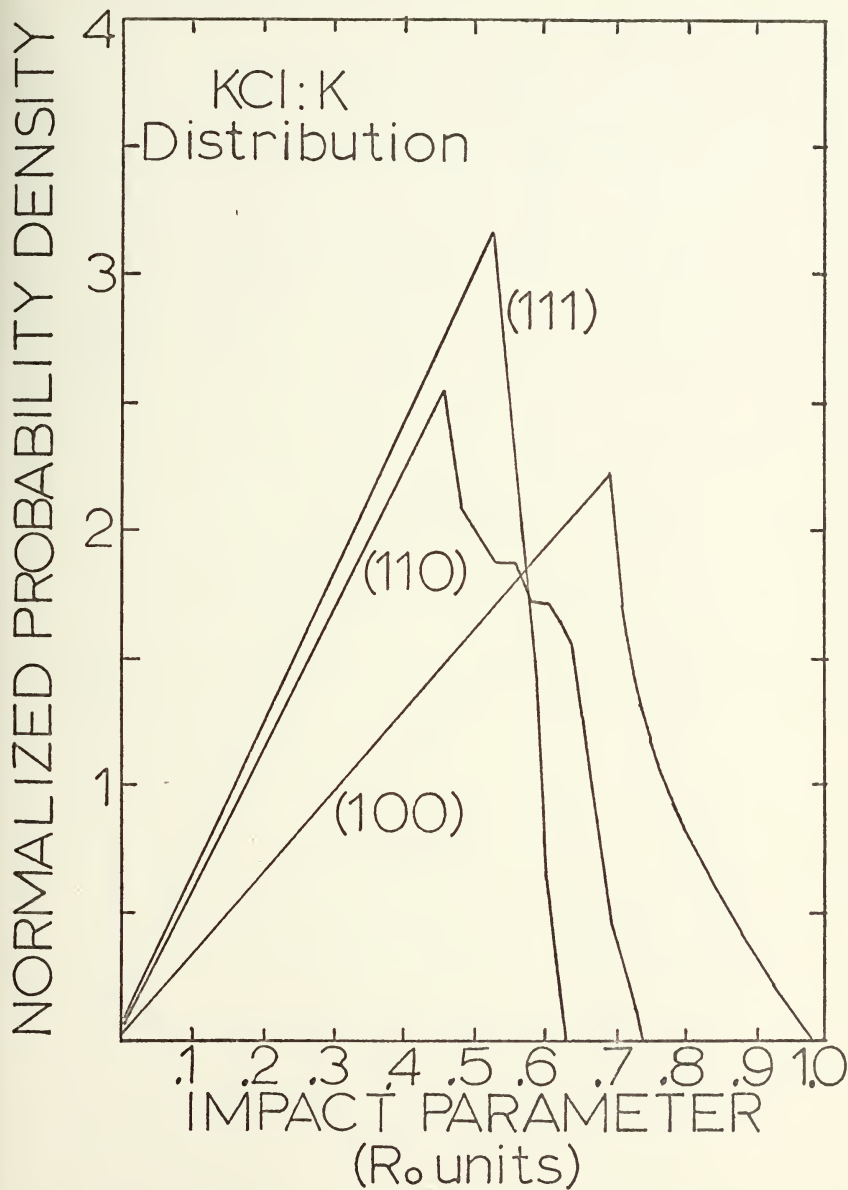


Figure 56. Potassium distribution of impact parameters in KCl.

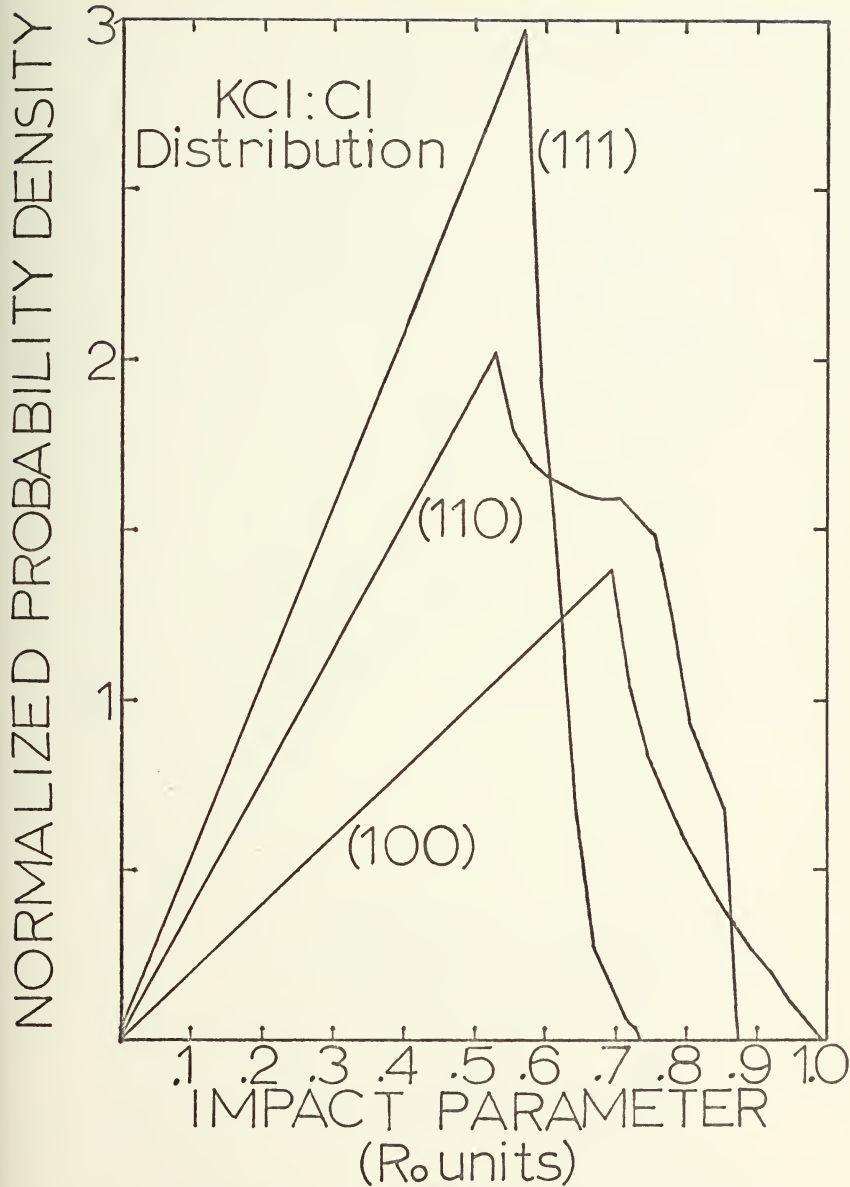


Figure 57. Chlorine distribution of impact parameters in KCl.

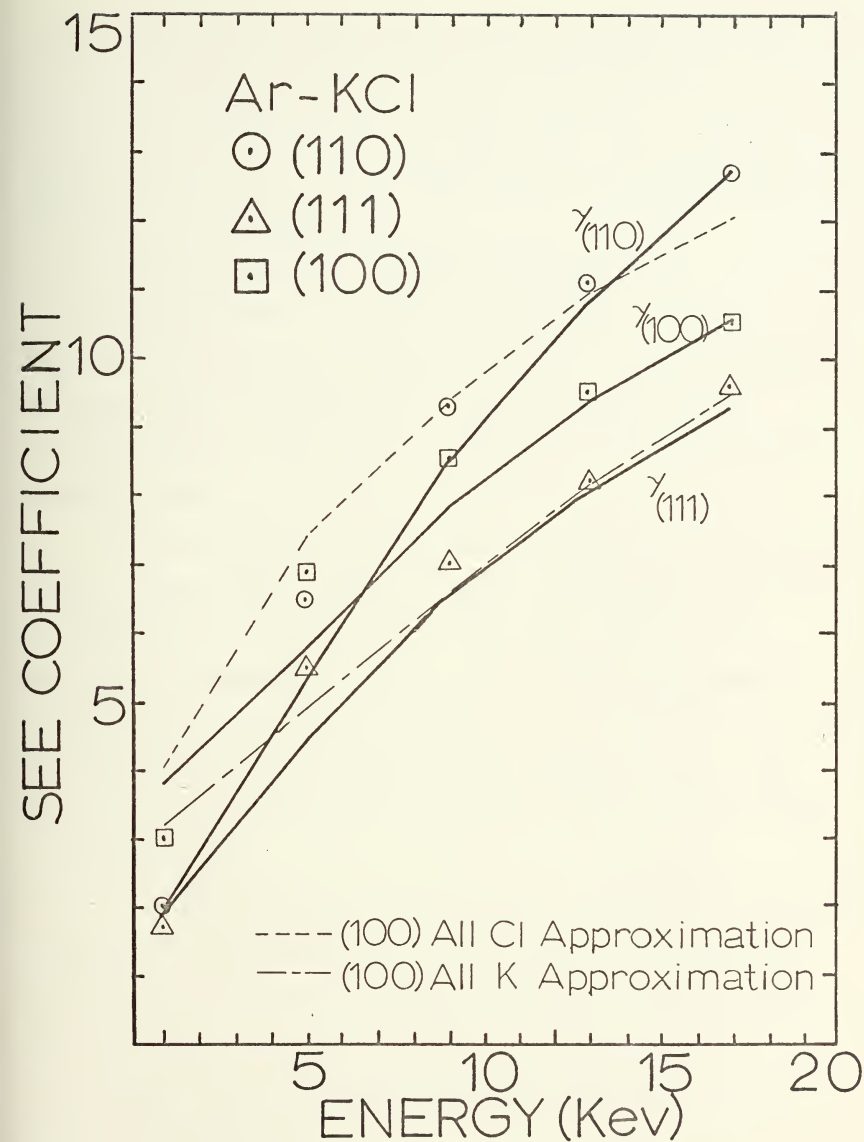


Figure 58. SEE coefficient as a function of energy for KCl bombarded by Ar⁺ ions.

coefficient for the (100) face crossed that of the (110) face in the five to six Kev region. This behavior, as well as that for the (111) and (110) faces, is predicted by the HCM modified model. A PSE contribution is evident but has not been investigated.

2. Potassium-Chloride Bombarded by Ne Ions

In the case of KCl bombarded by Ne^+ , the HCM modified model predicts a crossing of the (100) and (110) surfaces' SEE coefficients as a function of energy at approximately five Kev. Such a behavior is not confirmed experimentally.

In an attempt to explain this anomaly, two theories arose. First, such a behavior can be explained, if the KCl crystal tends to cleave on the (100) face with all the chlorine or potassium atoms up. Second, the crossing behavior might be due to preferential sputtering by the primary ion of one of the two types of atoms comprising the (100) face, leaving a surface that contains either all potassiums or all chlorines.

In the first case, the crystal structure of the (100) face should be the same for both Ar^+ and Ne^+ bombardment, as long as preferential sputtering does not occur. Hence, SEE from this face should be due to the bombardment of either pure chlorine or pure potassium, whichever is left in the "up" position.

In the second case, however, preferential sputtering of chlorine atoms by Ar^+ is the case most likely to occur,

since both the ion and target atom are of comparable mass. In this situation, preferential sputtering would affect the Ar^+ - KCl system more than it would the Ne^+ - KCl system. Since the Ar^+ - KCl system's SEE coefficient as a function of energy is accurately predicted for all surfaces examined, it appears that sputtering is not directly responsible for the results that are obtained from either system.

The effect of an all-potassium or all-chlorine approximation to the KCl (100) surface on the SEE coefficient as a function of energy and primary ion type is shown graphically in Figures 58 and 59.

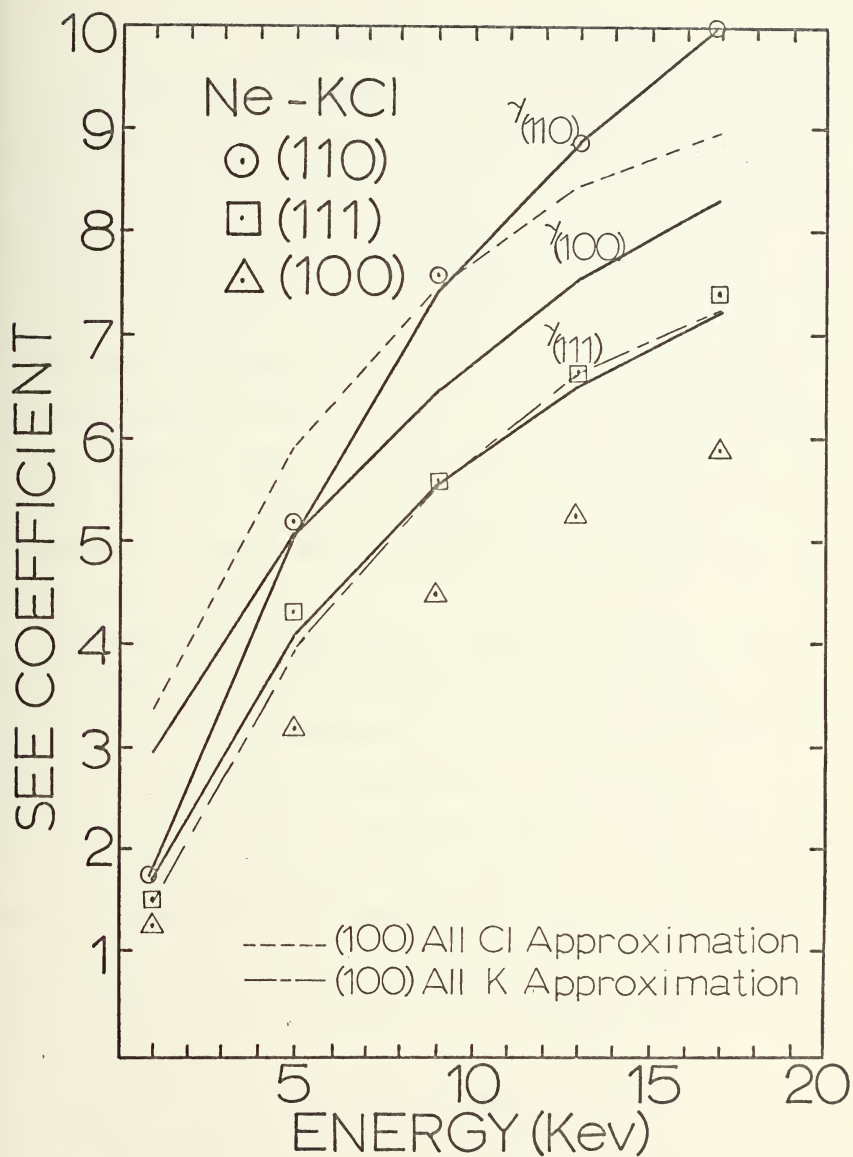


Figure 59. SEE coefficient, as a function of energy for KCl bombarded by Ne^+ ions.

VIII. CONCLUSIONS AND RECOMMENDATIONS

This thesis has attempted to predict the behavior of the coefficient of ion electron emission for various primary ion-target combinations using the Harrison, Carlston and Magnuson theory of secondary electron emission. Three aspects of secondary electron emission were investigated, including angularly dependent secondary electron emission from the (100) face of a copper single crystal rotated about $\langle \bar{1}10 \rangle$, secondary electron emission from Ar, Ne, Kr and Xe ions normally incident on the (100), (110) and (111) faces of Cu, Ag, Mo and Al single crystals, and secondary electron emission from Ar and Ne ions normally incident on the (100), (110) and (111) faces of KCl.

According to the HCM theory, angularly dependent results do not demonstrate the non-monotonic dependence on the angle of incidence found experimentally. Even so, the HCM theory does accurately model the dependence of the SEE coefficient of angle of incidence for inert gas ions normally incident on a polycrystalline metal surface. For this reason, it appears that the single collision model is not sophisticated enough and further modification must be made to it, if secondary electron emission from rotated, single-crystal faces is to be predicted.

In the case of metal targets bombarded by inert gas ions, it was found that the SEE coefficient as a function of energy, predicted by the modified HCM model, deviated from that experimentally obtained. This was contrasted with the results obtained using HCM's original model which yielded

reasonable results in almost all cases investigated. Since the modifications presented here were refinements to the original HCM model, it was hoped the results obtained would more accurately represent the secondary electron mechanism. For this reason, the difference between the SEE coefficient obtained here and the experimental result was identified as the potential secondary electron emission component operating at higher energies. Such a hypothesis is substantiated by experiment [1]. Analysis showed that the potential component in general rose to a peak and then decreased at higher energies. Furthermore, this component of secondary emission seemed to demonstrate behavior that could possibly be attributed to primary ion type as well as the face of the crystal being bombarded. The reason for this behavior was not positively identified, but the PSE process appears to be more complicated than was originally thought.

In the case of potassium-chloride bombarded by Ar ions, the HCM model fairly accurately predicted the SEE coefficient in the zero to 20 Kev energy range for all faces examined. On the other hand, potassium-chloride bombarded by Ne ions demonstrated a crossing of the SEE coefficient for the (100) and (110) faces as a function of energy which was not predicted experimentally. Two hypotheses were proposed that might possibly explain this behavior. The first hypothesis proposes that KCl cleaves with either all the potassium atoms or all the chlorine atoms up, essentially presenting a uniform layer of pure potassium or chlorine to the bombarding ion

beam. This hypothesis slightly improved the SEE coefficient for the Ne^+ KCl (100) surface, but adversely affected the results obtained for the Ar^+ - KCl system. The second hypothesis assumes that the (100) surface of KCl might demonstrate preferential sputtering. However, if this were the case, preferential sputtering should have been most evident in the Ar^+ - KCl system, because of the comparable mass of Ar and Cl. Since this system demonstrated the correct behavior without invoking the preferential sputtering assumption, it was surmised that preferential sputtering did not play an important role in the SEE process from the KCl (100) surface.

In all cases tested in the present investigation, the SEE coefficient as a function of energy tended to become a better approximation to the experimental results at higher energies. For this reason, it is recommended that primary ion-target atom combinations be run for primary ion energies between ten and 20 Kev. If in fact the potential component of secondary electron emission is real in this energy range, it should reach some constant value as primary ion energy is increased. Furthermore, because results obtained using the modified HCM model are dependent on the ion core configuration of the target atoms, it is recommended that more work be done in testing the influence of ion-target atom core ionization on secondary electron emission. Typically, for secondary electron emission from elements such as Cu and Ag, which appear in column I of the periodic table, the

ion core electron configuration is uniquely determined by considerations of the atomic valence, but the effect of the electronic structure of the ion core upon KSE for Mo and Al needs more investigation.

APPENDIX A

COMPUTER PROGRAMS

In this appendix, the parameters that appear in the computer programs are presented and explained. Variables that appear in the data input as constants are stated as such. A pictorial representation of how these data are entered into the programs is shown in Figures 12 - 16.

A. HERMAN SKILLMAN RADIAL ELECTRON DENSITY PROGRAM

CARD #	NAME	FORMAT	DESCRIPTION
1	HEADER CARD - CONTAINS 80 CHARACTERS OF INFORMATION DESCRIBING THE CASE TO BE RUN		
2	KEY	(I4)	SEE Reference (), 0
2	TOL	(F8.6)	" , 000001
2	THRESH	(I4)	" , 521
2	MESH	(I4)	" , 1
2	IPRATT	(I4)	" , 40
2	MAXIT	(I4)	" , 0
2	NOCOPY	(I4)	" , 0
2	KUT	(I4)	" , 0
3-A*	RU2(I)	(IPE15.7, IP4E14.7)	Normalized self-consistent potential as a function of X. Taken directly from Reference 16. This is a "starter" for generating the wavefunctions for the atom under investigation.
B	Z	(F4.0)	Atomic number of atom in question
B	NCORES	(I4)	No. of shells of atom in question
B	NVALES	(I4)	0
B	ION	(I4)	Degree of ionization of atom in question
C	NNLZ(I)	(I4)	n,l,m quantum no. for shells
C	WWNL(I)	(F4.0)	No. electrons in shell
C	EE(I)	(F8.4)	Trial eigenvalue for each shell, taken from Reference 16.

B. POTENTIAL PROGRAM

CARD #	NAME	FORMAT	DESCRIPTION
1	INUC	(I2)	0
1	KSTEP	(I3)	10
1	AZ	(F3.0)	Atomic no. of the first atom following the header card below.
1	AI	(F2.0)	Ionization of the first atom following the header card.
1	BZ	(F3.0)	Atomic no. of the second atom following the header card.
1	BI	(F2.0)	Ionization of the second atom following the header card.
1	DM	(F2.0)	5
1	RM	(F2.0)	5
1	RTEST	(F2.0)	5
1	DD	(F5.1)	.020
1	FRR	(F5.1)	1.20
1	DRS	(F5.1)	.010
1	IPN	(I4)	1
2	HEADER CARD - CONTAINS 30 CHARACTERS OF INFORMATION DESCRIBING THE CASE TO BE RUN		
3	OUTPUT FROM ELECTRON DENSITY PROGRAM WITH FIRST CARD REMOVED CORRESPONDING TO THE ATOM DESCRIBED BY AZ AND AI ABOVE		
4	OUTPUT FROM ELECTRON DENSITY PROGRAM WITH FIRST CARD REMOVED CORRESPONDING TO THE ATOM DESCRIBED BY BZ AND BI ABOVE		

C. DISTRIBUTION OF IMPACT PARAMETERS PROGRAM

CARD #	NAME	FORMAT	DESCRIPTION
1	HEADER CARD - 80 CHARACTERS OF INFORMATION DESCRIBING THE CASE TO BE RUN		
2	ICODE	(I3)	1, if representative area is a rectangle 2, if representative area is a triangle
2	A	(F10.4)	Height of representative area in Ro units.
2	B	(F10.4)	Length of representative area in Ro units.
2	INUMBER	(I3)	No. of atoms in representative area.

C. DISTRIBUTION OF IMPACT PARAMETERS PROGRAM (Continued)

CARD #	NAME	FORMAT	DESCRIPTION
3	LARGE(I)	(I2)	Logical array that indicates if any particular atom is larger than the other, i.e., Cl in KCl. 1, yes. 2, no. If yes the distribution is skewed to indicate preferential collision with the larger atom.
4	SCALEF	(F10.4)	1.0
4	RNA	(F10.4)	Ionic radius of smaller of two atoms.
4	RCL	(F10.4)	Ionic radius of larger of two atoms--Both RNA and RCL can be set to anything if atoms are both the same size.
5-7	A5(I,J)	(3F10.4)	An array that contains the (x,y) vertices of a triangular representative area in Ro units. If the area is not triangular, they can be set to anything.
8-11	A6(I,J)	(3F10.4)	An array that contains the (x,y,z) position of atoms in the representative area in Ro units. I runs from 1 to INUMBR, J runs from 1 to 3.
12	PHI	(F10.4)	Angle in radians x'-axis makes with x-axis.
12	XR	(F10.4)	(x) position of (x',y') origin.
12	YR	(F10.4)	(y) position of (x',y') origin.
12	ALPHA	(F10.4)	Angle in radians the representative area is rotated through.
12	RMAX	(F10.4)	Maximum impact parameter expected. The no. 250 is usually sufficient.

D. NUMERICAL INTERPOLATION PROGRAM

CARD #	NAME	FORMAT	DESCRIPTION
1	NPOINT	(I4)	No. points from the distribution of impact parameters program to be smoothed.
1	IFLAG	(I4)	1, indicates written output only. 2, indicates written output, card output and graphical output desired.
2	HEADER CARD - 46 CHARACTERS TO BE OUTPUT WITH GRAPHS		
3	HEADER CARD - 46 CHARACTERS TO BE OUTPUT WITH GRAPHS		
4	OUTPUT FROM DISTRIBUTION OF IMPACT PARAMETERS PROGRAM WITH ALL "NEW ATOM" CARDS REMOVED		

E. KSE PROGRAM

CARD #	NAME	FORMAT	DESCRIPTION
1	LCRYST	(A4)	Crystal type "FCC"/"BCC"
1	LTPE	(I2)	1
1	BMAX(I)	(3F6.4)	Maximum impact parameter in Ro units for each face.
1	PUD(I)	(3F6.4)	R _A for each face in Ro units.
1	ARO(I)	(3F6.4)	No. atoms per representative area in Ro units, for each face.
1	LM(I)	(3I3)	Total number of points in each distribution.
1	KM	(I4)	250
1	FACL	(F7.4)	(2) ^{1/2} /4 for FCC, (3) ^{1/2} /4 for BCC.
2-A	FLP(I)	(20I4)	Distribution of impact parameters from Interpolation Program.
B	IH1	80A1	80 characters of information.
C	IH3	19A4	76 characters of information from first card of output from Potential Program.
C	KMR	(I4)	250
D	APSI(I)	10F8.5	Wave functions from the Potential program, Atom A.
D	BPSI(I)	10F8.5	Wave functions from the Potential program, Atom B.

E. KSE PROGRAM (Continued)

CARD #	NAME	FORMAT	DESCRIPTION
E	V(I)	5F12.5	Potential between atoms A and B from the Potential Program.
F	EA(I)	8F8.4	Spectroscopic ionization potentials, numbers 11 to 18.
F+1	IAH	4A4	16 characters of accounting information.
F+1	EA(I)	10F8.4	Spectroscopic ionization potentials, numbers 1 to 10.
F+2	JFIT	I10	No. of values to which results are fit.
G	PSE(I)	(F5.3)	γ_{PSE} experimental for curve being fit.
G	FIT(J)	(F5.4)	γ experimental for (111) face at 10 Kev.
H	ZB	F4.0	Atomic no. for atom A.
H	ZT	F4.0	Atomic No. for atom B.
H	BMAS	F8.4	Atomic weight for atom A.
H	TMAS	F8.4	Atomic weight for atom B.
H	EOS	F8.0	Energy in Kev at which results are to start.
H	DEO	F3.0	Energy step in Kev.
H	KEOM	F3.0	Energy in Kev at which results are to end.
H	AO	F7.3	Lattice constant in angstroms.
H	LSKIP	I3	1
H	NM	I3	15
H	RES	F3.0	50
H	DRE	F3.0	50
H	REM	F5.0	5000
H	IH2	4A4	Accounting data.

*indicates that the actual card number varies from run to run and has been replaced by a letter to indicate the order in which the cards are arranged.


```

901C FCRMAT (F8.5,9F7.5)
902C FCRMAT (14,1P3E14.7,I4,1PE14.7)
903C FCRMAT (F4.0,3I4)
904C FCRMAT (5F8.8)
905C FCRMAT (6H,WWW) =F4.0,6H ZZZ= F4.0,6H Z =F4.0,11H NCORES = I4,
1 11H NVALUES = 14,11H NCSPVS= 14/25H CONTROL CARDS INCORRECT. )
906C FCRMAT (6F5.2,F10.3)
907C FCRMAT (14,F4.0,F8.4)
908C FCRMAT (17,F7.0,1PE14.7,OP2(I6,F9.3))
909C FCRMAT (15,1PE14.7))
910C FCRMAT (1PE15.7,1P4E14.7)
911C FCRMAT (10H,NCARDS= 14, 10H MCARCS = I4)
912C FCRMAT (14,2F8.6,5I4)
913C FCRMAT (2F4.0,2F7.3)
914C FCRMAT (6H,ZZI= F4.0,3H ZZZ= F4.0,10H BETA1= F7.3,
1 10H BETA2= F7.3)
915C FCRMAT (7H,KEY= I4)
916C FCRMAT (6H,ITER,7X,1HZ,4X5HDEL A,7X,30H1(DEL) I(CUT) X
1(CUT) )
917C FCRMAT (14,1P3E14.7,I4,1PE14.7,8X,1HZ,I3,I4)
918C FCRMAT (F4.0,3I4,50X,1HZ,I3,I4)
919C FCRMAT (1PE15.7,1P4E14.7,1X,1HZ,I3,I4)
920C FCRMAT (1PE15.7,57X,1HZ,I3,I4)
921C FCRMAT (27HOSIARTING POTENTIALS AND Z=,F4.0,9H,IN ERROR,2F4.0)
922C FCRMAT (140H1I,X,RU3,RUIN1,RUFNL1,RUINL2,RU
1 18,F10.4,1P6E16.7)
923C FCRMAT (18,F10.4,1P6E16.7)
NFILS = 0
10 READ(5,9000)
WRITE(6,9000)
READ(5,512C) KEY,TOL,THRESH,MESH,IPRATT,MAXIT,NOCOPY,KUT
NCARDS=90
WRITE(6,3150) KEY
IF(MAXIT) 20,20,30
MAXIT=20
3C NBLCK = MESH/40
I=1
X(I)=0.0
R(I)=0.0
DELTAX=0.0025
THIRD=1.0/3.0
R6=1.0/2.0
R24=1.0/24.0
R32=1.0/32.0
R315=1.0/315.82734
DC 40 J=1,NBLOCK
DC 35 K=1,40
I=I+1
35 X(I)=X(I-1)+DELTAX

```



```

40 DELTAX=DELTAX+DELTAX
   IF(KEY-1) 60,70,50
50 READ (5,9100) (RU2(M),M=1,441)
   READ (5,9100) (RU3(M),M=1,441)
   ZEG=-0.5*RU2(1)
   ZEE=-0.5*RU3(1)
   GC TO 100
60 READ (5,9010) (RU2(M),M=1,437,4)
   GC TO 100
70 READ (5,9100) (RU3(M),M=1,441)
   ZEE=-0.5*RU3(1)
100 READ (5,9030) Z,NCORES,NVALES,ICN
   IF (Z) 9593,10,110
110 NFILES =NFILES+1
   IZ=Z
   IZ=Z+Z
   NCSPVS=NCORES+NVALES
   C=0.885341387Z**THIRD
   TWCICN=ICN+ICN
   ZZZ=ICN+1
   TWCZZZ = ZZZ+ZZZ
   DC 120 I=2,MESH
   K(I)=C*X(I)
120 PR(I)=1.0/R(I)
   READ (5,9070) (NNLZ(I),WNL(I),EE(I),I=1,NCSPVS)
   WW=0.0
   DC 130 I=1,NCSPVS
130 WW=WW+WNL(I)
   IF(ABS(Z+1.0-WW-W-ZZZ)-0.001) 150,140,140
140 WRITE(6,9050) WW,ZZZ,Z,NCORES,NVALES,NCSPVS
   GC TO 9599
150 IF (KEY-1) 300,400,200
200 IF(ABS(ZE3-ZE2-Z+ZE3)-0.001) 220,220,210
210 WRITE(6,9210) Z,ZE2,ZE3
   GC TO 9999
220 DC 250 I=1,441
250 RU(I)=RU3(I)+RU3(I)-RU2(I)
   GC TO 500
300 TWCZ=IZ
   DC 310 I=1,437,4
310 RU(I)=-RU2(I)+TWCZ
   RU(441)=RU(437)
   RU(445)=RU(437)
   M=5
   DC 350 I=1,457,4
   N=M-1
   IF(M) 320,330,330
320 RU(I+1)=(22.0*RU(I)+11.0*RU(I+1)-RU(I+8))*R32

```



```

RL(I+2)=(10.0*RU(I)+15.0*RU(I+4)-RU(I+8))*R24
RL(I+3)=( 6.0*RU(I)+27.0*RU(I+4)-RU(I+8))*R32
M=9
CC TO 350
330 RU(I+1)=(21.0*RU(I)+14.0*RU(I+4)-3.0*RU(I+8))*R32
    RU(I+2)=( 3.0*RU(I)+ 6.0*RU(I+4)-    RU(I+8))*R8
    RU(I+3)=( 5.0*RU(I)+30.0*RU(I+4)-3.0*RU(I+8))*R32
350 CC CONTINUE
400 GL TO 500
410 IF (ABS(ZE3-Z)-0.001) 410,410,430
420 DC 420 I=1,441
430 RU(I)=RU3(I)
    CC TO 500
430 ZCZ=Z/ZE3
    CC 440 I=1,441
440 RU(I)=RU3(I)*Z0Z
500 V(I)=-S.9E35
    M=FINO(441,MESH)
    IF(RUT) 600,700,600
    CC 610 I=1,M
610 V(I)=RU(I)*RR(I)
620 IF(MESH-M) 620,620,640
630 DC 630 I=442,MESH
640 V(I)=-TWOICN*RR(I)
    LIMIT=MESH
    ICL=MESH
    IC=MESH
    CC TO 500
700 ICL=0
    CC 750 I=2,M
    IF (ICUT) 710,710,730
710 IF (TWOZZZ+RU(I)) 740,740,720
720 ICL=1
730 V(I)=-TWOZZZ*RR(I)
    CC TO 750
740 V(I)=RU(I)*RR(I)
750 CC CONTINUE
    IF (ICUT) 790,790,800
790 ICL=M
    LIMIT=ICUT
800 IF(MESH-M) 900,900,810
810 CC 850 I=442,MESH
850 V(I)=-TWOZZZ*RR(I)
900 DELTA=1000000.
    NITER=0
    NCNMM=3
    IPRSR=0
    WRITE(6,9160)

```



```

1000 MCARDS=9C
    IF (MAXIT-NITER) 110C,200C,2000
1100 WRITE(6,9220)
    DC 1500 I=1,MESH,5
    WRITE(6,9230) I,X(I),RUINLI(I),RUFNLI(I),
1    RUINL2(I),RUFNL2(I),RU(I)
1500 CCNTINUE
    GC TO 100
2000 DC 2010 I=1,MESH
    RSCORE(I)=C.0
2010 RSVALE(I)=0.0
    DC 2500 M=1,NCSPVS
    E=EE(M)
    NN=NNLZ(M)/100
    LAM=NNLZ(M)/10 -10*NN
    XL= LAM
    CALL SCHEQ(Z,E,LAM,NN,KKK,MESH,C,THRESH)
    IF (M-NCCKES) 2100,210C,2200
2100 DC 2150 I=1,KKK
    SAL(M,I)=SNLC(I)
2150 RSCORE(I)=RSCORE(I)+WWNL(M)*SNLC(I)*SNLG(I)
    GC TO 2500
2200 DC 2250 I=1,KKK
    SAL(M,I)=SNLG(I)
2250 RSVALE(I)=RSVALE(I)+WWNL(M)*SNLG(I)*SNLO(I)
2300 AKKK(M)=KKK
    MCARDS=MCARDS+2+((KKK-1)/40)*8
2500 EE(M)=E
    DC 2600 I=1,MESH
    RSATOM(I)=RSCORE(I)+RSVALE(I)
    RUEXCH(I)=-6.0*(I)*RSATOM(I)*R315)*THIRD
2600 A1=C.0
    ASUM=0..C
    RI=0..C
    PSUM=0..C
    F=0.0025*C
    I=1
    XI(I)=0.0
    XJ(I)=0.0
    DC 2620 J=1,NBLOCK
    DC 2610 K=1,40
    I=I+1
    A2=RSATOM(I)*0.5
    A1=A1+A2
    E2=A2*KKK(I)
    E1=E1+B2
    XI(I)=ASUM+A1*H
    XJ(I)=BSUM+B1*H

```



```

261C  A1=A1+A2
      B1=B1+B2
      ASUM=XJ(I)
      BSUM=XJ(I)
      A1=A2
      B1=B2
2620  F=F+H
      DC 2650 I=1,MESH
      XJ(I)=-T2+2.0*(XJ(I)+R(I))*(XJ(MESH)-XJ(I))
      XJ(I)=XJ(I)+RUEXCH(I)
265C  CUNTINUE
      DC 2700 I=1,MESH
      RUINL1(I)=RUINL2(I)
      RUENL1(I)=RUENL2(I)
      RUENL2(I)=RU(I)
      RUENL2(I)=XJ(I)
270C  NITER=NITER+1
      PDELTA=DELTA
      DELTA=C.0
      DC 2800 I=1,LIMIT
      SALC(I)=RU(I)-XJ(I)
      XJ(I)=ABS(SNLC(I))
      IF (XJ(I)-DELTA) 2800,2800,2750
275C  DELTA=XJ(I)
280C  CUNTINUE
      WRITE(9,9080) NITER,Z,DELTA,IDELTA,X(IDELTA),ICUT,X(ICUT)
      IF (DELTA-YCL)+.000,3000,3000
300C  IF (IPRSW) 310C,310C,315C
310C  DC 3110 I=2,LIMIT
311C  RU(I)=C.5*(RU(I)+XJ(I))
      IF (MESH-LIMIT) 3140,3140,3120
312C  RLZ=XJ(MESH)
      RATIO=(RUZM-RU(LIMIT))/(RUZM-XJ(LIMIT))
      DC 3130 I=LIMIT,MESH
      RU(I)=RUZM-RATIO*(RUZM-XJ(I))
313C  LIMIT=MESH
314C  IPRSW=IPRATT
      GC TO 3500
315C  IF (NCON) 3100,310C,3160
316C  IF (DELTA-DELTA) 3170,3170,3200
317C  NCON=NCON+1
      IF (NCON) 3100,310C,3200
320C  ALPH=0.5
      DC 3300 I=2,ICUT
      XAUM(I)=RUINL1(I)*RUFNL2(I)-RUINL2(I)*RUFNL1(I)
      DEAM(I)=RUENL2(I)-RUFNL2(I)+RUINL1(I)
      IF (ABS(DEAM(I)/RUINL2(I))-0.0001) 3210,3210,3220

```



```

3890 XI(I)=V(I)-VLAST
3900 XI(I)=0.0
NCARDS=50
CC 3990 M=1,NCSPVS
K={NKK(M)-1}/40
F=C.0025*C
FH=0.5*H
ASUM=0.0
AL=0.0
I=1
CC 3960 J=1,K
CC 3940 L=1,40
I=I+1
A2=XI(I)*SNL(M,I)*SNL(M,I)
AL=AL+A2*H
ASUM=ASUM+AL-A2*HH
F=F+H
F=F+H
AL=HH*A2
EE(M)=EE(M)+ASUM
3950 NCARDS=NCARDS+3*K+2
GC TO 1000
WRITE (6,9110) NCARDS,MCARDS
4000 NC=1
WRITE(6,9180) Z, NCCRES,NVALES,ICN,IZ,NC
CC 4190 I=1,441
IF(TWOION+RUINL2(I)) 4190,4190,4120
DC 4140 M=1,441
RUINL2(M)=-TWOION
GC TO 4200
4150 CONTINUE
4200 CC 4220 MIN=1,440,5
MAX=MIN+4
NC=NC+1
WRITE(6,9190)(RUINL2(M),M=MIN,MAX),IZ,NC
4220 WRITE(7,9970) Z,ICN
FORMAT(10.1,I5)
9970 WRITE(7,9960){RSATCM(I),I=1,441}
WRITE(6,9960){RSATCM(I),I=1,441}
FORMAT(5E15.7)
9960 NC=NC+1
WRITE(6,9200) RUINL2(441),IZ,NC
CC 4400 M=1,NCSPVS
ALZ=NLZ(M)
KKK=NKK(M)
XL=NLZ/10-10*(NLZ/100)
DP=XL+1.0
CC 4350 I=1,4

```



```

A(I,1)=1.0
A(I,2)=R(I+1)
A(I,3)=R(I+1)*R(I+1)
A(I,4)=R(I+1)*A(I,3)
A(I,5)=SNL(M,I+1)*RR(I+1)**LP
4350 CALL CRCSYM (4)
NC=NC+1
WRITE(6,9170) NLZ,XL,EE(M),WWNL(M),KKK,A(1,5),IZ,NC
K1=KKK-1
CC 4380 MIN=1,K1,5
NC=NC+1
MAX=MIN+4
WRITE(6,9190) (SNL(M,I),I=MIN,MAX),IZ,NC
4430 CCNTINUE
NC=NC+1
WRITE(6,9200) SNL(M,KKK),IZ,NC
44CC IF(KEY-1) 4420,4440,4480
442C KEY=1, I=1, MESH
444C DO 4460 I=1, MESH
4460 RU(I)=RU(I)
ZE3=Z
GC TO 100
448C CC 4490 I=1, MESH
RU(1)=RU(1)
4490 RU(1)=RU(1)
ZE2=ZE3
ZE3=Z
GC TO 100
9995 TIME=0.01*ITIME(XX)-START
STOP
END

SUBROUTINE SCHEQ(IZ,E,LAM,NN,KKK,MESH,C,TFRESH)
DIMENSION P(5),W(5),I(5),D(5)
COMMON CCMI,V(521),R(521),RU(521),RSATCM(521),RSVALE(521),
2 XI(521),XJ(521),RSCORE(521),RUFNL1(521),RUFNL2(521),RUFNL3(521),
3 RUINL1(521),RUINL2(521),RUINL3(521),RUINL4(521),RUINL5(521),
4 XNUM(521),DENM(521),SALD(521),CC(521),RR(521),
5 NLZ(24),WWNL(24),KKK(24),EE(24),A(4,5),SNL(24,521)
MANY = 200
MCRV=0
LESSV=0
LEMCRE=0.0
ELESS=0.0
MCRS=0
LESS=0

```



```

DE=0.0
NPRINT=C
LAMX=LAM-1
LAMP=LAM+1
XLP=LAMP
NCCR=MM-LAMP
B=LAM*LAMP
CC=R(12)
H=C
HSQ=H*H
B3=(V(3)-V(2))/H-Z/HSQ
Y=F+H*4*LAM+6
FLPS=4*LAM+6
SLPT=C*LAM+12
ELPT=3*LAM+20
AL=-Z/XLP
YSG=Y*Y
BI=-Z
A1=A*BI
A2=A*BI
A3=A*BI
RAISE H AND Y TO LAM+1
FIL=H
FIL=Y
IF(LAM) 105,120,100
105 NSTOP=105
GC 10 9900
100 I=1,LAM
FIL=FIL*H
110 YIL=YIL*Y
120 HI=HSQ
HCF=BI/H
RTH=BI/H
BQS=BOHS+BOH*BTH
BGL=0.25*BCHS+0.50*BOH+BTH+BTH
FPL=8*LAM
XIFC=C*.21701389E-4
START OUTWARD INTEGRATION
EG=E
200 NPRINT=NPRINT+1
EPS=E-EG
EG=E
IF (MANY-NPRINT) 9920,210,210
210 DC 220 I=1,MESH
220 SNLQ(I)=0.0
IF(NPRINT-1) 225,300,400
225 NSTOP=225

```



```

30C GC TO 9900
310 DC 310 I=4,MESH
31C CC(I)=V(I)+B*RR(I)*RR(I)-E
31E M=MESH
330 DC 330 I=4,MESH
32C IF(CQ(M)) 320,330,330
330 IK=R+1
33C GC TO 350
330 M=M-1
C Q IS EVERYWHERE POSITIVE
330 NSTCP=330
350 GC TO 9900
360 IF(MESH-1K) 360,360,430
36C EPS = E+EPS
400 DC 420 I=4,MESH
42C CC(I) = CQ(I)-EPS
430 GC TO 315
43C NCRCSS=0
L=CC
Y=F+H
BZ=3.0*Z/H-E+2.0*V(2)-V(3)
A2=(A1+B2)/FLPS
A3=(A2*B1+A1*B2+B3)/SLPT
A4=(A2*B1+A2*B2+A3B3)/ELPT
P(3)=(1.0+H*(A1+H*(A2+H*(A3+H*A4))))*HIL
P(4)=(1.0+Y*(A1+Y*(A2+Y*(A3+Y*A4))))*YIL
Q(3)=B3+B2
Q(4)=B4+B2
SNLL(2)=P(3)
SNLU(3)=P(4)
I=3
DX=CQ
H1=H**2
H2=H1/2.0
T(3)=P(3)*{(1.0-H2*C(3))}
T(4)=P(4)*{(1.0-H2*C(4))}
L(4)=T(4)-T(3)
NCCUNT=3
NIN=2
I=I+1
44C IF END OF MESH IS REACHED, MODIFY TRIAL EIGENVALUE
C IF (1-MESH) 460,450,450
45C IF(NCK-NCROSS) 800,500,900
C RETURN TO BEGINNING OF OUTWARD INTEGRATION IF NECESSARY
460 S(5)=Q(I)
IF(IK-I) 700,700,500

```



```

50C D(5)=D(4)+H1*Q(4)*P(4)
    T(5)=D(5)+T(4)
54C IF(1.0-ABS(H2*Q(5))) 450,450,540
    P(5)=T(5)/(1.0-H2*Q(5))
545 SNO(1)=P(5)
    IF(SIGN) 550,545,560
    NSTCP=545
    GO TO 5500
550 IF(P(5)) 580,580,570
56C IF(P(5)) 570,580,580
570 NCROSS=NCROSS+1
    CUNT CHANGES IN SIGN
    SIGN=SIGN
560 NCOUNT=NCOUNT+1
58E IF(7-ACOUNT) 585,590,600
    NSTCP=585
    GO TO 5900
59C NCOUNT=2
60C NINF=NINT+1
605,610,620 IF(40-NINT) 605,610,620
605 NSTCP=605
    GO TO 5900
61C DX=DX+DX
    H=DX
    F1=F**2
    F2=H1/I2.0
    NINT=0
620 T(5)=P(5)*(1.0-H2*Q(5))
    T(3)=P(3)*(1.0-H2*Q(3))
    D(5)=T(5)-T(3)
    CC 650 K=1,4
    P(K)=P(K+1)
    T(K)=T(K+1)
    C(K)=D(K+1)
    C(K)=C(K+1)
    GO TO 440
65C IF(ACOUNT-2) 705,710,500
70C IF(ACOUNT-2) 705,710,500
705 NSTCP=705
    GO TO 5900
71C IF(NINT-4) 500,500,720
    IF(MATCHING RADIUS HAS BEEN REACHED GOING OUT
72C IF(NUCH NOT EQUAL TO NCROSS,MODIFY TRIAL EIGENVALUE
    EIGEN=E-NCROSS) 800,1000,900
720 IF(NUCK-NCROSS) 800,1000,900
    MCREV=1
80C TCC MANY CROSSINGS, INCREASE ABSF(E)
    MCREV=MCREV+1
    IF(MCREV-1) 805,830,820

```



```

805 NSTOP=805
820 GC TO 9900
830 IF (E-MORE) 830,840,840
840 E-MORE=E-MORE
845 IF (LESS) 845,860,990
860 NSTOP=945
870 GC TO 9500
880 E=1.2*EG
890 GC TO 200
900 LESS=1
910 IF (CROSSINGS, DECREASE ABSF(E)
920 SV=SV+1
930 SV-1) 905,920,910
940 IF (LESS) 940,960,990
950 NSTOP=9500
960 GC TO 9500
970 IF (EL-ESS-E) 920,930,930
980 E-ESS=E
990 IF (MORE) 935,950,990
1000 NSTOP=995
1010 GC TO 9200
1020 E=0.75*EG
1030 GC TO 200
1040 E=C*.5*(E-MORE+E-LESS)
1050 GC TO 200
1060 IF (ABS(SNLC(I-1))-ABS(SNLC(I-2))) 1010,1040,1040
1070 CHECK TO SEE THAT WAVE IS IN THE DAMPED REGION (ABSCLUTE VALUE
1080 DECREASES AND SIGNS ALIKE)
1090 IF (P(3)) 1020,1500,1030
1100 IF (SNLC(I-2)) 1100,500,500
1110 IF (SNLC(I-2)) 500,500,1100
1120 IF (1.0E+25 -ABS(P(5))) 900,900,500
1130 LARGE ABSOLUTE VALUE OF P IN WHAT SHOULD BE THE DAMPED REGION
1140 INDICATES TOO FEW PEAKS, DECREASE ABSF(E)
1150 NCA-NCR=NCROSS AND MATCHING RADIUS LIES IN DAMPED REGION
1160 IMATCH=1-2
1170 XPMATCH=P(I-2)
1180 PPCUT=(I(4)-I(2))-0.5*(P(4)-P(2))/H
1190 S=PPCUT/P(3)
1200 INTEGRATION IS BY 8 APPLICATIONS OF NEWTON-COTES CLOSED
1210 QUADRATURE FOR FIVE INTERVALS ON EACH BLOCK
1220 XIFC=(5*H(BLOCK 1)/288)/2, H(1)=0.0025*SCALE FACTOR
1230 SUM1=0
1240 XIF=XIFC
1250 I=1
1260 VALUE=0.0
1270 MN=E
1280 SUM2=0.0
1290 XIF=XIF+XIF
1300
1310

```



```

112C Y=VALUE
      VALUE=SNLO(I+5)**2
      SUM2=SUM2+19.0*(VALUE+Y)+75.0*(SNLO(I+4)**2+SNLO(I+1)**2)
      I=I+50.0*(SNLC(I+2)**2+SNLO(I+3)**2)
      IF(IMATCH-I) 1125,1150,1130
1125 NSTOP=1125
      GC TO 9900
1130 MY=MY-1
      IF(MY) 1135,1140,1120
1135 NSTCP=1135
      GC TO 9900
1140 SLV1=SUM2*XIF+SUM1
      GC TO 1110
1150 SLV1=SUM1+SUM2*XIF
1160 P1=SUM1/P(3)**2
      P1*CH=P(3)
      IF(NN-1) 1165,1170,1180
1165 NSTOP=1165
      GC TO 9900
117C X1N=EP1*XMATCH
      FLR N=1, START INWARD INTEGRATION AT(8+LAM)*XMATCH CR X MAX
      GC TO 1200
118C X1N=FPL*XMATCH
      FLR N=1, START AT (5+LAM)*XMATCH OR X MAX (END CF MESH
120C GC 1220 I=1, MESH,40
      IF(X1N-R(I)) 1210,1210,1220
1210 KKK=I
      GC TO 1250
122C KKK=MESH
1250 I=KKK
      DX=R(I-1)-R(I)
      F=DX
      XIF=0.1736111E-1*DX
      FSC=H*H
      FSC12=H*SQ/12.0
      G(3)=G(1)
      P(3)=EXP(-R(I)*SQRT(G(3)))
      SUM3=P(3)/Q(3)
126C I=I-1
      G(4)=G(1)
      P(4)=EXP(-R(I)*SQRT(G(4)))
      IF(ABS(P(4))-1.0E-35) 1280,1280,1300
128C KKK=KKK-40
      IF(KKK-IMATCH) 129C,1250,1250
129C WRITE(6,5030) Z, NN, LAM, KKK
      P(3)=1.0E-35
      KKK=KKK+40

```



```

P(4) = 1.5E-35
1300 IF (PMATCH, 1310, 1305, 1320
1305 NSTCP=1305
GC TO 9500
1310 P(3)=-P(3)
1320 P(4)=-P(4)
SNLC(I+1)=P(3)
SNLC(I)=P(4)
T(3)=P(3)*{(1.0-HSQ12*Q(3))
T(4)=P(4)*{(1.0-HSQ12*Q(4))
D(4)=T(4)-T(3)
DC 1350 M=2,40
1330 I=I-1
G(5) = G(I)
G(5) = HSQ*G(4)*P(4)+D(4)
T(5) = D(5)+T(4)
P(5) = T(5)/(1.0-HSQ12*Q(5))
IF (MATCH, 1335
NSTCP=1335
GC TO 9500
1340 SNLC(I)=P(5)
DC 1350 K=1,4
P(K)=P(K+1)
T(K)=T(K+1)
Q(K)=D(K+1)
Q(K)=Q(K+1)
G(5) = G(I-2)*P(4)+D(4)
D(5) = D(5)+T(4)
T(5) = T(5)/(1.0-HSQ12*Q(5))
P(5) = 1.0335*P(4)+0.2734375*P(5)-0.546875*P(3)+0.21875*P(2)-
1 G.0396625*P(1)
I=I-1
DX=DX/2.0
Q(5) = Q(I)
H=DX
HSG=H*H
HSG12=HSG/12.0
T(5)=P(5)*{(1.0-HSQ12*Q(5))
T(4)=P(4)*{(1.0-HSQ12*Q(4))
D(5)=T(5)-T(4)
SNLC(I)=P(5)
DC 1380 L=1,4
P(L)=P(L+1)
T(L)=T(L+1)
Q(L)=D(L+1)
Q(L)=Q(L+1)
GC TO 1330
1380

```



```

C      MATCHING RADIUS HAS BEEN REACHED CCMING IN
1400  K=KKK
      VALUE=SNLC(K)*SNLC(K)
      GC TO 1420
1410  SUM3=SUM3+XIF*SUM4
      XIF=XIF*0.5
1420  MM=8
      SUM4=0.0
1430  Y=VALUE
      VALUE=SNLO(K-5)*SNLO(K-5)
      SUM4=SUM4+19.0*(VALUE+Y)+75.0*(SNLO(K-1)**2+SNLO(K-4)**2)
1      K=K-5
      IF(K-IMATCH) 1435,1450,1440
1435  NSTCP=1435
      GC TO 9500
1440  MM=MM-1
      IF(MM) 1445,1410,1430
1445  NSTCP=1445
      GC TO 9900
1450  SUM3=SUM3+XIF*SUM4
      S3=SUM3/P(4)**2
      PFIN=(I(5)-I(3))-0.5*(P(5)-P(3))/H.
      S4=PIN/P(4)
      DE=(S2-S4)/(S1-S3)
      DE*P=DE/E
      IF(ABS(DE/E)-THRESH) 2000,1460,1460
1460  E=E+DE
      IF(E) 200,1480,1480
1480  WRITE(6,9670) E,DE
9670  FORMAT(2E10.5)
      DE=0.5*DE
      GC TO 1460
C      IMPROVE TRIAL EIGENVALUE BY PERTURBATION THEORY IF NECESSARY
C      CALCULATE THE NORMALIZED WAVE FUNCTIONS
2000  PCP=PMATCH/P(4)
      DC 2010 J=IMATCH,KKK
2010  SNLC(J)=SNLC(J)*PCP
      SUM1=0.0
      J=1
      XIF=XIFC
      VALUE=C.0
2020  MM=8
      XIF=XIF+XIF
      SUM2=0.0
      SUM2=SUM2+XIF
      Y=VALUE
2030  VALUE=SNLC(J+5)*SNLC(J+5)

```



```

SUM2=SUM2+19.0*(VALUE+Y)+75.0*(SNL0(J+4)**2+SNL0(J+1)**2)
1  +50.0*(SNL0(J+2)**2+SNL0(J+3)**2)
J=J+5
MM=MM-1 2035,2040,2030
IF(MM) 2035
ASTCP=2035
GC TO 9900
2040 SUM1=SUM1+XIF*SUM2
2045 ASTCP=2045
IF(KKK-J) 2045,2050,2020
2050 GC TO 9900
C1=SQRT(SUM1)
IF(SNLC(3)) 2060,2055,2070
2055 NSTOP=2055
GC TO 9900
C1=-C1
2060 GC 2080 I=1,KKK
2070 SNLC(I)=SNLC(I)/C1
2080 RETURN
9900 WRITE( 6,9020) NSTOP
STOP
9920 WRITE (6,9010) NN,LAM,Z
STOP
9010 FORMAT (20H NO CONVERGENCE ON, I4, I1, F4.0)
9020 FORMAT (5HCSTOP, I4, 8HIN SCHEQ)
9030 FORMAT (6HOAT Z=, F6.0, 6H NL =, I3, I1, 7H KKK =, I5, 22H IS LESS THA
IN IATCH =, I5, 43H INWARD INTEGRATION WILL BE TRIED AT KKK+40)
9600 FORMAT (I4, 2F12.5)
END

```

```

CCCC
SUBROUTINE CPGSYM(M)
SIMULTANEOUS EQUATION SOLVER
WRITTEN BY I.C. HANSON, SCIENTIFIC COMPUTATION DEPARTMENT,
LOCKHEED MISSILES AND SPACE COMPANY, SUNNYVALE, CALIFORNIA
SOLVE M SIMULTANEOUS EQUATIONS BY THE METHOD OF CROUT
COMMON/CGM1/(521),R(521),RU(521),RU2(521),RU3(521),X(521),
X1(521),XJ1(521),RSCOFF(521),SATOM(521),RSVALE(521),
2 RUINL1(521),RUINL2(521),RUENL1(521),RUENL2(521),RUEXCH(521),
3 XNUM(521),DENM(521),SNLC(521),C(521),RR(521),
N=1
NNLZ(24),MMNL(24),INKKK(24),EE(24),A(4,5),SNL(24,521)
I1=1
I2=11
100 SUM=ABS(A(I1,I1))
DC 120 I=I1,M
IF(SUM-ABS(A(I1,I1))) 110,120,120
110 I2=I

```



```

12C SLN=ABS(A(I,I1))
    CC CONTINUE
13C IF(I3-I1) 130,15C,130
14C DC 140 J=1,N
    SUM=-A(I1,J)
15C A(I1,J)=A(I3,J)
    A(I1,J)=SUM
16C I3=I1+1
    I=I3,M
17C CC 160 I=I3,M
    A(I1,I1)=A(I,I1)/A(I1,I1)
    I3=I1+1
18C IF(J2) 18C,20C,18C
    CC 190 J=I3,N
19C DC 190 I=I1,J2
    A(I1,J)=A(I1,J)-A(I1,I)*A(I,J)
20C IF(I1-M) 200,220,200
    J2=I1+1
    I=I1+1
    CC 210 I=I1,M
    DC 210 J=I1,J2
21C A(I1,I1)=A(I,I1)-A(I,I)*A(J,I1)
22C IF(I1-M) 100,170,100
    CC 24C I=I,M
    J2=M-I
    I3=J2+1
    A(I3,N)=A(I3,N)/A(I3,I3)
    IF(J2) 230,250,230
230 CC 240 J=I,J2
24C A(J,N)=A(J,N)-A(I3,N)*A(J,I3)
25C RETURN
    END
//CC.SYSIN DD *

```


[illegible]


```

9030 READ(5,5030) IH
      ECRMAT(2044)
      CCUT=DM
      RS=DD
      RT2=K*TEST*RTTEST
      FLRS=0.5*DRS
      ZMAX=RTTEST
      CZ=DD
      HCC=0.5*DD
      FPD=4.0*PI*DD
      DCR=1.0*DD
      KCM=DM*DUCK
      KPM=KM-1
      KKM=1.0/KM
      KMR=RM*DCR
      KMRM=KMR-1
      KMR=1.0/KMR
      VCCE=AZ*BZ*RKMR
      VCCE=VCCE*RKMR
      CA=0.8853414/AZ**R3
      CB=0.8853414/BZ**R3
      C(1)=CA
      C(2)=CB
      NC=1
      CC TO (5,5,5,4,390,396),INUC
4  N=2
5  DK(1)=DX(1)*C(N)
      DC I=1,10
7  DX(I+1)=DX(I)+DX(I)
      DR(I+1)=DR(I)+DR(I)
      IP2=1
      IP3=1
      IP4=1
      IP5=1
      IP6=1
      IP7=1
      IP8=1
      IP9=1
      IP10=1
      IP11=1
      X(I)=0.0
      RU(I)=0.0
      K=1
      DC I=1,11
      C=DX(I)
      CC TO J=1,40
      K=K+1
      X(K)=X(K-1)+D

```

```

29 565
29 566
MOD9
29 557
29 558
29 559
MOD9
29 561
29 567
MOD9
MOD9
29 814
29 572
29 573
29 574
29 575
29 579
29 581
29 582
29 583
29 584
29 585
29 586
29 587
29 589
29 590
29 591
29 592
29 593
29 594
29 595
29 596
29 597
29 598

```


53 IP5=1
GC TO (61,62,63),IP6
61 IP6=2
CALL FILL(5,1)
GC TO 51
62 IP6=3
CALL FILL(5,21)
GC TO 51
63 IP6=1
GC TO (71,72,73),IP7
71 IP7=2
CALL FILL(6,1)
GC TO 61
72 IP7=3
CALL FILL(6,21)
GC TO 61
73 IP7=1
GC TO (81,82,83),IP8
81 IP8=2
CALL FILL(7,1)
GC TO 71
82 IP8=3
CALL FILL(7,21)
GC TO 71
83 IP8=1
GC TO (91,92,93),IP9
91 IP9=2
CALL FILL(8,1)
GC TO 81
92 IP9=3
CALL FILL(8,21)
GC TO 81
93 IP9=1
GC TO (101,102,103),IP10
101 IP10=2
CALL FILL(9,1)
GC TO 91
102 IP10=3
CALL FILL(9,21)
GC TO 91
103 IP10=1
GC TO (111,112,113),IP11
111 IP11=2
CALL FILL(10,1)
GC TO 101
112 IP11=3
CALL FILL(10,21)
GC TO 101

29 647
29 648
29 649
29 650
29 651
29 652
29 653
29 654
29 655
29 656
29 657
29 658
29 659
29 660
29 661
29 662
29 663
29 664
29 665
29 666
29 667
29 668
29 669
29 670
29 671
29 672
29 673
29 674
29 675
29 676
29 677
29 678
29 679
29 680
29 681
29 682
29 683
29 684
29 685
29 686
29 687
29 688
29 689
29 690
29 691
29 692
29 693
29 694


```

113 IF I1=1
GC TO 300
150 CCNINUE
RT=C.0
K=0
NFS=0
J=41
XX(41)=0.0
XX(41)=1.0E10
160 RT=RT+DD
K=K+1
IF(KMR.LT.K) GO TO 300
170 IF(J-41) 230,180,9999
180 IF(K-1) 9999,200,20
200 XX(1)=XX(41)
CC 210 I=2,41
XX(I)=I*(I-1,1)
XX(I)=I*(I-1,1)
210 UU(I)=I*(I-1,1)
J=J+1
220 IF(J-41) 230,230,20
230 IF(RT-XX(J)) 250,240,220
240 R(K)=RT
R(K)=1.0/RT
FPR20(K)=FPR*RT*RT
245 IF(N-1) 9999,245,345
ACQ(K)=CD*UU(J)
GC TO 260
250 R(K)=RT
R(K)=1.0/RT
FPR20(K)=FPR*RT*RT
IF(N-1) 9999,255,355
255 ACQ(K)=DU*((RT-XX(J-1))*RDX*(UU(J)-UU(J-1))+UU(J-1))
260 ARHO(K)=ADQ(K)/FPR20(K)
APSI(K)=SQRT(ARHO(K))
ARFT(K)=ARHO(K)**FT
AKFOI(K)=AKHO(K)**FCT
J=J-1
IF(K-1) 9999,270,280
270 AQ(K)=ADQ(K)
GC TO 160
280 AQ(K)=AQ(K-1)+ADQ(K)
GC TO 160
300 CCNINUE
IF(N-1) 9999,310,320
310 WRITE(6,9550) AZ,AI

```



```

9550 FCRMAT(IH,1,20X,'NUCLEAR CHARGE WAS',F4.0,' THE ATOM WAS',F4.0,' T
      2 TIMES IONIZED',//)
9580 WRITE(6,9580) ((R(I),ADQ(I),ARHO(I)),I=1,KMR)
      FORMAT(3(F58.3,2F10.5,E10.2))
      WRITE(6,9500)
      GC TO (390.4,400,400), INUC
320 WRITE(6,9535) BZ,BI
9555 FCRMAT(IH0,20X,'NUCLEAR CHARGE WAS',F4.0,' THE ATOM WAS',F4.0,' T
      2 TIMES IONIZED',//)
      WRITE(6,9580) ((R(I),BDQ(I),BRHO(I)),I=1,KMR)
      WRITE(6,9500)
      GC TO 400
345 BQ(K)=DD*UU(J)
      GC TO 360
355 BQ(K)=DD*((RT-XX(J-1))*RDX*(UU(J)-UU(J-1))+UU(J-1))
360 BHC(K)=BC(K)/FPR2D(K)
      BPSI(K)=SQRT(BRHO(K))
      BRFT(K)=BRHU(K)**FT
      BRFOT(K)=BRHO(K)**FOT
      J=J-1
      IF(K-1) 999,370,380
370 BQ(K)=BC(K)
      GC TO 160
380 BQ(K)=BQ(K-1)+BDQ(K)
      GC TO 160
390 CC 395 I=1,KM
      BQ(I)=AQ(I)
      BRQ(I)=ADQ(I)
      BRFO(I)=ARHO(I)
      BPSI(I)=APSI(I)
      BRFT(I)=ARFT(I)
      BRFOT(I)=ARFOT(I)
395 GC TO 400
356 CC 399 K=1,KM
      AC(K)=BC(K)
      ADQ(K)=BDQ(K)
      ARQ(K)=BRQ(K)
      APSI(K)=BPSI(K)
      ARFT(K)=BRFT(K)
      ARFOT(K)=BRFOT(K)
399 CCNTINUE
400 WRITE(6,9530) IH
41C FCRMAT(IH,1,20X,20A4,/,30X,'HETERONUCLEAR MDEL, AUGUST 1969 FORM'
      X,/)
9530 CCNTINUE
50C WRITE(6,9540) DZ,DRS,FRK,RTEST,DD,KSTEP,RM
9540 FCRMAT(10X,DZ=1,F6.3,'DRS=',F6.3,'FRK=',F5.2,'RTEST WAS',
      2 F5.2,' DD WAS',F6.3,' RUN EVERY',13,' STEPS, RMAX =',F5.2,/) MOD9

```

29 770

29 773

MOD9
MOD9
MOD9
MOD9
MOD9
MOD9

MOD9
MOD9
MOD9

MOD7
MOD9

MCD1
MOD6
MOD6
MOD6
MCD9

29 825

MCD7
MOD7
MOD7
MOD7
MOD7

```

VBA1=VBA1+BDQ(J)*RR(J)
VBB1=VBB1+ADQ(J)*RR(J)
VEA2=VBA2+BDQ(J)
VEB2=VBB2+ADQ(J)
VEA3=VBA3+BDQ(J)*R(J)
VEB3=VBB3+ADQ(J)*R(J)
VEA=HRD*(CC1*VBA1+CC2*VBA2+CC3*VBA3)
VEB=HRD*(CC1*VBB1+CC2*VBB2+CC3*VBB3)
VAB=0.0
VAA=0.0
CC 570 J=JPP,KMR
VAA=VAA+BDQ(J)*RR(J)
VAB=VAB+ADQ(J)*RR(J)
DVEE=ADQ(I)*(VAA+VBA+VCA)+BDQ(I)*(VAB+VBB+VCB)
VEE=VEE+DVEE
VSZ=VSZ+DVEE+DVSZ
VSZ=VSZ+JVNN
VSN=VNN+VEE+VNE
VNA=VNN+Q.5*VNE
CALL CLAP(EDD,EXX,FT,FOT,KMR)
VDXC=2.C*(EDD-EXX)
VNA=VNG+VDXC
VK(K)=VSZ+VDXC
VXA=R3*(EDD-2.0*EXX)
VA=VSNA+VDXA
WRITE(6,9600) D,VP(K),VSZ,EDD,EXX,VSNA,VNN,VNE,VEE,VA,VSNA
9600 FORMAT(F10.3,11F10.3)
DVS=0.0
IF(K-KSTEP) 9999,620,700
620 DVS=DVS+D
VNSD=VSZ*D
DC 350 I=1,KSM
DVS=DIS+DD
VP(I)=VNSD/DIS+VDXC
GC TO 1000
KL=K-KSTEP
DVP=(VP(KL)-VP(K))*FKSR
DC 750 I=1,KSM
VP(KL+I)=VP(KL+I-1)-DVP
CONTINUE
IF(IPN) 1010,2,1010
CONTINUE
WRITE(7,9610) (IH(I),I=1,15),KM
9610 FORMAT(1 DIFFERENT,TRUE,15A4,14)
WRITE(7,9630) (APSI(I),I=1,20)
9630 FORMAT(10F8.4)
WRITE(7,9635) (APSI(I),I=21,KM)
9635 FORMAT(10F8.5)
WRITE(7,9630) (BPSI(I),I=1,20)

```



```

MOD9
IF(RB*GT.RT2) GO TO 200
RB=SQRT(RA)
R=SQRT(RB)
I=AA*DDR+HDD
J=RB*DDR+HDD
RDR=R*UR
CR=DR*ERR
IF(I.LT.I) I=1
IF(J.LT.J) J=1
IF(I.GT.KMR) GO TO 200
IF(J.GT.KMR) GO TO 200
EDD=EDD+((ARHO(I)+BRHO(J))*FT-ARFT(I)-BRFT(J))*RDR
EXX=EXX+((ARHO(I)+BRHO(J))*FCT-ARFCT(I)-BRFCT(J))*RDR
150 R=R+DR
    GC TO 100
    N=Z+DZ
200 IF(Z.GT.ZMAX) GO TO 1000
IF(ABS(Z)-DD) 260,250,220
220 IF(ABS(Z-D).GE.DD) GO TO 260
250 R=R+S
    CR=CRS
    GC TO 100
260 R=DD
    CR=FDRS
    GC TO 100
1000 EDD=18.C39Q2*DZ*EDD
    IF(EDD.LT.C.O) EDD=0.0
    EXX=4.64076*DZ*EXX
    IF(EXX.LT.C.O) EXX=0.0
    RETURN
END
//GO.FTC6FC01 DD SYSOUT=A,DCB=BLKSIZE=133
//GC.SYSIN DD *

```

MOD9
MOD9
MOD9

MOD9
MOD9
MOD9
MOD9
MOD9


```

5 PFR=.005/SCALEF
6 PFR1=SCALEF/.005
7 CC 5 I=1,1500
8 IAL(I)=C
9 THIS SECTION CONVERTS ATOM POSITIONS TO SCALED COORDINATES
10 CC 10 I=1,INUMBR
11 CC 9 J=1,3
12 AC(I,J)=AC(I,J)*PFR1
13 WRITE(6,950)
14 CONTINUE
15 IF (ICLDE-2) 51,20,999
16 THIS SECTION CONVERTS VERTICES INTO SCALED COORDINATES
17 CC 25 I=1,3
18 CC 24 J=1,2
19 AS(I,J)=AS(I,J)*PFR1
20 CONTINUE
21 CRITX IS THE X VALUE AT WHICH WE CHANGE THE CONDITIONS WHICH MUST BE
22 MET IF THE GRIDED COORDINATE IS TO FALL IN THE REPRESENTATIVE AREA.
23 CC CRITX=A5(2,1)
24 THIS SECTION CALCULATES THE EQUATIONS OF THE LINES BOUNDING THE TRIANGLE
25 CC 35 I=1,2
26 B1(I)=(A5(I+1,2)-A5(I,2))/(A5(I+1,1)-A5(I,1))
27 WRITE(6,950)
28 B2(I)=(A5(I,2)-B1(I)*A5(I,1)+A5(I+1,2)-B1(I+1,1))/2.0
29 B1(3)=C.0
30 B2(3)=A5(3,2)
31 THIS SECTION CALCULATES THE NEW COORDINATES OF THE ATOMS IN THE
32 REPRESENTATIVE AREA
33 CC 50 I=1,INUMBR
34 IF (A6(I,1)) 40,44,40
35 THETA=ATAN(A6(I,2)/A6(I,1))
36 WRITE(6,950)
37 CC 10 45
38 TLETA=1.5707963
39 R=SQRT((A6(I,2)**2+A6(I,1)**2)
40 AC(I,1)=FX(R,THETA)
41 AC(I,2)=FY(R,THETA)*COS(ALPHA)-A6(I,3)*SIN(ALPHA)
42 WRITE(6,950) ((A6(I,J),J=1,3),I=1,INUMBR)

```



```

FCRMT(3F10.3)
THIS SECTION CALCULATES THE ACTUAL DISTRIBUTION OF IMPACT PARAMETERS
C
IX=IA+1
IXX=IB+1
CC 75 I=1, IX
CC 74 J=1, IXX
ACK1=I-1
ACK2=J-1
IF (ICODE-2) 54,53,54
IF (ACK1-CRITX) 100,100,150
IF (ACK1-(B1(1)*ACK2+B2(1))) 54,54,74
IF (ACK1-(B1(2)*ACK2+B2(2))) 54,54,74
IF (ACK2) 55,60,55
THETA=ATAN(ACK1/ACK2)
CC TO 65
THETA=1.707963
R=SQRT(ACK1**2+ACK2**2)
ACK1=FY(R,THETA)*CCS(ALPHA)
ACK2=FX(R,THETA)
THIS SECTION CALCULATES THE SHORTEST IMPACT PARAMETER AND
ASSIGNS IT TO THE CORRECT ATOM
RANGE=6.25E04
KEEP=0
DO 180 K=1, INUMBR
B3(K)=(AG(K,1)-ACK2)**2+(AG(K,2)-ACK1)**2
IF (LARGE(K)-1) 179,178,999
B3(K)=B3(K)*SCALE2
IF (B3(K)-RANGE) 182,192,180
RANGE=B3(K)
KEEP=K
CC TO 180
CALL RANDOM(0.0,2.0,0.2,0.5,0,TAU,2.0,0,NN,ALFA,RN1,SN,SN1)
IF (.5-SN) 180,555,555
RANGE=B3(K)
KEEP=K
CC CONTINUE
IF (LARGE(KEEP)-1) 186,185,999
RANGE=RANGE/SCALE2
RANGE=SQRT(RANGE)+1.0
ITALLY=(KEEP-1)*250+IRANGE
IA(ITALLY)=IA(ITALLY)+1
CC CONTINUE
CC CONTINUE
DC 300 I=1, INUMBR

```



```

ISUM=0
IS(I)=0
JMIN=(I-1)*250+1
JMAX=JMIN+249
CC 299 J=JMIN,JMAX
ISUM=ISUM+IAL(J)
IS(I)=ISUM
CONTINUE 556, CHAR
FORMAT(1,23X,80A1,///)
WRITE(7,550) CHAR
FORMAT(80A1)
CC 347 I=1,INUMBR
JMIN=(I-1)*250+1
J1=JMIN+15
J2=J1+20
J3=J2+20
J4=J3+20
J5=J4+20
J6=J5+20
J7=J6+20
J8=J7+20
J9=J8+20
J1=J0+20
J2=J1+20
J3=J2+10
WRITE(6,951)(IAL(J),J=JMIN,J1)
WRITE(7,951)(IAL(J),J=JMIN,J1)
JMIN=J1+151
WRITE(6,951)(IAL(J),J=JMIN,J2)
WRITE(7,951)(IAL(J),J=JMIN,J2)
JMIN=J2+151
WRITE(6,951)(IAL(J),J=JMIN,J3)
WRITE(7,951)(IAL(J),J=JMIN,J3)
JMIN=J3+151
WRITE(6,951)(IAL(J),J=JMIN,J4)
WRITE(7,951)(IAL(J),J=JMIN,J4)
JMIN=J4+151
WRITE(6,951)(IAL(J),J=JMIN,J5)
WRITE(7,951)(IAL(J),J=JMIN,J5)
JMIN=J5+151
WRITE(6,951)(IAL(J),J=JMIN,J6)
WRITE(7,951)(IAL(J),J=JMIN,J6)
JMIN=J6+151
WRITE(6,951)(IAL(J),J=JMIN,J7)
WRITE(7,951)(IAL(J),J=JMIN,J7)
JMIN=J7+151

```

299

360

556

550


```

951 WRITE(6,951)((IAL(J),J=JMIN,J8)
    WRITE(7,951)((IAL(J),J=JMIN,J8)
    JMIN=J8+1
952 WRITE(6,951)((IAL(J),J=JMIN,J9)
    WRITE(7,951)((IAL(J),J=JMIN,J9)
    JMIN=J9+1
953 WRITE(6,951)((IAL(J),J=JMIN,J0)
    WRITE(7,951)((IAL(J),J=JMIN,J0)
    JMIN=J0+1
954 WRITE(6,951)((IAL(J),J=JMIN,JJ1)
    WRITE(7,951)((IAL(J),J=JMIN,JJ1)
    JMIN=JJ1+1
955 WRITE(6,951)((IAL(J),J=JMIN,JJ2)
    WRITE(7,951)((IAL(J),J=JMIN,JJ2)
    JMIN=JJ2+1
956 WRITE(6,951)((IAL(J),J=JMIN,JJ3)
    WRITE(7,951)((IAL(J),J=JMIN,JJ3)
    JMIN=JJ3+1
957 FCFRMT(2014)
    WRITE(7,914)
958 FCFRMT(1,NEW ATGM')
    WRITE(6,915),TOTAL NUMBER OF IMPACT POINTS TALLIED',///)
959 FCFRMT(28X,'ATOM',11,'=',15,' POINTS',///)
    WRITE(6,913),I,IS(I)
    FCFRMT(6,558)
    FCFRMT(1,1)
    GO TO 1
    STOP
    END

```

```

1 SUBROUTINE RANDOM(A,B,SIGMA,MU,TAU,LAMBDA,G,NN,ALFA,
    RN1,SN,SN1)
C
C SUBROUTINE RANDOM GENERATES THREE PSEUDORANDOM NUMBER DISTRIBUTIONS:
C 1) UNIFORM, 2) NORMAL, 3) EXPONENTIAL. IF TAU=1,2,3, ONE GETS A
C UNIFORM, NORMAL, EXPONENTIAL DIST. RESP. A DEFINITION OF THE
C OTHER TERMS, USED IN THIS ROUTINE, MAY BE FOUND IN THEESIS
C BOOK 1, K.-L. ALLEN. THE ROUTINE WAS TAKEN FROM RALSTON AND WILF
C NUMERICAL METHODS FOR DIGITAL COMPUTERS.
C
C INTEGER TAU,ALFA,G,RN,RN1
C REAL MU,LAMBDA
C RN=RN1*ALFA
C RSN=RN
C RSN=RSN*2.0**(-31)
C IF (TAU-2) 2,3,4
C EXPONENTIAL DISTRIBUTION

```



```

29 3 IF(RSTN) 9,9,8
      RSTN=ABS(RSTN)
      SN=-(1.C/LAMBDA)*ALCG(RSTN)
      GC TO 5
      UNIFORM DISTRIBUTION
      SN=(B-A)*RSTN+A
      GC TO 5
      NORMAL DISTRIBUTION
      IF (G-1) 7,6,7
      NN=NN+1
      G=G+1
      NN=NN
      RSTN=KSTN
      GC TO 1
      IF (RSTN) 11,11,10
      KSTN=ABS(RSTN)
      Z=SGRT(+2.0*ALCG(RSTN))*SIGMA
      SN1=Z*UCS(6.28318*RSTN)+MU
      SN=Z*STN(6.28318*RSTN)+MU
      C=C
      NN=NN+1
      NN1=NN
      RETURN
      END
//GO.SYSIN DD *

```



```
// EXEC FCRTCLGP,REGION.GC=150K
//FCRT.SYSIN DD *
```

THE PROGRAM TAKES THE RAW DATA FROM THE QUESTIONNAIRE, PERFORMS SOME PRELIMINARY SORTING, AND THEN CALCULATES THE SPENDING FUNCTION. THIS IS DONE BY USING AN INTERPOLATION PROCEDURE WHICH ASSUMES THAT THE SPENDING FUNCTION IS LINEAR BETWEEN THE SPENDING POINTS. THE PROGRAM TAKES THE RAW DATA FROM THE QUESTIONNAIRE, PERFORMS SOME PRELIMINARY SORTING, AND THEN CALCULATES THE SPENDING FUNCTION. THIS IS DONE BY USING AN INTERPOLATION PROCEDURE WHICH ASSUMES THAT THE SPENDING FUNCTION IS LINEAR BETWEEN THE SPENDING POINTS.

DATA INPUT: CARD 1; NUMBER OF POINTS TO BE FITTED, ID NUMBER
INDICATING IF CARD AND GRAPHICAL OUTPUT IS WANTED (1=NO, 2=YES);
CARD 3; TWO CARDS WITH INFORMATION TO BE COMPUTED WITH GRAPH...
MUST BE INSERTED FOR EVERY RUN; CARD 4-N: DATA FROM THE DISTRIBUTION
OF IMPACT PARAMETER PROGRAM

```
COMMON/PCPLY/INTERUS,B(300),C(500),D(300)
DIMENSION X(300),F(300),W(300),ERRCR(300),PJW1(300),PJ(300)
DIMENSION XX(300),YY(300),YY1(300),XX1(500),IIF(300)
DIMENSION IIF1(300)
```

```

REAL LAST
REAL*8 TITLE(12)
REAL LABEL1/F(X),/
REAL LABEL2/P(X),/
REAL LABEL3/E(X),/
REAL LABEL4/END=999
REAL(5,859,END=999) NPOINT,IFLAG

```

```

      TITLE
      READ(5,500)
      FCRMAT(648)
      READ(5,500)
      FCRMAT(2014)
      WRITE(6,907)
      FCRMAT(1,1)

```

```
NTERMS=2
ICCOUNT=0
AFT=NPCINT
KEEP=0
```

```

TERMS=DEGREE OF FIT+1; ICOUNT=A COUNTER;KEEP=
THE IMPACT PARAMETER DISTRIBUTION IS A MAXIMUM;
ICRANGE= THE RANGE VALUE AT WHICH
CORRESPONDING TO THE MAXIMUM IMPACT PARAMETER;

```

```

RANGE=C
CC 777 I=1,NPCINT
IF (IRANGE-IIF(I)) 778,778,777
KEEP=I

```

822


```

777  RANGE=IIF(I)
      CCNTINUE
5000  WRITE(6,9000) KEEP
      FORMAT(' ',25X,'KEEP= ',15,///)
101  NPCINT=KEEP
      ICCUNT=ICCUAT+1
      IF (ICCUAT.EQ.2) GO TO 779
760  CC TO 102
779  CC 767 I=1,NPCINT
787  IIF(I)=PJ(I)
      ATERMS=11
      NPCINT=NPT-NPCINT
      CC 781 I=1,NPCINT
      IIF(I)=IIF(KEEP+I)

781  X(I)=X VALUES OF DISTRIBUTION TO BE FITTED; F(I)= VALUES OF THE
      FUNCTION CORRESPONDING TO X; W(I)= WEIGHTING FACTORS FOR THE
      ORTHOGONAL POLYNOMIALS;
      CC 5 I=1,NPCINT
102  ACK=1
      X(I)=ACK*.005
      F(I)=IIF(I)
      W(I)=1.C
      CCNTINUE
5  CALL CKTPCL(NPCINT,X,F,W,ERROR,PJM1,PJ)
      WRITE(6,601)(J,B(J),C(J),D(J),J=1,NTERMS)
601  FCRMAT(' ',25X,14,3016.8)
      CC 60 I=1,NPCINT
      IIF(I)=F(I)
60  PJ(I)=CKTRVAL(X(I))
      WRITE(6,600)(X(I),IIF(I),PJ(I),ERRCR(I),I=1,NPCINT)
600  FCRMAT(' ',10X,F5.3,14,F10.5,EL3.3,/)
      IF (IFLAG.EQ.1) GC TO 72
      IF (IFLAG.EQ.2) GC TO 73
73  CALL DRAW(NPCINT,X,F,1,0,LABEL,TITLE,.1, 40.C,1,0,2,2,8,12,0,
      1 LAST)
      1 CALL DRAW(NPCINT,X,PJ,2,0,LABEL1,TITLE,.1, 40.0,1,0,2,2,8,12,0,
      1 LAST)
      1 CALL DRAW(NPCINT,X,ERRCR,3,0,LABEL2,TITLE,.1, 40.0,1,0,2,2,8,12,
      1 0,LAST)
      IF (ICCUAT.EQ.2) GO TO 888
72  GC TO 101
888  CC 889 I=1,NPCINT
889  IIF(I+KEEP)=PJ(I)
74  WRITE(7,500)(IIF(I),I=1,NPT)
      GC TO 1
959  STOP

```


ENC

FLACTION ORTVAL(X)

C
C
C

SLBROUTINE ORTVAL EVALUATES THE ORTHOGONAL POLYNOMIALS AT A
SPECIFIED VALUE CF X

COMMON/PCLY/NTERMS,B(300),C(300),D(300)
K=NTERMS
ORTVAL=D(K)
PREV=0.

10

K=K-1 RETURN

IF (K.EQ.0)

PREV2=PREV

PREV=ORTVAL

ORTVAL=D(K)+(X-B(K))*PREV-C(K+1)*PREV2

GO TO 10

END

SLBROUTINE ORTPOL(NPOINT,X,F,W,ERRCR,PJML,PJ)

C
C
C

SLBROUTINE ORTPOL CALCULATES THE COEFFICIENTS OF THE TERMS IN
THE ORTHOGONAL POLYNOMIAL USED IN THE LEAST SQUARES FIT

COMMON/POLY/NTERMS,B(300),C(300),D(300)
DIMENSION X(300),F(300),W(300),ERRCR(300),PJML(300),PJ(300)
DIMENSION S(300)

C

DO 9 J=1,NTERMS

B(J)=0.

D(J)=0.

S(J)=0.

DO 10 I=1,NPOINT

D(I)=D(I)+F(I)*W(I)

B(I)=B(I)+X(I)*W(I)

S(I)=S(I)+W(I)

D(I)=D(I)/S(I)

DO 11 I=1,NPOINT

ERRCR(I)=F(I)-D(I)

IF (NTERMS.EQ.1)

B(1)=B(1)/S(1)

DO 12 I=1,NPOINT

PJML(I)=1.

PJ(I)=X(I)-B(I)

J=J+1

RETURN

9

10

11

12


```

C20      J=J+1
         I=1,NPOINT
         P=PJ(I)*W(I)
         Q(J)=D(J)+ERRCR(I)*P
         R=P*PJ(I)+X(I)*P
         S(J)=B(J)+X(I)*P
         S(J)=S(J)+P
         CC 21 I=1,NPOINT
         Q(J)=D(J)/S(J)
         ERRCR(I)=ERROR(I)-C(J)*PJ(I)
         RETURN
         IF (J.EQ. NTERMS)
           C(J)=B(J)/S(J)
           CC 22 I=1,NPOINT
           Q(J)=S(J)/S(J-1)
           P=PJ(I)
           PJM1(I)=X(I)-B(I)-C(J)*PJM1(I)
           PJM1(I)=P
           CC 27 I=1,NPOINT
           GO TO 20
         END
//GO.FTC6F001 DD SYSOUT=A,SPACE=(CYL,(3,1))
//GC.SYSIN DD *

```



```

// EXEC FORTCLG, REGION.GC=150K
//FCRT SYSIN DD INLCSS
FCGRATION BMAP(3), PUD(3), ARC(3), LM(3), TFL(3), XM(3), KXM(3)
DIMENSION FLPD(750), IH2(4), IAH(4), PSE(8), FIT(8), EAV(3)
DIMENSION EA(20), ENN(20), BC(40), LCLT(40), IH3(19), IH4(19)
DIMENSION E(100), ERN(100), DREL(100), PP(100), EI(100)
DIMENSION RHG(1000), EIN(1000), ELEC(1000), FN(1000), RX(1000),
2 RXZ(1000), RXZR(1000), RMIN(1000), E(1000)
DIMENSION V(1000), SIG(1000), APSI(1000), BPSI(1000)
DIMENSION ELECS(30,3), PEL(30,3), ECU(30)
EQUIVALENCE(PCNI,PCZZ)
START=0.01*ITIME(XX)
CALL EP
CCCL=1, L=1, 100
ER(1)=0.0
ERN(1)=C.0
EL(1)=0.0
ET(1)=0.0
EA(1)=0.0
LCLT(1)=0.0
1 DREL(1)=0.0
CCZ=1, 1, 1000
RFC(1)=0.0
EIN(1)=C.0
ELEC(1)=0.0
FN(1)=0.0
RX(1)=0.0
RXZ(1)=0.0
RXZR(1)=0.0
RMIN(1)=0.0
E(1)=0.0
V(1)=0.0
SIG(1)=C.0
APSI(1)=0.0
2 BPSI(1)=0.0
FPAR=1.05443E-27
PI=3.14159265
ECHRGE=4.80286E-10
CVD=0.525172E-8
CVE=1.6021E-12
CVM=1.67239E-24
CAH=1.0E-8/CVD
ECI=3.0/3.0
FCI=4.0/3.0
KSTEP=5
9000 FCRMAT(A4, I2, 9F6.4, 3I3, I4, F7.4)

```

7JCB, 722
7JCB, 723
7JCB, 724
7JCB, 725
7JCB, 726
7JCB, 727
7JCB, 728
7JCB, 729
7JCB, 730
7JCB, 731

7JCB, 733
7JCB, 734
7JCB, 735
7JCB, 736
7JCB, 737
7JCB, 738
7JCB, 739
7JCB, 740
7JCB, 741


```

      READ (5,9000) LCRYST,LTPE,(BMAX(1),I=1,3),(PUD(1),I=1,3),
2      (ARO(1),I=1,3),(LM(1),I=1,3),KN,FACL
      PUDM=AMAX1(PUD(1),PUD(2),PUD(3))
      PUDM2=PUDM*PUDM
      DO 5 I=1,3
      L=LM(I)
      FCFMAT(2CF4,0)
      READ (5,5010) (FLP(L),L=1,LF)
      PT=0.0
      DO 3 L=1,LF
      PT=PT+FLP(L)
      TFL(I)=PT
      L=ARO(I)/PT
      DO 5 L=1,LF
      FFLP(L,I)=FLP(L)*SF
      CONTINUE
      BMM=AMAX1(BMAX(1),BMAX(2),BMAX(3))
      READ (5,5020) IH1
      FCFMAT(20A4)
      DO 2C I=1,3
      IH3,KMR
      FCFMAT(19A4,I4)
      DO 25 I=1,KMR
      FCFMAT(10F8.5)
      READ(5,5030) (BPSI(I),I=1,KMR)
      READ(5,5025) IH4,KMV
      READ(5,5032) (V(I),I=1,20)
      FCFMAT(5F12.5)
      DO 32 I=1,20
      FCFMAT(5,5035) (V(I),I=21,KMV)
      FCFMAT(6F10.5)
      DO 35 K=1,KMR
      KMVR=MINO(KM,KMV,KMR)
      KMVP=KMVR+1
      KMVF=KMVR+1
      KMN=KM-1
      KMP=KM+1
      FKRP=KMP
      KND=KN+KM
      DX=0.02
      TCX=3.0*DX
      LXX=DX*DX
      DXR=1.0/DX
      FK=KMVP
      XMV=FK*DX
      PDX=0.5*DX
      CES=0.005
      FCR=1.0/DBS
      FCFMAT(10F8.4)
      READ (5,9050) (EA(N),N=11,18),IAH
901C      FCFMAT(I10)
902C
9025
9030
9032
9035
904C
906C

```

```

7J08,743
7J08,743
7J08,745
7J08,746
7J08,747
7J08,748
7J08,749
7J08,750
7J08,751
7J08,752
7J08,753
7J08,754
7J08,755
7J08,756
7J08,757
7J08,760
7J08,761
7J08,762
7J08,763
7J08,764
7J08,765
7J08,766
7J08,767
7J08,768
7J08,769
7J08,770
7J08,771
7J08,772
7J08,773
7J08,774
7J08,775
7J08,776
7J08,777
7J08,778
7J08,780
7J08,781
7J08,782
7J08,784
7J08,785
7J08,786
7J08,787
7J08,788
7J08,789
7J08,790
7J08,791

```



```

905C READ(5,9040) (EA(N),N=1,10)
      FCRMAT(8F8.4,4A4)
      READ (5,9060) JEIT
      IF (JEIT) 9999,15,10
907C FCRMAT(16F5.3)
      READ(5,9070) (PSE(J),J=1,JFIT)
908C FCRMAT(2F4.0,2F8.4,2F3.0,14,F7.3,213,2F3.C,F5.0,6X,4A4)
15 READ(5,908C) ZB,ZT,BMAS,IMAS,EOS,DEC,KEOM,AC,LSKIP,NM,RES,DRE,REM,
      IF2
20 IF(ZB) 9999,9999,20
      ACA=AO/O.529172
      HACAT=O.5*ACA
      IFIT=3
      KCA=FACT*AOA
      KCOB=ROA/OBS
      AM=IMAS/BMAS
      BM=BMAS*CVM/CVE
      COM=AM/(1.C+AM)
      ERY=73.502388
      CEC=CCM*ERY
      7.28926 = .75*PI*(3*PI**2)**1/3
      ECCC=1.0
      EIC=ECC*7.28926*DX*HBAR/(CVE*CVC)
      TCRV=2.O/BM
      ECE=EOS
      ECEV=EOS*1000.
      DECEV=DEC*1000.
      FL=LSKIP
      DEL=O.O1*FL
      CER=1.O/OBL
      BML=BM*RGCA
      LML=BML*DBSR
      SCB=CB*JUM*DXK*ROA
      KLB=PUJUM*DXK*ROA
      L2SKIP=LSKIP+LSKIP
      L3SKIP=L2SKIP+LSKIP
      L4SKIP=L3SKIP+LSKIP
      AE=O
25 CC 25 I=1,3
      XM(I)=ROA*SQRT(BMAX(I)**2+PUD(I)**2)
      KXP(I)=XM(I)*DXR*HDX
      KLM=MAXO(KXM(1),KXM(2),KXM(3))
      KLM=MINO(KLM,KM)
      KLMN=KLM-1
      MAKE THE RUSSEK ENERGY-ELECTRON PRODUCTION TABLE
      CC 30 M=1,40
      BC(M)=O.O
C

```

```

7JCB,792
7JCB,793
7JCB,794
7JCB,795
7JCB,796
7JCB,797
7JCB,798
7JCB,799
7JCB,800
7JCB,801
7JCB,802
7JCB,803
7JCB,804
7JCB,805
7JCB,806
7JCB,807
7JCB,808
7JCB,809
7JCB,810
7JCB,811
7JCB,812
7JCB,813

7JCB,815
7JCB,816
7JCB,817
7JCB,818
7JCB,819
7JCB,820
7JCB,821
7JCB,822
7JCB,823
7JCB,824

7JCB,825
7JCB,826
7JCB,827
7JCB,828
7JCB,829
7JCB,830
7JCB,831
7JCB,832
7JCB,833
7JCB,834
7JCB,835
7JCB,836
7JCB,837

```



```

30  LCLT(M)=0.0
    NMP=NM+1
    NM=NM-1
    WRITE(6,9505) IH2
9505  FORMAT(IH1,52X,4A4,/)
    BC(1)=NM
    ENN(1)=EA(1)
    EN(1)=EA(1)
    CC 40 N=2,NM
    IF(EA(N)-1.0E-10) 42,42,37
37  ENN(N)=ENN(N-1)+EA(1)*EA(N)
    FFK=N
    EN(N)=ENN(N)/FFN
    J=NM+1
    FJ=J
    J=N-1
40  BC(N)=FJ*BC(J)/FFN
    GC TO 45
42  NM=NM-1
    NM=NM+1
45  WRITE(6,9510) IH1,IAH,LCRYST,AC,KM,DX
9510  FORMAT(27X,20A4,/,20X,4A4,/,
           2  IGNIZATION ENERGIES, 1,A4,
           3  LATTICE CONSTANT WAS, F6.3,/,
           4  DGNE WITH, 14, STEPS, AND,
           5  F6.3, BCHR STEP SIZE,/)
    DC 41 M=1,400
47  BCZZ(M)=0.0
    DCR=1.0/DCR
    FDE=(REM-RES)*DRER+1.001
    JM=FDE
    NM=NM-1
    E(1)=RES
    ERN(1)=(1.0/E(1))*NM
    CC 50 J=2,JM
    E(J)=E(J-1)+DE
50  ERN(J)=(1.0/E(J))*NM
    DC 200 N=1,NM
    NR=NM-N
    ECNI(N,1)=-NR
    NRP=NR+1
60  IF(NR-2) 200,200,60
    CC 100 I=2,NR
    FI=1
    K=NRP-I
    FK=K
100  BCNI(N,I)=-BCNI(N,I-1)*FK/FI
200  CCNI=IUE
    CC 500 L=1,JM

```

```

7JOB,838
7JOB,839
7JOB,840
7JOB,841
7JOB,842
7JOB,843
7JOB,844
7JOB,845
7JOB,846
7JOB,847
7JOB,848

7JOB,851
7JOB,852
7JOB,853

7JOB,855
7JOB,856
7JOB,857
7JOB,858
7JOB,859

7JOB,865
7JOB,866
7JOB,867
7JOB,868
7JOB,869
7JOB,870
7JOB,871
7JOB,872
7JOB,873
7JOB,874
7JOB,875
7JOB,876
7JOB,877
7JOB,878
7JOB,879
7JOB,880
7JOB,881
7JOB,882
7JOB,883
7JOB,884
7JOB,885

```



```

202 DC 202 I=1,100
202 PP(I)=C.O
202 PZ=1.O
202 PZT=O.O
202 FK=E(L)/EN(I)
202 K=FK
202 IF(K-NM) 210,210,205
205 K=NM
210 DC 220 I=1,K
220 FI=1
220 PZT=PZT+((-1.O**I)*((E(L)-FI*EN(I))-ENNM)*BC(I)
220 PZ=PZ+PZT*ERN(L)
220 DC 400 N=1,NM
220 IF(LCUT(N)) 400,29C,400
29C IF(E(L)-ENN(N)) 400,390,300
300 NP=N+1
300 FK=(E(L)-ENN(N))/EN(NP)
300 K=FK
310 IF(K) 390,39C,310
315 IF(K-NM) 320,320,315
320 DC 350 I=1,K
320 FI=1
320 IF=E(L)-ENN(N)-FI*EN(NP)
320 IF(EF) 390,390,350
350 PP(N)=PP(N)+(EF*NM)*BCNI(N,I)
39C PP(N)=BC(N)*((E(L)-ENN(N))-ENNM)+PP(N))*ERN(L)
400 CONTINUE
410 IF(PZ) 410,420,420
41C PZ=C
42C PP=PZ
42C DC 430 N=1,NM
42C IF(PP(N)) 425,430,430
425 PP(N)=O.O
425 LCUT(N)=-1
42C PP=PPT+PP(N)
43C PPTR=1.O/PP
43C PZ=PPT*PZ
43C EL(L)=O
43C ET(L)=O
43C DC 440 N=1,NM
440 PP(N)=PP(N)*PPT
440 FFN=N
440 TE=PP(N)*FFN
440 EL(L)=EL(L)+TE*EN(N)
45C ET(L)=ET(L)+TE*EN(N)
45C CONTINUE
45C CC=CONTINUE
45C
460
470
480
490
500

```

```

7JCB,886
7JCB,887
7JCB,888
7JCB,889
7JCB,890
7JCB,891
7JCB,892
7JCB,893
7JCB,894
7JCB,895
7JCB,896
7JCB,897
7JCB,898
7JCB,899
7JCB,900
7JCB,901
7JCB,902
7JCB,903
7JCB,904
7JCB,905
7JCB,906
7JCB,907
7JCB,908
7JCB,909
7JCB,910
7JCB,911
7JCB,912
7JCB,913
7JCB,914
7JCB,915
7JCB,916
7JCB,917
7JCB,918
7JCB,919
7JCB,920
7JCB,921
7JCB,922
7JCB,923
7JCB,924
7JCB,925
7JCB,926
7JCB,927
7JCB,928
7JCB,929
7JCB,930
7JCB,931

```



```

C
65C DE1=E(1)-EA(1)
      DEIR=1.0/DE1
      FCDE=EL(1)*DEIR
      CC 650 J=1,JMM
      DREL(J)=DREK*(EL(J+1)-EL(J))
      MAKE THE CROSS SECTION TABLE
      K=KMK
      KMF=KM/2
      KPF=KMR-KMH
      FK=K
      XMP=DX*FKMP
      X=DX*FK
      XCX=X*DX
      SIG(KM)=0.0
      CC 700 M=1,KH
      K=K-1
      XCX=XDX-DX2
      SIG(KM)=SIG(KM)+XDX*(APSI(K)+BPSI(K))*EOT
      K=KM
      J=KMH
      KP=KMH-1
      CC 750 M=1,KP
      XCX=XDX-DX2
      J=J-1
      K=K-2
      750 SIG(K)=SIG(K+2)+XDX*(APSI(J)+BPSI(J))*EGT
      SIG(1)=SIG(2)+0.5*DX2*(APSI(1)+BPSI(1))*ECT
      CC 800 K=3,KMM,2
      SIG(K)=0.5*(SIG(K+1)+SIG(K-1))
      WRITE(6,5820) (SIG(K),K=1,KMR)
      WRITE(6,5820) (V(K),K=1,KMV)
      982C PCRMAT(IX,IOF11,5)
      MAKE CALCULATIONS FOR A SINGLE ION ENERGY
      100C WRITE(6,9505) IH2
      CC 2500 NE=1,KEOM
      DC 1010 L=1,1000
      E(L)=0.0
      RMIN(L)=C.C
      EMIN(L)=C.C
      EMAX(L)=0.0
      101C CCN INCE
      CC 1020 M=1,3
      EAV(M)=0.0
      VC=SQRT(ECEV*TOBM)
      EIF=EIC*VC
      ECP=EC*CEC
      ECPK=1.0/EOIP
      LOCATE THE DISTANCE OF CLOSEST APPROACH

```

```

7JCB,932
7JCB,933
7JCB,934
7JCB,935
7JCB,936
7JCB,937
7JCB,938
7JCB,939
7JCB,940
7JCB,941
7JCB,942
7JCB,943
7JCB,945
7JCB,946
7JCB,947
7JCB,948
7JCB,950
7JCB,951
7JCB,952
7JCB,953
7JCB,954
7JCB,955
7JCB,956
7JCB,959
7JCB,960
7JCB,962
7JCB,963
7JCB,964
7JCB,965
7JCB,966
7JCB,967
7JCB,968
7JCB,969
7JCB,970
7JCB,971
7JCB,972
7JCB,973

```



```

K=KMVP
X=XMV
CC 1050 M=1,KMV
K=X-K-1
X=X-DX
FN(K)=1-C-EGPR*V(K)
IF(FN(K)) 1060,1040,1040
104C RA(K)=X
RA2(K)=X*X
RX2R(K)=1.0/RX2(K)
CCCONTINUE
X=CX
KMIN=1
CC TO 1065
KMIN=K
X=X+DX
KMPO=KMIN+1
CC 1070 M=1,KMIN
RX(M)=0.0
RX2(M)=C.0
RX2R(M)=0.0
FN(M)=0.0
CCCONTINUE
107C RX(KMIN)=X-DX
CX1=DX
CC 1090 M=1.5
DX1=0.1*DX1
CC 1080 MM=1.10
X=X-DX1
PUT=V(K)+(X-RX(K))*DXR*(V(K+1)-V(K))
IF(1.0-EGPR*POT) 1090,1080,1080
108C CCCONTINUE
109C X=X+DX1
RXIN(1)=X
R(1)=0.0
KSS=KMIN-1
PSI=0.0
C THIS IS THE INTEGRAL WITH ZERC IMPACT PARAMETER
PSI=0.5*SQR(FN(KMPO))*SIG(KMPO)
FIC=FSI*(RX(KMPO)-X)*DXR
CC 1100 K=KMPO, KLB
1=SIG(K)*SQR(FN(K))
110C FSI=PSI+1
EIN(1)=EIF*(PSI+FSI-0.5*1+FI0)
C CALCULATE THE NUMBER OF ELECTRONS FROM THE RUSSEK MODEL
M=EIN(1)*DRER
IF(M-1) 1110,1140,1140
111C IF(EIN(1)-EA(1)) 1120,1120,1130

```

```

7JCB,974
7JCB,975
7JCB,976
7JCB,977
7JCB,978
7JCB,979
7JCB,980
7JCB,981
7JCB,982
7JCB,983
7JCB,984
7JCB,985
7JCB,986
7JCB,987
7JCB,988
7JCB,989
7JCB,990
7JCB,991
7JCB,992
7JCB,993
7JCB,994
7JCB,995
7JCB,996
7JCB,997
7JCB,998
7JCB,999
7JCB,000
7JCB,001
7JCB,002
7JCB,003
7JCB,004
7JCB,005
7JCB,006
7JCB,007
7JCB,008
7JCB,010
7JCB,011
7JCB,012
7JCB,014
7JCB,015
7JCB,016
7JCB,018
7JCB,019
7JCB,020
7JCB,021

```



```

1120 ELEC(1)=0.0
1121 GC TO 1170
1130 ELEC(1)=(EIN(1)-EA(1))*FDEL
1131 GC TO 1150
1140 ELEC(1)=EL(M)+(EIN(1)-E(M))*DREL(M)
1150 DC 1160 I=1,3
1160 EAV(1)=ELEC(1)*FLPD(1,1)
1170 EMAX=0.0
1171 LMAX=0

C      THIS IS THE INTEGRAL FOR A SINGLE B(L)
DC 1990 L=2,LML,LSKIP
LS=L
      FIND RC FOR GIVEN B(L)
P(L)=B(L-LSKIP)+DBL
IF(B(L)-BML) 1171,1171,2000
1171 K=KSS+KSTEP
X=RX(K)*B(L)
B2=B(L)*B(L)
DC 1172 M=1,KSTEP
K=K-1
IF(L=0-ECPR*V(K)-B2*RX2R(K)) 1173,1173,1172
1173 CCNTINUE
KSS=K
X=RX(K+1)
LXI=0
CC 1175 M=1,3
DXT=0.1*DXT
CC 1174 MM=1,10
X=X-DXT
PCT=(K)+(X-RX(K))*DXR*(V(K+1)-V(K))
IF(L=0-ECPR*POT-B2/(X*X)) 1175,1174,1174
1174 CCNTINUE
1175 X=X+DXT
RC=X
RC2=RC*RC

C      FIRST INCREMENT AT SINGULARITY FOR B(L)
KI=QA*CAR*SQRT(PUDM2+B2)
IF(KI-KLMM) 1177,1177,1176
1176 KI=KLMM
1177 RMIN(L)=RC
KB=K+2
CRB=0.1*(RX(KB)-RO)
DRB=1.0/CRB
CLC=0.5*RO*DXT
CL=0.5*RC2*DXT
PCT=V(K)+(RO-RX(K))*DXR*(V(K+1)-V(K))
SIGR=SIG(K)+(RO-RX(K))*DXR*(SIG(K+1)-SIG(K))

```

7JCB, 022
 7JCB, 023
 7JCB, 024
 7JCB, 025
 7JCB, 026
 7JCB, 027
 7JCB, 028
 7JCB, 029
 7JCB, 030

 7JCB, 032
 7JCB, 033
 7JCB, 034
 7JCB, 035
 7JCB, 036

 7JCB, 039
 7JCB, 041
 7JCB, 042
 7JCB, 043
 7JCB, 044
 7JCB, 045
 7JCB, 046
 7JCB, 047
 7JCB, 048
 7JCB, 049
 7JCB, 050
 7JCB, 051
 7JCB, 052
 7JCB, 053
 7JCB, 054
 7JCB, 055
 7JCB, 056

 7JCB, 058
 7JCB, 059
 7JCB, 060
 7JCB, 061
 7JCB, 062
 7JCB, 063
 7JCB, 064
 7JCB, 065

 7JCB, 067
 7JCB, 068
 7JCB, 069


```

AL=1.0-ECPR*POT
RN=EC+DRB
PCT=V(K)+(RN-RX(K))*DXR*(V(K+1)-V(K))
AN=1.0-ECPR*POT
N=C
DADX=(AN-AL)*DRBR
IF(CADX) 2000,2000,1182
PSI=0.5*SIG*AL*DU/SQRT(2.0*(DADX*RC2*RO+B2))
INTEGRATE THE REST OF THE FIRST STEP FOR B(L)
C
1182
RN=RO
DC 1190 M=1,10
RN=RN+DRB
AL=AN
PCT=V(K)+(RN-RX(K))*DXR*(V(K+1)-V(K))
AN=1.0-ECPR*POT
C=RC/RN
U2=1.0-C
U=SQRT(U2)
DU=DC/SQRT(RN*RN*(RN-RO))
SIG=SIG(K)+(RN-RX(K))*DXR*(SIG(K+1)-SIG(K))
T=SIGR*AN*DU/(C*C*SQRT(RO2*(AN-AL)/(U2+B2*(2.0-U2)))
PSI=PSI+T
CONTINUE
EIN(L)=EIF*CB*(PSI-0.5*T)
AN=FN(KB)
PSI=0.5*SIG(KB)*AN/SQRT(AN-B2*RX2R(KB))
COMPLETE THE INTEGRAL FOR B(L)
C
KEP=KB+1
CC 1290 K=KB,KT
T=SIG(K)*FN(K)/SQRT(FN(K)-B2*RX2R(K))
PSI=PSI+T
EIN(L)=EIN(L)+EIF*(PSI-0.5*T)
CALCULATE ELECTRONS FROM RUSSEK MCEEL FOR THIS B(L)
C
1410
1420
N=EIN(L)*DRER
IF(M-1) 1410,1440,1440
ELEC(L)=0.0
GC TO 1600
ELEC(L)=(EIN(L)-EA(1))*FDEL
GC TO 1500
IF(M-JM) 1460,1460,1450
ELEC(L)=(EIN(L)-E(M))*DREL(M)+EL(M)
ADD ELECTRONS FROM THIS B(L) TO AVERAGE
C
1500
1510
J=B(L)*DBSR
EAV(I)=EAV(I)+ELEC(L)*FLPD(J,I)*SCB

```

```

7JCB,070
7JCB,071
7JCB,072
7JCB,073
7JCB,074
7JCB,075
7JCB,076
7JCB,077
7JCB,078
7JCB,079
7JCB,080
7JCB,081
7JCB,082
7JCB,083
7JCB,084
7JCB,085
7JCB,086
7JCB,087
7JCB,088
7JCB,089
7JCB,090
7JCB,091
7JCB,092
7JCB,093
7JCB,094
7JCB,095
7JCB,096
7JCB,097
7JCB,098
7JCB,099
7JCB,100
7JCB,101
7JCB,103
7JCB,104
7JCB,105
7JCB,106
7JCB,107
7JCB,108
7JCB,109
7JCB,110
7JCB,111
7JCB,112
7JCB,113
7JCB,114
7JCB,115
7JCB,116

```



```

3100 DC 3500 I=1,JFIT
      FIX=FIT(I)/ELECS(KEOM,IIFIT)
      DC 3200 M=1,3
      DC 3200 N=1,KEOM
3200 PEL(N,M)=FIX*ELECS(N,M)+PSE(I)
      WRITE(6,9505) I,H2
      WRITE(6,9510) I,H1,IAH,LCRYST,AO,KM,DX
      WRITE(6,9720)
9720 FCRMAT(///,30X,5H ION,/,30X,4CH ENERGY N(100) N(110)
      2 (111,///)
      WRITE(6,9730) (EQU(N),(PEL(N,M),N=1,3),N=1,KEOM)
9730 FCRMAT(26X,F10,0,5X,3F10,5)
      WRITE(6,9740) PSEL,I,FIT(I)
9740 FCRMAT(///,30X,20HPSE CONTRIBUTION WAS,F6.3,13H, FIT WAS AT ,F6.3,
      14H ELECTRONS/ION )
3500 CONTINUE
      GC TO 15
9999 STOP
      ENC
      //CC.SYSIN DD *

```

JCB,165
 JCB,166
 JCB,167
 JCB,168
 JCB,169
 JCB,171
 JCB,172
 JCB,174
 JCB,175
 JCB,179
 JCB,177
 JCB,180
 JCB,181
 JCB,183

LIST OF REFERENCES

1. Medved, D. B., Mahadevan, P., and Layton, J. K.,
"Potential and Kinetic Electron Ejection from
Molybdenum by Argon Ions and Neutral Atoms,"
Physical Review, v. 129, p. 2086-2087, 1 March 1963.
2. Harrison, D. E., Jr., Carlston, C. E., Magnuson, G. D.,
"Kinetic Emission of Electrons from Monocrystalline
Targets," Physical Review, v. 139, p. A737-A745,
2 August 1968.
3. Carter, G. and Colligon, J. S., Ion Bombardment of Solids,
American Elsevier Publishing Co., Inc., 1968.
4. Parilis, E. S., and Kishinevskii, L. M., "The Theory of
Ion Electron Emission," Soviet Physics - JETP,
v.3., p. 885-891, October 1960.
5. Firsov, O. B., "A Qualitative Interpretation of the
Electron Excitation Energy in Atomic Collisions,"
Soviet Physics - JETP, v. 36, p. 1076-1080,
November 1959.
6. Wolff, P. A., "Theory of Secondary Electron Cascade,"
Physical Review, v. 95, p. 56, 1954.
7. Harrower, G. A., "Auger Electron Emission in the Energy
Spectra of Secondary Electrons from Mo and W,"
Physical Review, v. 102, p. 340, 1956.
8. Torrens, I. M., Interatomic Potentials, Academic Press,
1972, 247 p.
9. Russek, A., "Ionization Produced by High Energy Atomic
Collisions," Physical Review, v. 132, p. 246-261,
1 October 1963.
10. March, N. H., "The Thomas-Fermi Approximation in Quantum
Mechanics," Advances in Physics, v. 53, p. 206, 1957.
11. Gombas, P., Die Statische Theorie des Atoms und ihre
Anwendungen, Springer-Verlag, 1952.
12. Wedepohl, P. T., "Influence of Electron Distribution on
Atomic Interaction Potential," Proc. Phys. Soc.,
v. 92, p. 79-93, 22 March 1967.
13. Harrison, D. E., "Semiclassical Interaction Potential for
Atoms and Ions," Bull. Am. Phys. Soc. II, v. 14,
p. 315, 1969.

14. Wilson, W. D., Bisson, C. L., "Inert Gases in Solids: Interatomic Potentials and Their Influence on Rare Gas Mobility," Physical Review, v. 3, p. 3984, 1971.
15. Günther, K., "Über die Existenz eines Maximalprinzips als äquivalente Formulierung des Thomas-Fermi-Dirac Modells and das TFD Wechselwirkungspotential von Atomen," Ann. Physik. (7), v. 14, p. 296, 1964.
16. Herman, F. and Skillman, S., Atomic Structure Calculations, Prentice-Hall, Inc., 1963.
17. Ralston, A. and Wilf, H. S., Mathematical Methods for Digital Computers, v. 2, John Wiley and Sons, p. 249-263, 1968.
18. Conte, S. D and de Boor, C., Elementary Numerical Analysis, 2d. ed., McGraw-Hill Book Co, 1972.
19. Mashkova, E. S., Molchanov, V. A., and Odintsov, D. D., "Anisotropy of the Ion-Electron Emission Coefficient of Single Crystals," Soviet Physics - Doklady, v. 8, p. 806-807, Feb. 1964.
20. Carlston, C. E., Magnuson, G. D., Mahadevan, P. and Harrison, D. E., Jr., "Electron Ejection from Single Crystals due to 1- to 10- Kev Noble Gas Ion Bombardment," Physical Review, v. 139, p. A729-A736, 2 August 1965.
21. Baboux, J. C., Pedrix, M., Goutte, R., and Guillaud, C., "Emission Electronique Secondaire d'un Monocristal de NaCl Bombarde par des Ions de Gaz Rares," J. Phys. Appl. Phys., v. 4, p. 1617-1623, 9 June 1971.
22. Babous, J. C. and Pedrix, M., unpublished data, private communication.

INITIAL DISTRIBUTION LIST

	No. Copies
1. Defense Documentation Center Cameron Station Alexandria, Virginia 22314	2
2. Library, Code 0212 Naval Postgraduate School Monterey, California 93940	2
3. Professor D. E. Harrison, Codes 61 Hx Department of Physics and Chemistry Naval Postgraduate School Monterey, California 93940	5
4. MM H. Perdrix and J. C. Baboux Institut National des Sciences Appliquees de Lyon 20 Avenue Albert Einstein 69261 Villeurbanne Lyon, France	1
5. Ensign Kristin Lloyd Allen 505 Sweeney Road Virginia Beach, Virginia 23452	1

UNCLASSIFIED

Security Classification

DOCUMENT CONTROL DATA - R & D

(Security Classification of title, body of abstract and indexing annotation must be entered when the overall report is classified)

ORIGINATING ACTIVITY (Corporate author)

Naval Postgraduate School
Monterey, California 93940

2a. REPORT SECURITY CLASSIFICATION

Unclassified

2b. GROUP

REPORT TITLE

Secondary Electron Emission from Monocrystalline Metal and
Alkali-Halide Crystals

DESCRIPTIVE NOTES (Type of report end, inclusive dates)

Master's Thesis; June 1973

AUTHOR(S) (First name, middle initial, last name)

Kristin Lloyd Allen

REPORT DATE

June 1973

7a. TOTAL NO. OF PAGES

174

7b. NO. OF REFS

22

CONTRACT OR GRANT NO.

9a. ORIGINATOR'S REPORT NUMBER(S)

PROJECT NO.

9b. OTHER REPORT NO(S) (Any other numbers that may be assigned
this report)

DISTRIBUTION STATEMENT

Approved for public release; distribution unlimited

SUPPLEMENTARY NOTES

12. SPONSORING MILITARY ACTIVITY

Naval Postgraduate School
Monterey, California 93940

ABSTRACT

This thesis is a computer simulation of secondary electron emission (SEE) from monocrystalline metals and alkali-halides using a modified version of the Harrison, Carlston and Magnuson single collision theory of SEE. Three cases of SEE are investigated: the angular dependence of SEE from Cu bombarded by Ar⁺, the dependence of SEE as a function of energy for rare gas ions normally incident on the (100), (110) and (111) faces of metal single crystals, and the dependence of SEE as a function of energy for Ar⁺ and Ne⁺ ions normally incident on the (100), (110) and (111) faces of KCl. The theory does not accurately describe the angular dependence of SEE for monocrystalline Cu targets, but does accurately predict the modified sec θ dependence found experimentally in polycrystalline studies. For the metal targets, the difference between the theoretical kinetic secondary emission result and the experimental datum is identified as potential secondary emission. The alkali-halide SEE simulation agrees reasonably well with experiment.

FORM 1473 (PAGE 1)

1 NOV 68 101-807-6811

173

UNCLASSIFIED
Security Classification

A-31408

KEY WORDS	LINK A		LINK B		LINK C	
	ROLE	WT	ROLE	WT	ROLE	WT
Secondary						
Electron						
Emission						
Ion						
Bombardment						

16 FEB 77

23882

Thesis
A3778
c.1

Allen

143438

Secondary electron
emission from monocrystal-
line metal and alkali-
halide crystals.

16 FEB 77

23882

Thesis

A3778 Allen

c.1

143438

Secondary electron
emission from monocrystal-
line metal and alkali-
halide crystals.

thesA3778

Secondary electron emission from monocr



3 2768 001 91020 1

DUDLEY KNOX LIBRARY